U.S. Department of Transportation
Federal Highway Administration

CONCRETE BRIDGE SHEAR LOAD RATING GUIDE AND EXAMPLES

USING THE MODIFIED COMPRESSION FIELD THEORY

Publication No: FHWA-HIF-22-025

Office of Bridges and Structures

April 2022

FOREWORD

Bridge owners load rate concrete bridges to ensure safe operation, meet regulatory requirements and identify management needs. However, engineers face challenges when applying the current provisions of the AASHTO LRFD Bridge Design Specifications, 8th Edition (2017) to conduct shear load rating for existing concrete bridges designed with previous standards.

The objective of this Guide is to illustrate to load rating engineers how to apply Modified Compression Field Theory (MCFT) when load rating concrete bridges in shear and to identify how load rating differs from design in its application. To meet this objective, this Guide contains shear load rating examples for three concrete bridges that illustrate the application of MCFT for commonly encountered bridge types and situations.

Joseph L. Hartmann, PhD, P.E.
Director, Office of Bridges and Structures
Office of Infrastructure
Federal Highway Administration

Notice

This document is disseminated under the sponsorship of the U.S. Department of Transportation (USDOT) in the interest of information exchange. The U.S. Government assumes no liability for the use of the information contained in this document.

The U.S. Government does not endorse products or manufacturers. Trademarks or manufacturers' names appear in this report only because they are considered essential to the objective of the document. They are included for informational purposes only and are not intended to reflect a preference, approval, or endorsement of any one product or entity.

Non-Binding Contents

The contents of this document do not have the force and effect of law and are not meant to bind the public in any way. This document is intended only to provide clarity to the public regarding existing requirements under the law or agency policies. However, compliance with applicable statutes or regulations cited in this document is required.

Quality Assurance Statement

The Federal Highway Administration (FHWA) provides high-quality information to serve Government, industry, and the public in a manner that promotes public understanding. Standards and policies are used to ensure and maximize the quality, objectivity, utility, and integrity of its information. FHWA periodically reviews quality issues and adjusts its programs and processes to ensure continuous quality improvement.

Cover Photos: **Top Right:** Photo taken by Mark Bewley, courtesy Texas Department of Transportation. **Bottom Right:** Photo courtesy Matt Farrar, Idaho Transportation Department. **Left:** Photo courtesy Gregg Reese, Modjeski and Masters, Inc.

TECHNICAL REPORT DOCUMENTATION PAGE

1. Report No. FHWA-HIF-22-025	2. Government Accession No.	3. Recipient's Catalog No.
4. Title and Subtitle Concrete Bridge Shear Load Rating Guide and Examples: Using the Modified Compression Field Theory		5. Report Date April 2022
		6. Performing Organization Code:
7. Author(s) John Holt, Oguzhan Bayrak, Pinar Okumus, Andreas Stavridis, Thomas Murphy, Dhaval Panchal, Animesh Dutta, Akshay Randiwe		8. Performing Organization Report No.
9. Performing Organization Name and Address University at Buffalo, the State University of New York 12 Capen Hall Buffalo, NY 14260 Modjeski and Masters, Inc 100 Sterling Parkway, Suite 302 Mechanicsburg, PA 17050		10. Work Unit No. 11. Contract or Grant No. DTFH6114D00050
12. Sponsoring Agency Name and Address Federal Highway Administration U.S. Department of Transportation Washington, D.C.		13. Type of Report and Period Covered Final Report. 7/2019 to 4/2022 14. Sponsoring Agency Code HIF/HIBS-10

15. Supplementary Notes

FHWA Task Order COR (Task Order Manager): Lubin Gao, Ph.D., P.E.
FHWA Contracting Officer Representative (COR): Tuonglinh Warren, P.E.
University at Buffalo Project Manager: Pinar Okumus, Ph.D.

Technical Review Panel: Matt Farrar (Idaho Transportation Department), Murugesu Vinayagamoorthy (California Department of Transportation), Yihong Gao (Minnesota Department of Transportation), and Jon Rooper (Oregon Department of Transportation)

16. Abstract

This Guide provides information to load rating engineers in the application of Modified Compression Field Theory (MCFT) when load rating concrete bridges in shear. It includes a literature review of recent research on load rating and summarizes a research study on the effects of minimum shear reinforcement amounts relative to load rating. This Guide also highlights the differences in design and load rating with MCFT. Presented are flow charts with three potential controlling cases of shear strength and proc edures to ascertain the limiting shear strength for a concrete element. Load rating examples are provided, illustrating the application of AASHTO provisions for shear load rating for three concrete bridges.

17. Key Words	18. Distribution Statement
Highway, Bridges, Concrete Shear, Load Rating, Design, Design Loads, Legal Loads, Permit Loads, LFR, LRFR, LFD, LRFD, Modified Compression Field Theory, MCFT	No restrictions. This document is available through the National Technical Information Service, Springfield, VA 22161. http://www.ntis.gov

19. Security Classif. (of this report)	20. Security Classif. (of this page)	21. No. of Pages	22. Price
Unclassified	Unclassified		

Form DOT F 1700.7 (8-72) Reproduction of completed page authorized.

APPROXIMATE CONVERSIONS FROM SI UNITS

SI* (MODERN METRIC) CONVERSION FACTORS

APPROXIMATE CONVERSIONS TO SI UNITS

Symbol	When You Know	Multiply By	To Find	Symbol
		LENGTH		
in	inches	25.4	millimeters	mm
ft	feet	0.305	meters	m
yd	yards	0.914	meters	m
mi	miles	1.61	kilometers	km
		AREA		
in^2	square inches	645.2	square millimeters	mm^2
ft^2	square feet	0.093	square meters	m^2
yd^2	square yard	0.836	square meters	m^2
ac	acres	0.405	hectares	ha
mi^2	square miles	2.59	square kilometers	km^2
		VOLUME		
fl oz	fluid ounces	29.57	milliliters	mL
gal	gallons	3.785	liters	L
ft^3	cubic feet	0.028	cubic meters	m^3
yd^3	cubic yards	0.765	cubic meters	m^3
		NOTE: volumes greater than 1000 L shall be shown in m^3		
		MASS		
oz	ounces	28.35	grams	g
lb	pounds	0.454	kilograms	kg
T	short tons (2000 lb)	0.907	megagrams (or "metric ton")	Mg (or "t")
		TEMPERATURE (exact degrees)		
°F	Fahrenheit	5 (F-32)/9 or (F-32)/1.8	Celsius	°C
		ILLUMINATION		
fc	foot-candles	10.76	lux	lx
fl	foot-Lamberts	3.426	candela/m^2	cd/m^2
		FORCE and PRESSURE or STRESS		
lbf	poundforce	4.45	newtons	N
lbf/in^2	poundforce per square inch	6.89	kilopascals	kPa

APPROXIMATE CONVERSIONS FROM SI UNITS

Symbol	When You Know	Multiply By	To Find	Symbol
		LENGTH		
mm	millimeters	0.039	inches	in
m	meters	3.28	feet	ft
m	meters	1.09	yards	yd
km	kilometers	0.621	miles	mi
		AREA		
mm^2	square millimeters	0.0016	square inches	in^2
m^2	square meters	10.764	square feet	ft^2
m^2	square meters	1.195	square yards	yd^2
ha	hectares	2.47	acres	ac
km^2	square kilometers	0.386	square miles	mi^2
		VOLUME		
mL	milliliters	0.034	fluid ounces	fl oz
L	liters	0.264	gallons	gal
m^3	cubic meters	35.314	cubic feet	ft^3
m^3	cubic meters	1.307	cubic yards	yd^3
		MASS		
g	grams	0.035	ounces	oz
kg	kilograms	2.202	pounds	lb
Mg (or "t")	megagrams (or "metric ton")	1.103	short tons (2000 lb)	T
		TEMPERATURE (exact degrees)		
°C	Celsius	1.8C+32	Fahrenheit	°F
		ILLUMINATION		
lx	lux	0.0929	foot-candles	fc
cd/m^2	candela/m^2	0.2919	foot-Lamberts	fl
		FORCE and PRESSURE or STRESS		
N	newtons	0.225	poundforce	lbf
kPa	kilopascals	0.145	poundforce per square inch	lbf/in^2

TABLE OF CONTENTS

LIST OF FIGURES

LIST OF TABLES

LIST OF ABBREVIATIONS AND SYMBOLS

AASHO	American Association of State Highway Officials
AASHTO	American Association of State Highway and Transportation Officials
ACI	American Concrete Institute
ADTT	Average Daily Truck Traffic
AS	Australian Standard
BDS	Bridge Design Specifications
CFT	Compression Field Theory
CIP	Cast-in-Place
COV	Coefficient of Variation
CSA	Canadian Standards Association
DOT	State Department of Transportation
FEA	Finite Element Analysis
FHWA	Federal Highway Administration
fib	International Federation for Structural Concrete
JSCE	Japan Society of Civil Engineers
LFD	Load Factor Design
LFR	Load Factor Rating
LHS	Left-hand side [of equation]
LLDF	Live Load Distribution Factors
LRFD	Load and Resistance Factor Design
LRFR	Load and Resistance Factor Rating
MBE	AASHTO Manual for Bridge Evaluation
MCFT	Modified Compression Field Theory
NCHRP	National Cooperative Highway Research Program
PCI	Precast Concrete Institute
PDF	Portable Document Format

PT	Post-Tensioned
RC	Reinforced Concrete
RHS	Right-hand side [of equation]
STM	Strut and Tie Modeling
UTDBD	University of Texas Deep Beam Database
UTPCSDB	University of Texas Prestressed Concrete Shear Database
WWR	Welded Wire Reinforcement

CHAPTER 1. INTRODUCTION

1.1 CONCRETE BRIDGE SHEAR LOAD RATING

Accurate bridge load ratings are important to maintain safe transportation networks that do not unduly hinder commerce. Public safety is paramount, and the role bridges play in the economy of the nation is directly indicated by the heavy truck loadings bridges carry. Loads exceeding legal loads can exceed the design loads; hence, States depend on accurate load ratings to effectively manage maintenance, rehabilitation, and replacement of their bridge inventory.

The Federal Highway Administration's (FHWA) Concrete Bridge Shear Load Rating Synthesis Report (Holt et al. 2018) described challenges States experience, along with the many changes in how shear was addressed since the first edition of the American Association of State Highway Officials (AASHO) Bridge Design Specifications (BDS) in 1931. Three major developments in shear design were the transition from allowable stress design to a factored load and ultimate strength-based design, the widespread introduction of prestressed concrete, and the introduction of both the Modified Compression Field Theory (MCFT) and Strut and Tie Modeling (STM). All represent advancements in structural engineering, largely made possible by Federal and State investment in transportation research.

The intent of this Guide is to assist with implementation of MCFT, and STM to a limited extent, when load rating concrete bridges in shear. This Guide will also identify the differences between design and load rating when applying MCFT.

1.2 SPECIFICATIONS, MANUALS, AND ADDITIONAL RESOURCES

AASHTO Load and Resistance Factor Design (LRFD) Bridge Design Specifications, 8th Edition (2017). These specifications are incorporated by reference in 23 CFR 625.4(d)(1)(v) and are applicable to design for new construction, reconstruction, resurfacing, restoration, or rehabilitation of a highway on the NHS [23 CFR 625.3(a)(1)]. These specifications contain provisions for MCFT and STM. Unless noted otherwise, all references to AASHTO LRFD Specifications in this Guide are to these binding design specifications. All other versions of the LRFD Specifications that do not reflect binding regulatory standards are noted as nonbinding in this Guide.

AASHTO Manual for Bridge Evaluation (MBE), 3rd Edition (2018). This manual is not incorporated by reference and is not a binding regulatory standard. This manual is a voluntary industry specification and is not a Federal requirement. Unless noted otherwise, all references to AASHTO MBE in this Guide are to this nonbinding manual.

AASHTO Standard Specifications for Highway Bridges, 17th Edition (2002). These specifications are incorporated by reference in 23 CFR 625.4(d)(1)(iii) and are applicable to modification design for existing bridges on the NHS that are originally designed to any edition of the AASHTO Standard Specifications for Highway Bridges [23 CFR 625.3(a)(1); 23 CFR

625.4(b)(1)]. These specifications are referenced in this Guide as an additional resource and are noted as nonbinding.

Note that this Guide deals with load rating, not design, of highway bridges. For bridge load rating, the National Bridge Inspection Standards (NBIS) [23 CFR Part 650, Subpart C] provide Federal requirements [23 CFR 650.313(c)]. The NBIS incorporates the first Edition MBE (2008) [23 CFR 650.317(b)(1)]. All AASHTO bridge design specifications (including any edition of the AASHTO Standard Specification or LRFD Specifications) are not directly incorporated by reference in the NBIS. However, AASHTO MBE, including the binding first Edition 2008 MBE and the nonbinding 3rd Edition 2018 MBE, refers to specific articles or provisions provided in the design specifications.

The focus of this Guide is the MCFT, which is not included in any editions of the AASHTO Standard Specifications.

In a brief summary, this Guide is only to provide additional technical information for bridge owners to consider when load rating concrete bridges in shear. No part of this Guide constitutes or is to be considered as new Federal requirements.

1.3 MODIFIED COMPRESSION FIELD THEORY, MCFT

The MCFT was widely introduced to the United States' bridge engineering community with the first edition of the American Association of State Highway and Transportation (AASHTO) Load and Resistance Factor Design (LRFD) Bridge Design Specifications in 1994. Although it is versatile as it addresses both prestressed concrete and reinforced concrete, and accounts for axial load in addition to vertical loading, its iterative approach to designing for shear was new to engineers. AASHTO acknowledged challenges in implementing MCFT and introduced simplified shear design provisions in AASHTO LRFD in 2007 (Hawkins et al. 2005; AASHTO 2007). A non-iterative approach with MCFT was introduced in the 2008 interim revisions to the AASHTO LRFD Bridge Design Specifications. This non-iterative approach is made possible through incorporation of simplifying assumptions in MCFT (Bentz et al. 2006).

Chapters 2 and 3 identify multiple studies where MCFT and other shear strength methodologies have been researched and evaluated for bridge design. MCFT has been shown to be an accurate, adequately conservative, and versatile shear strength prediction methodology.

While designing for shear with MCFT is straightforward, load rating with MCFT is somewhat more challenging in that an iterative procedure is used to determine a member's shear strength as the strength is dependent on the moment, shear, and axial loads on the member. This Guide presents one way to perform these iterations when load rating, with three load rating examples.

Other load rating challenges with MCFT include members that have some but less than the minimum shear reinforcement and members where prestressing is not within the flexural tensile zones.

1.4 STRUT AND TIE MODELING, STM

STM provides a way to design and assess disturbed regions of members, such as near supports and points of application of concentrated loads. Common bridge elements that may benefit from STM to determine their capacity are substructure elements such as deep pier caps, pile caps and footings with short shear spans. STM is also useful for post-tensioning anchorage zones, diaphragms, deep beams, beam ledges or corbels.

Chapter 3 presents study results that may be beneficial when load rating bridge members without the minimum crack control reinforcement specified for new designs.

1.5 LOAD AND RESISTANCE FACTOR RATING, LRFR

In this Guide, the MCFT and STM approaches to determining concrete shear strength are outlined in the binding AASHTO LRFD Bridge Design Specifications 8th Edition (AASHTO 2017) , referred to in this Guide as AASHTO LRFD. Load and Resistance Factor Rating (LRFR) is provided in the nonbinding AASHTO Manual for Bridge Evaluation 3rd Edition (AASHTO 2018), referred to as AASHTO MBE in this Guide.

MCFT and STM may be used with Load Factor Rating (LFR) as both are strength-based methodologies. It is suggested to use the strength reduction factors listed in the nonbinding AASHTO Standard Specifications (AASHTO 2002) when using MCFT or STM with LFR.

The focus of this Guide is implementation of MCFT with load rating. The Guide assumes the reader is familiar with the various load rating methods in AASHTO MBE, types of ratings, when they are used, and when concrete bridges are to be load rated and for which loads.

CHAPTER 2. LITERATURE REVIEW

2.1 INTRODUCTION

This document builds on the work compiled in the Concrete Bridge Shear Load Rating Synthesis Report (Holt et al. 2018). The history of AASHTO LRFD and AASHTO Load and Resistance Factor Rating (LRFR) methods, loads, load combinations, live load distributions, and shear strength in both reinforced and prestressed concrete were reviewed in the synthesis report. The synthesis report also included a survey to nine State DOTs to understand their practices and challenges, in addition to reviewing some of the most recent research on concrete shear strength, design and load rating. The following were among the main findings. This study focuses on findings 7, 8, 9, 10 and 12. The finding numbers refer to those in the synthesis report.

- **Finding 7:** The locations where the strains are calculated per Chapter 5 (closed form solution) and Appendix (iterative solution) of binding AASHTO LRFD BDS (AASHTO 2017) (incorporated by reference at 23 CFR 625.4(d)(1)(v)) are not the same.
- **Finding 8:** When prestressing is on the compressive flexural side, MCFT can provide incorrect shear strength, particularly if the section is not cracked.
- **Finding 9:** With MCFT, it is important to use the strain consistent with the applied loads when computing the shear resistance. To achieve consistency between the applied loads, the strain, and the shear resistance, numerical analysis should converge.
- **Finding 10:** Members that have stirrups, but less than binding AASHTO LRFD BDS's (AASHTO 2017) minimum shear reinforcement amount, may have higher shear strength than predicted by AASHTO LRFD BDS's MCFT based design and load rating methods.
- **Finding 12:** Reinforcement detailing and anchorage should be checked when load rating.

The literature review provided in this section complements the synthesis report. The literature review covers the evolution of the AASHTO's shear provisions including the compression field theory (CFT) and MCFT, their bases, assumptions, simplifications, and adoption by codes; methods for load rating using MCFT and for predicting the capacity of members with less than the suggested minimum reinforcement amount; and provisions of international codes that utilize MCFT. Databases compiled by other researchers are also summarized here.

2.2 AASHTO LRFD MCFT SHEAR PROVISIONS

2.2.1 Basis of Compression Field Theory

The Compression Field Theory (CFT) was proposed (Collins 1987; Mitchell and Collins 1974) in the 1970s as a method based on mechanics and supported by empirical data. In the 1980s, CFT was expanded to account for the average concrete tension stresses between cracks. Inclusion of these stresses can improve the shear resistance of reinforced concrete and allows for the prediction of capacity of members without shear reinforcement (Bentz and Collins 2006). This method, called the Modified Compression Field Theory (Vecchio and Collins 1986) (MCFT) is the basis of shear design provisions of AASHTO LRFD Bridge Design Specifications 8th Edition (AASHTO 2017) (binding).

Key variables to characterize the shear behavior are hard to identify using traditional beam tests (e.g., simple span beams). To identify these variables, CFT and MCFT researchers developed a testing method where a membrane element can be loaded under pure shear and biaxial loading. Both CFT and MCFT start with a small membrane element with an orthogonal grid of reinforcement. CFT and MCFT then use equilibrium over this membrane element to describe the replacement of concrete tensile stress when concrete cracks with reinforcing bar stress (before rebar yielding) or concrete shear stress across crack interface (after rebar yielding). The latter is a function of aggregate interlock and therefore crack width. The principal strains and crack angle are determined using compatibility of rebar and concrete, constitutive relation of steel, constitutive relation of *cracked* concrete considering aggregate interlock (Walraven 1981). The properties of cracked concrete are obtained through membrane testing.

Unlike most other models, MCFT and CFT take into account axial loading combined with shear and allow variable shear crack angles, which can be particularly beneficial for prestressed members. CFT and MCFT are also general enough to predict the behavior of both reinforced and prestressed members with and without shear reinforcement (Vecchio and Collins 1986).

2.2.2 Assumptions of MCFT

The main assumptions of the original MCFT (Vecchio and Collins 1986) are: 1) loading history does not have a significant influence on stress states, 2) stresses and strains are averaged over areas or lengths that cross several cracks, 3) there is no slip between rebar and concrete, and 4) longitudinal and transverse rebar are uniformly distributed. MCFT also assumes that average stress-strain relation of concrete and rebar are completely independent from each other, the axial rebar stress is only a function of axial rebar strain, average out-of-plane shear stress on rebar is zero, and axes of principal stresses and strains in concrete coincide.

2.2.3 Code Adaptation of MCFT

MCFT theory was transformed into design equations with the following simplifications in the 1990s (Collins et al. 1996): 1) Shear stress was assumed uniform over shear area ($b_v d_v$), 2) Maximum longitudinal strain in the web (a parameter used to calculate the maximum principal tensile strain in cracked concrete in MCFT) was approximated as the strain in the flexural tension reinforcement, 3) Principal compressive stress was simplified to be the uniform shear stress multiplied by the sum of tangent and cotangent of shear crack angle (neglecting the principal tensile stress term), and 4) Clamping stresses across member direction were assumed zero.

When MCFT was initially developed, the calculation of shear stresses in concrete and reinforcement needed iterations (or tables), where the principal tensile strain in concrete and the angle of principal strains were varied until convergence. The results of 528 reinforced and prestressed beam tests were compared to the MCFT predictions as adopted by the early editions of AASHTO LRFD BDS (nonbinding) with iterations and the simplifications given above. Mean of measured-to-predicted strength ratio was 1.44, with a coefficient of variation (COV) of 18.2 percent. As a point of reference, the mean was 1.32 and COV was 30.1 percent for American Concrete Institute (ACI) specification ACI 318-95 (ACI 318 1995) (Collins et al. 1996). A

similar but larger database analysis of 1329 reinforced and prestressed beam tests showed that mean ratio was 1.38 and COV was 26.2 percent when the strength was estimated using the earlier editions of AASHTO LRFD BDS with iterations (Kuchma et al. 2008).

2.2.4 Simplifications to MCFT and Code Equations

The AASHTO LRFD Bridge Design Specification, 8th Edition (AASHTO 2017) (binding) uses simpler equations than the previous versions to determine the ability of cracked concrete to resist shear (β) and crack angle (θ) as functions of the longitudinal strain and crack widths. It eliminates iterations and tables for β and crack angle θ, and reduces the number of equations needed to calculate shear strength (Kuchma et al. 2008). These changes were consistent with the ones to the Canadian standard (CSA Group 2004) proposed by Bentz et al. (Bentz and Collins 2006; Bentz et al. 2006). The following were the assumptions that allowed simplifications to latest versions of AASHTO LRFD (Bentz and Collins 2006) and further simplifications to MCFT:

- To eliminate iterations, β was expressed by relating aggregate interlock to crack width (i.e., crack spacing and average strain perpendicular to cracks). The nonlinear relation between longitudinal strain at mid-depth and diagonal crack width was simplified as linear (**Figure 1a**).
- Curve fitting was used to determine an adjustment factor to β that accounts for the size effect on shear strength as a function of crack spacing parameter (**Figure 1b**).
- The crack angle was assumed to be linearly proportional to the longitudinal strain at mid-depth. A linear equation was developed to represent a relatively narrow range of crack angle-longitudinal strain pairs that allow stirrups to yield before failure and prevent concrete to crush before reaching the desired shear stress (**Figure 1c**).
- Finally, in calculating the longitudinal strain, the force in the bottom chord due to shear ($0.5V\cot\theta$) was conservatively simplified by assuming $0.5\cot\theta = 1$ so that the force is no longer a function of crack angle.

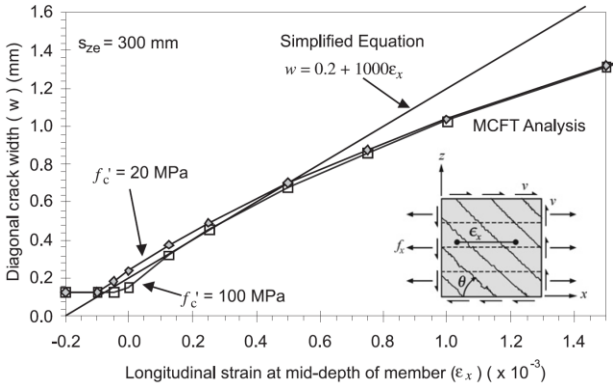

a. Longitudinal strain at mid-depth vs diagonal crack width

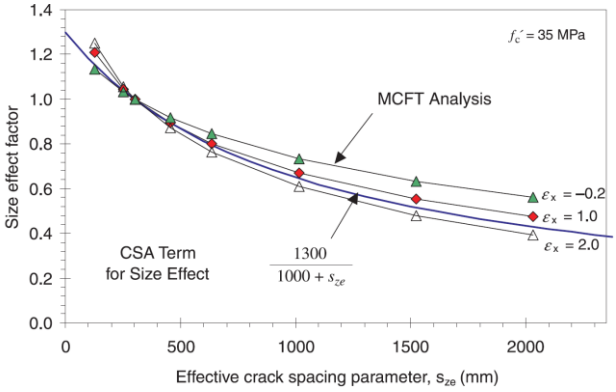

b. Effective crack spacing parameter vs size effect factor (multiplier for β)

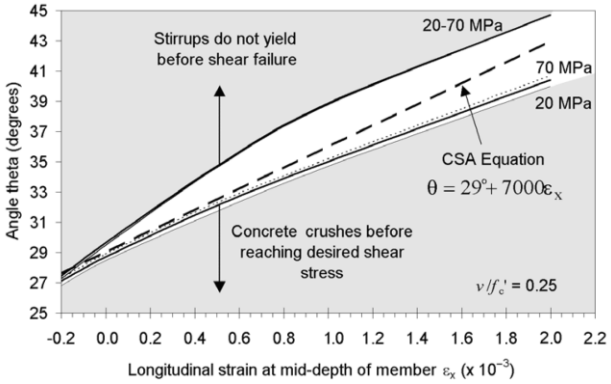

c. Longitudinal strain ad mid-depth vs crack angle

Figure 1. Simplifications to MCFT and to AASHTO LRFD BDS in 2000s.

Equations of β and θ that resulted from these simplifications are given in equations (Equation 1) and (Equation 2), respectively. When members have AASHTO LRFD BDS's (AASHTO 2017) (binding) suggested minimum shear reinforcement amount, crack spacing parameter, s_{ze}, is assumed to be 12 inches (300 mm). Therefore, the second term in the equations become unity. For members without the minimum shear reinforcement of AASHTO LRFD BDS (AASHTO 2017) (binding), shear strength decreases and angle increases, with increasing crack spacing. The MCFT equations shown in equations (Equation 1) and (Equation 2) by Bentz and Collins (2006) differ slightly from those in AASHTO LRFD BDS (AASHTO 2017) (binding) due to the differences in units and in the calculation of longitudinal strain, but they are otherwise equivalent.

$$\beta = \frac{0.4}{1 + 1500\varepsilon_x}\left(\frac{1300}{1000 + s_{ze}}\right)[mm] \quad \text{(Equation 1)}$$

$$\theta = (29^o + 7000\varepsilon_x)\left(0.88 + \frac{s_{ze}}{2500}\right)[mm] \quad \text{(Equation 2)}$$

National Cooperative Highway Research Program (NCHRP) Report 549 (Hawkins et al. 2005) analyzed test results of 64 reinforced concrete and 82 prestressed concrete members that have at least the AASHTO LRFD BDS's 8th Edition (AASHTO 2017) (binding) suggested minimum reinforcement amounts and compared them to code predictions. The simplified AASHTO LRFD (versions after 2008, nonbinding other than the 8th Edition) led to a mean ratio of measured-to-predicted strength of 1.105 (for reinforced concrete members) and 1.245 (for prestressed concrete members), with a COV of 15.6 percent (for reinforced concrete members) and 13.4 percent (for prestressed concrete members). As a reference, when the same dataset was used to evaluate earlier versions of AASHTO LRFD before simplifications (nonbinding), the mean ratios were 1.214 (for reinforced concrete members) and 1.227 (for prestressed concrete members). The corresponding COVs were 17.9 percent (for reinforced concrete members) and 14.5 percent (for prestressed concrete members).

2.2.5 MCFT on Members without the Minimum Shear Reinforcement

The minimum reinforcement amount suggested by AASHTO increased over the years. The amount suggested by the binding AASHTO LRFD BDS 8th Edition (AASHTO 2017) is 50 percent higher than the one suggested by nonbinding AASHTO Standard Specifications (AASHTO 2002) (Kuchma et al. 2008). NCHRP Report 549 considers this increase reasonable by citing members with less than the minimum reinforcement failing at loads less than predicted by codes (Hawkins et al. 2005; Kuchma et al. 2008).

A minimum amount of shear reinforcement is needed for ductility (Zararis 2003) and to keep shear crack widths small so that cracked concrete can resist shear (Hawkins and Kuchma 2007; Hawkins et al. 2005). MCFT provides shear capacity equations for members without any web reinforcement as a function of crack width that controls the ability of cracked concrete to transmit shear through aggregate interlock (Collins et al. 1996). Crack width is calculated as principal tensile strain multiplied by crack spacing in MCFT. Therefore, for members without any web reinforcement, shear strength is a function of aggregate size and crack spacing. Crack spacing is controlled by longitudinal reinforcement location.

MCFT equations that were developed for members with no shear reinforcement are now used in AASHTO LRFD BDS 8th Edition (binding) to predict the strength of members that have less than the minimum specified reinforcement. In other words, AASHTO LRFD provisions address beams with no reinforcement but do not explicitly address beams with less than the minimum reinforcement amount (Angelakos et al. 2001). This can explain why there is a drop in shear capacity predictions of a beam with minimum reinforcement and a beam reinforced with less than the minimum reinforcement, as documented by the FHWA study (Holt et al. 2018). The drop can also be explained by the large number of tested beams in databases with no shear reinforcement, which were used to develop, refine, and evaluate AASHTO equations.

In principle, MCFT's indicator of the ability of cracked concrete to carry shear (β) covers members with less than the minimum suggested amount of reinforcement, as long as crack spacing can be identified for these members (as opposed to using crack spacing of members with no shear reinforcement). A crack spacing term in the equation of β for members with more than

the minimum amount of web reinforcement is not present, because MCFT conservatively assume a spacing of 12 inches for these members (Bentz and Collins 2017; Bentz et al. 2006).

2.3 MEMBERS WITH LOW LOAD RATINGS

Only a few studies, as summarized in this section, proposed methods for members with low load ratings or for members with less than the minimum specified amount of shear reinforcement. These methods include detailed MCFT analyses, interpolation, iterative analyses, and load rating adjustment factors as summarized in this section.

2.3.1 Detailed MCFT Analysis

Bentz (2010) evaluated two methods with different levels of accuracy and complexity as compared to measured shear capacities of eight beams tested by Higgins et al. (2007). **Figure 2** shows shear capacity predictions of MCFT with simplification (similar to AASHTO LRFD 8th Edition (AASHTO 2017) (binding), called Level III in **Figure 2**) and detailed MCFT (sectional analysis conducted with software (Bentz and Collins 2019), called Level IV in **Figure 2**) compared to test results shown with dots on plots. There is a jump in level III and IV predictions with increasing stirrup quantity. The jump in strength is smaller with detailed MCFT analysis than Level III that uses simplified MCFT. The figures present that detailed MCFT analyses with the use of a computer program such as Response2000 may predict higher strengths as compared to the predictions of MCFT with simplifications.

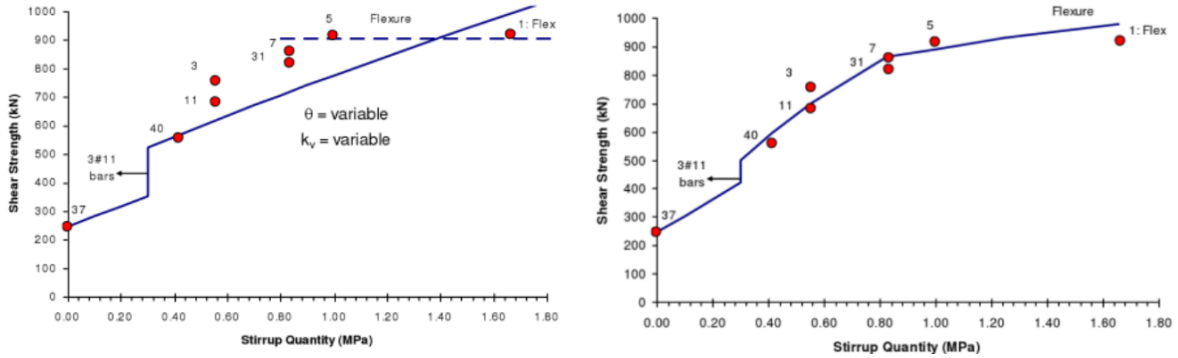

a) Level III Approximation b) Level IV approximation using Response2000

Figure 2. Shear strength predicted by Level III and IV with varying stirrup amounts.

A study conducted for the AASHTO Committee on Bridges and Structures (Sivakumar 2016) focused on shear load rating of post-tensioned multi-cell box girders with strands that follow a parabolic profile. These girders can have low shear ratings within the vicinity of the inflection points because the area of prestress within the flexural tension side of the girder (area of prestress that can be used to calculate the longitudinal tensile strain) is very small or zero, causing an increase in longitudinal tensile strain (ε_s). To overcome this problem, near the inflection points,

Sivakumar (2016) suggested replacing the shear capacity obtained using AASHTO LRFD BDS (binding) (or AASHTOWare Bridge™ Rating) with an analysis performed using Response2000, an MCFT based software (Bentz and Collins 2019). The method proposed by Sivakumar (2016) had the following steps:

- Step 1: Determine the length near the inflection points over which load ratings are problematic,
- Step 2: Use Response2000 analysis to obtain a moment-shear diagram and include resistance factors if needed,
- Step 3: Mark the moment and shear created by dead loads on the moment-shear (M-V) diagram and connect it to origin, i.e., point (0,0),
- Step 4: Mark the moment and shear created by dead and live loads on the M-V diagram and connect it to the point created in step 3,
- Step 5: Estimate the shear and moment capacity of the section as the intersection of the line or the projection of the line created in step 5 with the M-V diagram.

2.3.2 Linear Interpolation

The AASHTO LRFD BDS 8th Edition (AASHTO 2017) (binding) shear predictions for members with less than the minimum reinforcement were developed for members with no reinforcement, following MCFT. To prevent low strength predictions for beams that have reinforcement less than the minimum amount, Angelakos et al. (2001) suggested linear interpolation. In this method, shear strength is calculated for the member by assuming there is no shear reinforcement and by assuming there is the minimum specified reinforcement. Shear capacity of the member with some, but less than the minimum, amount of reinforcement is determined by using linear interpolation between these two capacities.

Figure 3 shows a comparison of an earlier versions of AASHTO LRFD (nonbinding) prediction with minimum reinforcement (the top line), AASHTO prediction with no reinforcement (the bottom line), and prediction using linear interpolation for five beams that have the same $A_v f_y / b_v s$ ratios. The results are compared to results of five beams tested by Angelakos et al. (2001) with less than the minimum amount of reinforcement as marked with circles on the figure. The earlier version AASHTO LRFD (nonbinding) prediction with no reinforcement was conservative for all five beams. Linear interpolation method was conservative for two out of five beams.

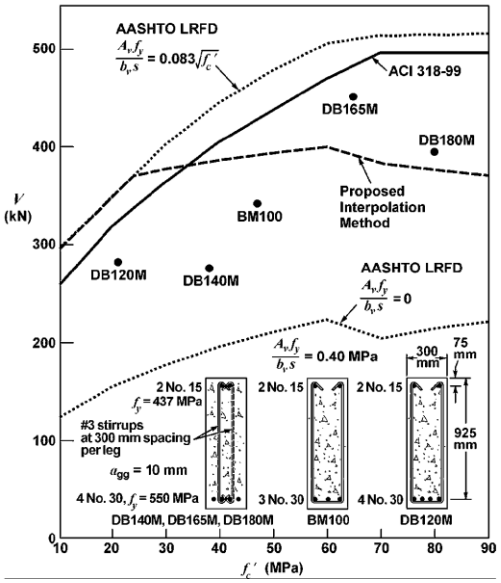

Figure 3. Capacity prediction with linear interpolation.

2.3.3 Iterations

Caprani and Melhem (2019) observed that when assessing a bridge, as opposed to designing a bridge, shear capacity "…both depends on the longitudinal strain and causes the longitudinal strain." They proposed an iterative process to calculate the shear capacity. The procedure starts with an initial guess of longitudinal strain using ultimate shear as the shear demand. It then continues by calculating ratios of moment, torsion, and axial load to shear from analysis, calculating shear resistance as a sum of shear resistance of reinforcement and concrete (both functions of longitudinal strain). Iterations are continued until shear resistance is equal to the shear demand. A similar iterative process was proposed for evaluating tension in longitudinal reinforcement due to shear. This method was shown to have similar errors for calculating shear capacity of five beams. However, for calculating tension in longitudinal reinforcement due to shear, this method with iterations reduced error from +49 percent to +58 percent to -16 percent to -6 percent compared to calculations without iterations. In reporting error, + and – refer to overestimating and underestimating of capacities, respectively. Baseline for the error calculations of the Caprani and Melhem (2019) study was detailed MCFT performed by Response2000 (Bentz and Collins 2019).

2.3.4 Adjusted Shear Capacity based on Regression Analysis

A study conducted for Michigan Department of Transportation (DOT) (Chehab and Eamon 2018; Chehab et al. 2018; Eamon et al. 2014) evaluated the capacity 16 cracked prestressed concrete bridge members, tested 6 full-scale beams, and performed a parametric study using finite element modeling. Finite element analyses were performed in 2-D using a software based

on MCFT (Vector Analysis Group 2019). This model can simulate nonlinear behavior through a smeared crack modeling approach.

Using the finite element models, which were validated by test data, the study created 414 cases by varying the following parameters: beam type, load position, strand geometry, concrete strength, section axial stress, stirrup spacing and longitudinal steel reinforcing ratio. For these cases, ratios of capacities predicted by finite element analysis and by an earlier version of AASHTO LRFD (nonbinding) were calculated, as shown in **Figure 4** with blue triangles. The mean and COV of the ratio were 2.25 and 0.26, respectively. The ratios were then adjusted using linear and nonlinear regression analysis so that they were closer to but above 1.0. The red circles on **Figure 4** show the ratios adjusted by linear regression. The mean and COV after adjustment with linear regression were 1.37 and 0.14, respectively. Nonlinear regression led to 1.39 and 0.23 for mean and COV, respectively.

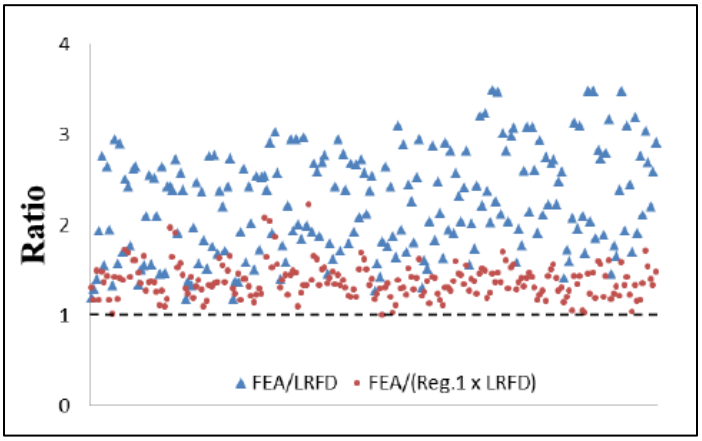

Source: Eamon, Parra-Montesinos, Chehab. Reproduced from Eamon, C. D., Parra-Montesinos, G. J., and Chehab, A. (2014). "Evaluation of Prestressed Concrete Beams in Shear." Michigan Department of Transportation, Report No: RC-1615, Lansing, MI, 324.

Figure 4. Ratios of capacity by finite element analysis (FEA) to AASHTO LRFD (blue triangles in figure) and adjusted ratios using linear regression (red circles in the figure).

Regression equations were provided as a function of concrete compressive strength (f'_c), gross area of beam divided by total prestress force (σ), stirrup spacing (s) and beam height (h). The adjustment factor (k_{mL}) obtained from linear regression for capacity calculated per LRFD is given in equation 3. Nonlinear regression was also performed but is not summarized here.

$$k_{mL} = (0.009f'_c + 0.2\sigma + 0.035s + 0.018h + 0.01), \text{ where } 1.18 \le k_{mL} \le 3.49 \quad \text{(Equation 3)}$$

The study suggested that shear capacity be determined (using iterations until $V_u=V_n$) and be adjusted by multiplying the shear capacity with the adjustment factor, k_{mL}, from equation 3.

2.3.5 Methods That Are Not Based on MCFT

Other methods have been proposed to determine the shear capacities of members with shear reinforcement, regardless of how small the reinforcement amount may be (e.g., Zararis (2003)).

However, these methods utilize rationales that are different from the one of MCFT. These methods are not reviewed in-depth here.

2.4 INTERNATIONAL CODES

International codes and standards were reviewed to understand if provisions developed elsewhere reduce the level of conservatism included in shear capacity prediction methods and address members that do not have minimum shear or longitudinal reinforcement amounts. At the focus of the review are codes and standards based on MCFT, as these are compatible with binding provisions in AASHTO LRFD Bridge Design Specifications, 8th Edition (2017). Standards based on other rationales are acknowledged but are not reviewed in detail.

2.4.1 Canadian Highway Bridge Design Code 2019

AASHTO followed the Canadian Highway Bridge Design Code in the adoption of MCFT and in the adoption of simplified MCFT. Therefore, the two codes are very similar. Equations given in this report earlier as (Equation 1) and (Equation 2) were developed by Bentz and Collins (2006) and were incorporated into CSA S6:19 (CSA Group 2019a).

In the Canadian Standard, the longitudinal strain, ε_x, is taken as half the longitudinal strain in the flexural tensile side reinforcement, by assuming the flexural compression side reinforcement longitudinal strains are small. Note that the multipliers of ε_x in equations (Equation 1) and (Equation 2) are twice that of binding AASHTO LFRD BDS 8th Edition resulting in the same β and θ values.

CSA commentary (CSA Group 2019b) provides a more accurate method to estimate the longitudinal strain at mid-depth, ε_x, as shown in **Figure 5** as the algebraic average of the strain in the flexural tension side and the strain in the compression side of the section. **Figure 6** is provided to determine axial strains in flanges from axial forces. The longitudinal strain at mid-depth can then be determined as the algebraic average of the longitudinal strains in top and bottom flanges. When the longitudinal compression strain (usually a small negative quantity) is small and assumed zero, this leads to the assumption of longitudinal mid-depth strain to be half of longitudinal tension flange strain.

A more accurate method of separating reinforcement area into the ones in flexural tension and compression zones is provided in CSA S6:19. This method includes picking reinforcement areas that ensure the centroid of reinforcement remains at its original location. However, the commentary acknowledges that the additional accuracy gain may not justify the added complexity.

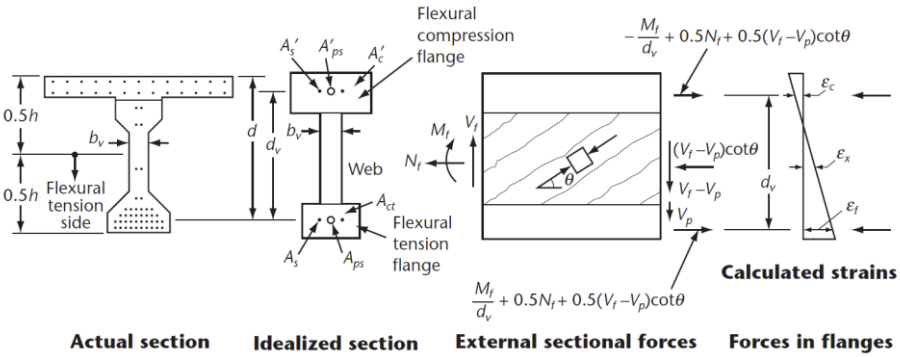

Source: Figure C8.12, CSA S6:19, Canadian Highway Bridge Design Code. © 2019 Canadian Standards Association. Please visit store.csagroup.org[1].

Figure 5. More accurate calculation procedure for longitudinal strain at mid-depth per Figure C8.12 of CSA S6:19.

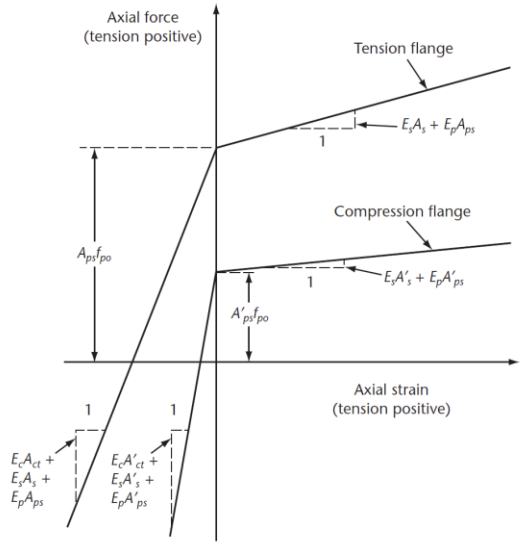

Source: Figure C8.12, CSA S6:19, Canadian Highway Bridge Design Code. © 2019 Canadian Standards Association. Please visit store.csagroup.org[2].

Figure 6. Assumed relationship between axial force in flange and axial strain of flange per Figure C8.13 of CSA S6:19.

[1] With the permission of Canadian Standards Association, (operating as "CSA Group"), 178 Rexdale Blvd., Toronto, ON, M9W 1R3, material is reproduced from CSA Group's standard **CSA S6:19, *Canadian Highway Bridge Design Code***. This material is not the complete and official position of CSA Group on the referenced subject, which is represented solely by the Standard in its entirety. While use of the material has been authorized, CSA Group is not responsible for the manner in which the data is presented, nor for any representations and interpretations. No further reproduction is permitted. For more information or to purchase standard(s) from CSA Group, please visit store.csagroup.org or call 1-800-463-6727.

[2] With the permission of Canadian Standards Association, (operating as "CSA Group"), 178 Rexdale Blvd., Toronto, ON, M9W 1R3, material is reproduced from CSA Group's standard **CSA S6:19, *Canadian Highway Bridge Design Code***. This material is not the complete and official position of CSA Group on the referenced subject, which is represented solely by the Standard in its entirety. While use of the material has been authorized, CSA Group is not responsible for the manner in which the data is presented, nor for any representations and interpretations. No further reproduction is permitted. For more information or to purchase standard(s) from CSA Group, please visit store.csagroup.org or call 1-800-463-6727.

CSA S6:19 commentary also covers the design of longitudinal reinforcement on both the flexural tensile and compression sides of a section. Provisions for the latter are meant to cover sections with significant tension in longitudinal reinforcement on the flexural compression side, caused by small moment and large shear forces, i.e., near points of inflection.

2.4.2 Australian Standard AS 5100:2017

MCFT without iterations for β and θ was adopted by the Australian Standard for design of new bridges and assessment of existing bridges, Australian Standard (AS) AS 5100, in 2017 (Caprani and Melhem 2019). Provisions of AS 5100 are similar to Canadian Highway Bridge Design Code (and therefore similar to binding AASHTO LRFD BDS 8th Edition) with the exception of the crack spacing parameter that is adjusted by a factor to account for thin sections with larger aggregates.

2.4.3 *fib* Model Code 2010

The International Federation for Structural Concrete *(fib)* Model Code 2010 provides four options for the calculation of a coefficient of concrete contribution (similar to β) and the inclination of shear crack angle. These options are called "levels of approximation," with level I being the simplest and the least accurate, and level IV being the most complex and the most accurate. Levels I and III are based on MCFT (Bentz 2010). These levels are summarized as follows:

- In Level I analysis, inclination of shear crack angle is assumed 36°. A coefficient of concrete contribution accounts for the size effect for members without stirrups.
- Level II ignores concrete contribution to shear resistance and determines shear crack angle range as a function of longitudinal strain.
- Level III is equivalent to earlier versions of AASHTO LRFD specifications (nonbinding) based on MCFT with iterations necessitated by the $0.5\cot\theta$ term. Coefficient of concrete contribution to shear is calculated either for members without reinforcement ($t_{wo} = 0$) and separately for members with more than the minimum reinforcement ($W \geq 0.08\sqrt{f_{ck}}/f_{yk}$). Reinforcement ratios between these two limits are not addressed.
- Level IV is detailed analysis, such as a non-linear finite element analysis.

Implications of Level III and IV analyses on strength prediction are summarized in Section 2.3.1. Comparisons of all levels of analyses are available by Bentz (2010).

2.4.4 ACI318-19: Building Code

The provisions for shear members were updated in 2019 (ACI 318 2019) to account for the size effect in shear for non-prestressed members (Frosch et al. 2017). ACI 318 is not consistent with AASHTO LRFD BDS 8th Edition (AASHTO 2017) (binding) as the shear calculation methods are based on methods other than MCFT (MacGregor and Hanson 1969), and therefore is not reviewed here in detail. Previous editions of ACI 318 provisions have been found to be less conservative and less precise than earlier versions of nonbinding AASHTO LRFD when compared to test or detailed analysis results (Kuchma et al. 2008).

2.4.5 New Zealand Bridge Manual and Concrete Structures Standard

The New Zealand Transportation Agency Bridge Manual SP/M/022 (New Zealand Transportation Agency 2013) refers the users to nonbinding AASHTO LRFD, 6th Edition (2012) for shear design of prestressed concrete members. New Zealand Concrete Structures Standard, NZS 3101.1:2006 and NSZ 3101.2.2006 (Standards New Zealand 2006), includes shear strength calculation methods for non-prestressed and prestressed members. These methods are similar to the ones given in earlier and current versions of ACI 318 and earlier versions of AASHTO LRFD (nonbinding).

2.5 AVAILABLE DATABASES

As this research relies heavily on existing experimental data, some of the largest databases on shear of concrete beams are reviewed here. Note that test results of some beams may have been included in multiple databases as databases often build up on each other.

- NCHRP 12-61 (Hawkins et al. 2005) provides a comprehensive database containing test results for 2,187 reinforced concrete or prestressed concrete beams. More than 62 percent of the beams had no stirrups.
- NCHRP 12-56 (Hawkins and Kuchma 2007) set up a database of 1,874 test results on reinforced and prestressed beams, building up on the NCHRP 12-61 database.
- Reineck et al. (2003) compiled test results of 439 rectangular beams with no shear reinforcement to assess code predictions of shear strength.
- ACI-DAfStb Database (Reineck et al. 2013) expanded the database by Reineck et al. (2003) and has test results on 784 beams with no shear reinforcement.
- University of Texas, Austin (Nakamura et al. 2013) maintains a database with 1,146 tests on prestressed concrete beams that failed under shear.
- Naji et al. (2018) investigated bond-loss failure, a less common type of shear-flexure failure associated with shear cracking, using test results from 120 beams. Bond-loss failure is influenced by longitudinal tie resistance.

The contents of the databases indicate that while many researchers have focused on beams with no shear reinforcement, the number of tests on beams that had shear reinforcement without meeting the code is limited.

2.6 SUMMARY

The literature review covered the basis of CFT and MCFT, simplified MCFT and adaptation of MCFT with simplifications to AASHTO LRFD BDS 8th Edition (AASHTO 2017) (binding). Approximations utilized in simplifying MCFT and the AASHTO LRFD 8th Edition (AASHTO 2017) (binding) were outlined as they can be used to understand the level of conservatism of AASHTO LRFD 8th Edition (AASHTO 2017) (binding). The review showed that MCFT's equations for members that do not meet the minimum specified shear reinforcement were originally developed for members with no shear reinforcement. Only a few methods exist in the literature to improve shear capacity prediction of members that have some, but less than the prescribed, amount of reinforcement. These methods include linear interpolation, detailed MCFT analyses and iterative analyses. MCFT equations that describe shear capacity as a function of

crack spacing can also be utilized if crack spacing is identified for members with less than the prescribed amount of reinforcement.

Guides and codes from Canada, Australia, Europe, and New Zealand were reviewed to identify provisions that may address members with less than the prescribed amount of reinforcement and members with strands on the compression side. Most international codes that utilize MCFT, including AASHTO LRFD BDS 8th Edition (AASHTO 2017) (binding), followed the Canadian Highway Bridge Design Code, CSA S6:19 in their adaption of MCFT. CSA S6:19 suggests methods to calculate the longitudinal strain more accurately when there is reinforcement on both tension and compression sides of members.

CHAPTER 3. CHALLENGES USING STM AND MCFT WITH LOAD RATING

3.1 STRUT AND TIE MODELING IN LOAD RATING

3.1.1 Crack Control Reinforcement

The AASHTO LRFD Bridge Design Specifications, since their inception in 1994, prescribed the use of 0.3 percent crack control reinforcement in elements designed by using the Strut and Tie Modeling (STM) provisions. With that stated, and with many difficulties encountered in the application of STM in bridge design, nonbinding STM provisions were recently revised in 2017. However, the use of 0.3 percent minimum crack control reinforcement remains unchanged in the current provisions similar to the legacy provisions they replaced. The new STM provisions are primarily based on research completed at the University of Texas at Austin (Birrcher et al. 2009; Williams et al. 2012; Larson et al. 2013).

A potential drawback of the new STM efficiency factors, as they were adopted in the binding provisions of AASHTO LRFD Bridge Design Specifications, 8th Edition (2017) (incorporated by reference at 23 CFR § 625.4(d)(1)(v)), arises in the application of the new STM provisions in evaluating the capacity of structural components in the existing inventory of bridges. If the 0.3 percent crack control reinforcement specification is met, high efficiency factors can be used in an STM. If the 0.3 percent minimum reinforcement is not met the efficiency factor drops down to 0.45.

3.1.1.1 Purpose of Crack Control Reinforcement

An examination of the University of Texas research (Birrcher et al. 2009; Williams et al. 2012; Larson et al. 2013) indicates that 0.3 percent crack control reinforcement serves two purposes: i. by allowing proper redistribution of internal stresses, it gives an assumed STM model a chance to materialize/develop at ultimate, in a fully "plastified" concrete element and ii. by restraining the widths of the cracks, should they form at service level loads. In a nutshell, the dual purpose of the crack control reinforcement is to satisfy "strength" and "serviceability." Decoupling objectives that relate to strength from those that relate to serviceability offers advantages in load rating. Many existing bridges do not comply with modern detailing standards.

3.1.2 Study of Existing Bridges and Their Crack Control Reinforcement Detailing

The research team studied the performance of the current STM provisions for bridge components that do not comply with the detailing standards as specified in the binding 8th Edition of the AASHTO LRFD Bridge Design Specifications. This objective is achieved by leveraging the findings of the recent research at the University of Texas (Zaborac et. al., 2020). Zaborac et al. (2020) used a deep beam database and a case study of an approximately 60-year-old recently decommissioned bent cap (Perez et al., 2019). This Guide benefits from the insights gained from the use of the University of Texas Deep Beam Database (UTDBD), for reinforcement details that do not comply with the binding 8th Edition of AASHTO LRFD Bridge Design Specifications (2017).

3.1.2.1 Database and Filtering

Tuchscherer et al. (2014) assembled the UTDBD that contains results from 868 deep beam shear tests ($a_v/d \leq 2.5$) from the literature (Clark 1951; Moody et al. 1954; Ferguson 1956; Morrow and Viest 1957; Chang and Kesler 1958; Watstein and Mathey 1958; de Cossio and Siess 1960; Van Den Berg 1962; Bresler and Scordelis 1963; Leonhardt and Walther 1964; de Paiva and Siess 1965; Krefeld and Thurston 1966b; a; Rajagopalan and Ferguson 1968; Ramakrishnan and Ananthanarayana 1968; Kong et al. 1970; Manuel et al. 1971; Kani et al. 1979; Smith and Vantsiotis 1982; Hara 1985; Hsuing and Frantz 1985; Rogowsky et al. 1986; Subedi et al. 1986; Ahmad and Lue 1987; Johnson and Ramirez 1989; Shioya 1989; Roller and Russel 1990; Bažant and Kazemi 1991; Sarsam and Al-Musawi 1992; Walraven and Lehwalter 1994; Xie et al. 1994; Tan et al. 1995, 1997a; b; Yoon et al. 1996; Foster and Golbert 1998; Furuuchi et al. 1998; Kong and Rangan 1998; Stanik 1998; Angelakos 1999; Ozcebe et al. 1999; Shin et al. 1999; Tan and Lu 1999; Vecchio 2000; Yoshida 2000; Angelakos et al. 2001; Cao 2001; Ghoneim 2001; Oh and Shin 2001; Matsuo et al. 2002; Rigotti 2002; Uzel 2003; Yang et al. 2003; Tanimura and Sato 2005; Brown et al. 2006b; Quintero-Febres et al. 2006; Zhang and Tan 2007; Alcocer and Uribe 2008; Hassan et al. 2008). Further University of Texas researchers contributed results from their 37 full-scale bent cap specimen tests (Tuchscherer et al. 2010, 2011; Birrcher et al. 2013, 2014), to the UTDBD. Tuchscherer et al. (2014) referred to this collection of 905 tests as the "collection database," and performed two stages of filtering which resulted in an "evaluation database" that they used to develop the new STM provisions used in designing new bridges. Zaborac et. al (2020) have recently performed a very similar filtering exercise to study the performance of the current AASHTO LRFD STM provisions for deep beams which do not meet the crack control provisions of Article 5.8.2.6 (AASHTO 2017).

Following Tuchscherer et al. (2014), many test results were removed because there was not enough information to develop a STM. Furthermore, many specimens were filtered out due to their small-scale or unrealistic material strengths. To reduce discrepancies between deep beam and sectional shear-strength predictions, specimens with shear-span-to-depth ratios (a_v/d) larger than 2.0 were also filtered from the present investigation, because their behavior is typically modeled more accurately with sectional shear methods (Tuchscherer et al. 2016). Lastly, specimens that were detailed in accordance with current AASHTO provisions (2020) were removed. These filtering criteria resulted in an evaluation database of 253 deep beam shear tests which are realistically scaled and violate modern crack control reinforcement detailing practices, as shown in **Table 1**.

Table 1. Database Filtering (Adapted from Zaborac et al., 2020)[3]

Filtering criteria	Tests
Total tests	905
Incomplete plate size info	-284
Subjected to uniform loading	-7
Stub column failure	-3
f'_c < 2.0 ksi	-4
b_w < 4.5 in.	-220
$b_w d$ < 100 in^2	-75
d < 12 in.	-13
a_v/d > 2.00	-24
AASHTO compliant crack control*	-22
Evaluation Database	253

*$\rho_v \geq 0.003$, $\rho_h \geq 0.003$, and $s <$ min (d/4, 300 mm)

The aforementioned violations can be violation of maximum reinforcement spacing specifications and/or quantity of crack control reinforcement in the vertical or horizontal directions. The following overall attributes of the database are important to note:

- A majority of the 253 deep beam tests were conducted on specimens shallower than 40 inches.
- Nearly all of the tests were conducted on specimens fabricated with concrete with $f_c' <$ 7.5 ksi.

3.1.2.2 Assessing Performance without Minimum Crack Control Reinforcement

The newly assembled/filtered evaluation database was used to assess the performance of current STM provisions for estimating the capacity of existing structures with insufficient crack control reinforcement. To assess the predictive performance of the AASHTO LRFD STM provisions for members which violate the crack control provisions, a STM was developed for each of the 253 beams in the evaluation database. Furthermore, six methods for determining the appropriate nodal efficiency factors were investigated. Zaborac et. al (2020) used $\rho_\perp$ (Equation 4) originally proposed by Brown et al. (2006a)

$$\rho_\perp = \rho_v \cos\theta + \rho_h \sin\theta \geq \rho_{\perp,min} = \frac{v f_c' A_c \sin\theta}{f_y b d k} \qquad \text{Equation 4}$$

where $\rho_\perp$ is the perpendicular reinforcement ratio, ρ_v is the vertical reinforcement ratio, ρ_h is the horizontal reinforcement ratio, θ is the inclination of the strut, v is the concrete efficiency factor, f'_c is the specified compressive strength of concrete, A_c is the minimum cross-sectional area of the strut, f_y is the yield strength of the web reinforcement, b is the beam width, d is the beam effective depth, and k is the slope of the dispersion of compression. The slope of the dispersion

[3] Reprinted from Engineering Structures, Volume 218, Zaborac, J., Choi, J., Bayrak, O., Assessment of deep beams with inadequate web reinforcement using strut-and-tie models, 16, 2020, with permission from Elsevier.

of compression is traditionally taken as 2:1 (AASHTO 2017). It is important to note that as the strut inclination (θ) changes, the contribution of horizontal (skin) and vertical (shear) reinforcement to $\rho_{\perp}$ changes. This fact offers a benefit to load rating existing structures since different contributions from horizontal and vertical reinforcement will help meet the $\rho_{\perp}$ limit, as discussed later in this Guide.

The average estimated value of minimum perpendicular reinforcement for the 253 specimens in the database was 0.14 percent. A perpendicular reinforcement ratio of 0.15 percent corresponds to an approximately 66 percent reduction, on average, in the amount of vertical and horizontal reinforcement specified by AASHTO LRFD 2017 (these provisions are binding per 23 CFR 625.4(d)(1)(v)) for strength and serviceability (approximately 0.1 percent each way compared to 0.3 percent each way).

The 253 specimens were evaluated using the minimum concrete efficiency factor, 0.45, and the concrete efficiency factor per AASHTO LRFD 2017 (these provisions are binding per 23 CFR 625.4(d)(1)(v)) Table 5.8.2.5.3a-1 (2017) for adequately detailed crack control reinforcement. **Figure 7** summarizes the results of these analyses, with the experimental-to-calculated-strength ratio on the vertical axis and various member properties on the horizontal ones.

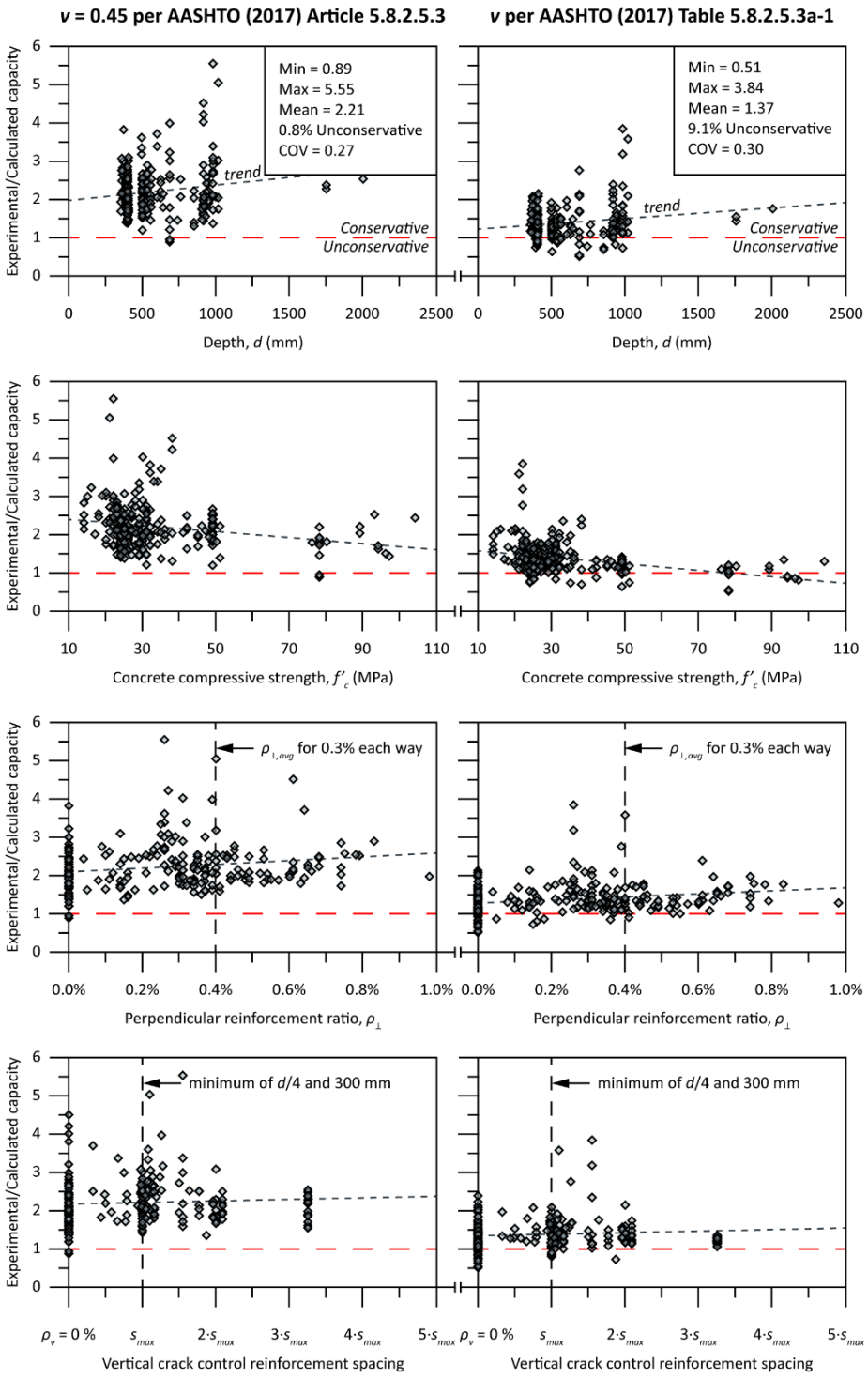

Figure 7. Comparison of results computed with minimum (left) and maximum (right) efficiency factors using evaluation database (N = 253) (Adapted from Zaborac et al., 2020). [4]

[4] Reprinted from Engineering Structures, Volume 218, Zaborac, J., Choi, J., Bayrak, O., Assessment of deep beams with inadequate web reinforcement using strut-and-tie models, 16, 2020, with permission from Elsevier.

Furthermore, there are long-dashed lines delineating the strength prediction ratios greater and less than 1, as well as short-dashed lines marking the general trends in the results. Lastly, there is a statistical summary provided in the upper right of each column of plots. The results computed with the minimum concrete efficiency factor are too low, with a mean experimental-to-calculated-strength ratio of 2.21 and a maximum value of 5.55. The results computed with the normal efficiency factors, on the other hand, have more desirable mean and maximum values (1.37 and 3.84, respectively) but suffer from an unacceptable increase in high strength predictions, from 0.8 to 9.1 percent.

3.1.3 Study Observations and Suggestions when Using STM for Load Rating

A detailed examination of database analyses reveals the following observations:

- The concrete efficiency factors per AASHTO LRFD Table 5.8.2.5.3a-1 (2017), for adequately detailed crack control reinforcement, can be used in evaluating the existing inventory of bridges for structural elements in which a minimum perpendicular reinforcement ratio of 0.2 percent is used (i.e., $\rho_{\perp,min} = 0.2$ percent). This is equivalent to a quantity of vertical and horizontal crack control reinforcement that is one-half of that suggested by the 8th Edition of AASHTO LRFD Specifications for new design. In this context, it is important to recall the dual intent (strength and serviceability) of the Specifications and the singular intent (strength) of the load rating.
- The selection of $\rho_{\perp,min} = 0.2$ percent was driven by the following facts: There are very few tests in which a perpendicular reinforcement ratio less than or equal to 0.2 percent is used. This is approximately 15 percent of the reinforced cases ($\rho_{\perp} > 0.0$ percent) in the database. In this slim population of tests (0.2 percent $> \rho_{\perp} > 0.0$ percent) 10 percent of the tests are predicted to be too high, by using the suggestion in item 1. Unacceptably high percentage of strength predictions coupled with the few tests available in this range, does not permit relaxing the $\rho_{\perp,min} = 0.2$ percent suggestion any lower.
- $\rho_{\perp,min} = 0.2$ percent can be met by being in compliance or violation of bar spacing rules of the binding AASHTO LRFD Bridge Design Specifications (2017). In other words, the database analyses do not highlight any discernable trends for cases in which the $\rho_{\perp,min} = 0.2$ percent was met by specimens with crack control reinforcement spacings out of compliance with the specifications. This observation is expected to provide some relief in load rating bridges that do not meet the maximum reinforcing bar spacing specifications.
- Serviceability performance of structures evaluated by using the suggestion described in item 1 should be checked separately. Depending on the exposure conditions and the local policies put forth by the bridge owners, different levels of service performance can be acceptable to different owners. For example, a 30-year-old substructure element exhibiting flexural and shear cracks with no visible signs of corrosion, is not likely to suffer from corrosion in the near future. Similarly, a 20-year-old substructure element with no visible signs of flexural or shear cracks is likely to perform similarly in the future. The examples given above, and others like them, can inform the inspection frequency and rigor, moving forward. Undoubtedly, acceptable crack widths and crack

distributions will vary depending on the environmental exposure conditions and presence of corrosive agents such as chlorides.

- In a case where the flexural reinforcement (i.e., primary longitudinal tie) is not in compliance with the minimum reinforcement specifications of AASHTO LRFD, the STM constructed for that substructure element will be controlled by the capacity of that tie. STM modeling does cover all aspects of conventional design in a convenient package where all aspects of shear, flexure and reinforcement anchorage are checked.
- It would be highly beneficial to test realistically sized specimens with 0.2 percent> $\rho_{\perp}$ > 0.0 percent. Some older bridges are likely to fall in this category and load rating those bridges would greatly benefit from this information.

3.2 USE OF MODIFIED COMPRESSION FIELD THEORY IN LOAD RATING

3.2.1 Evaluating Accuracy and Conservatism of MCFT with Shear Database

To investigate the accuracy and safety of sectional shear design procedures for prestressed concrete members, the University of Texas researchers assembled a database over the course of a decade. The first version of University of Texas Prestressed Concrete Shear Database (UTPCSDB) was compiled by Avendaño and Bayrak (2008) and it was expanded by Nakamura (2011). Subsequently, Nakamura et al. (2013) conducted a statistical evaluation of the currently available shear design procedures in various code provisions including ACI, AASHTO, CSA, Japan Society of Civil Engineers (JSCE), and *fib* using the most recent UTPCSDB. They concluded that MCFT-based procedures offered the most accurate and sufficiently safe strength estimation, for specimens that were in compliance with the detailing specifications of AASHTO LRFD (2010 and 2017). This finding is important in the context of shear load rating of bridges.

3.2.1.1 Study of MCFT with Non-Compliant Reinforcement Detailing

Choi et al. (2021) took a similar approach to Nakamura et al. (2013), albeit with an entirely different objective. With the ultimate goal of developing suggestions for estimating the shear strength of members that do not comply with required detailing specifications of AASHTO LRFD (2017), focus was directed to specimens that would inform the behavior of prestressed concrete beams with non-compliant details. This focus resulted in filtering out a great majority of 1696 tests in the UTPCSDB. 300 tests displaying shear failures without anchorage zone distress and/or horizontal shear failure informed the database analyses of Choi et al. (2021) and resulted in important conclusions. For context, the following attributes of the database are important to note:

- Overall member depth of all test specimens included in the database was less than 48 inches
- 266 of the 300 test specimens were fabricated with concrete with $f_c' \leq 9$ ksi. The remaining 34 specimens were fabricated with higher strength concrete with 9 ksi < f_c' < 15 ksi.

3.2.1.2 Simplified MCFT for Design

The current general shear design procedure of the nonbinding AASHTO LRFD (2020) has recently been revised and it is based on the simplified version of MCFT. The simplification was

necessary to eliminate an iterative process to calculate the shear capacity of the reinforced and prestressed concrete members, with the ultimate goal of expediting shear design. Importantly, the original MCFT-based shear design procedure is dependent on the applied loads (i.e., M_u ,V_u , and N_u) necessitating iterations in estimating the actual shear capacity of a member. To simplify MCFT, for the purposes of design, assumptions on the safe side were made. In using simplified MCFT for structural evaluation of existing inventory of bridges, this "design simplification" results in an unintended consequence of providing strength estimates that are low in some cases. In effect, the use of simplified MCFT expressions in load rating is somewhat inconsistent with the original intent of the simplification as further discussed below.

3.2.2 Load Rating Existing Bridges with MCFT

To estimate the shear capacity of existing pretensioned girders, iterations are necessary to establish consistency between the load effects and capacities (Choi et al. 2021, Caprani and Melhem 2019, Nakamura et al. 2013, and Hawkins et al. 2005). In addition, to calculate the structural capacity of a prestressed concrete member, anchorage distress and horizontal shear failure should be also checked in parallel, and the minimum among those should be the governing shear capacity. Considering the aforementioned failure modes, the structural capacity of a member can be calculated using a procedure described in the flowchart presented in **Figure 8**. It is essential to note that the process summarized in **Figure 8** takes into account the shear strength of the web, the horizontal shear strength of the web-to-bottom flange connection and the anchorage of the longitudinal tie.

3.2.2.1 Use Concurrent Force Effects

With respect to the use of MCFT, as shown in **Figure 8**, it is essential to use concurrent bending moments (M_u) and shear forces (V_u), in estimating the shear capacity. MCFT-based shear strength is a function of the loads imposing longitudinal (i.e., axial) strains on the element under consideration. Both bending moments (M_u) and shear forces (V_u), in addition to axial loads (N_u) and 'self-equilibrating-loads' due to pre- or post-tensioned strands influence the axial strain experienced by the member. This axial strain influences the shear strength as shown in **Figure 8**. Further, combining maximum bending moments from a load combination with shear forces from another load combination is both theoretically unjustified and produce strength estimates that are low and therefore is not suggested. The use of approximate structural analysis, live load distribution factors for bending moments and shear forces that were not intended to yield concurrent results will lead to low strength estimates, and therefore are not suggested for load rating. Taking an overly conservative approach can be justified as the first cut analysis and may produce satisfactory results in some cases. In other cases with challenging loading conditions, refined analyses may be necessary to obtain satisfactory load ratings. The methodology described in **Figure 8** is intended to outline the framework that can be used in assessing the structural capacity. The application of this framework to a range of practical problems is covered in later sections through examples.

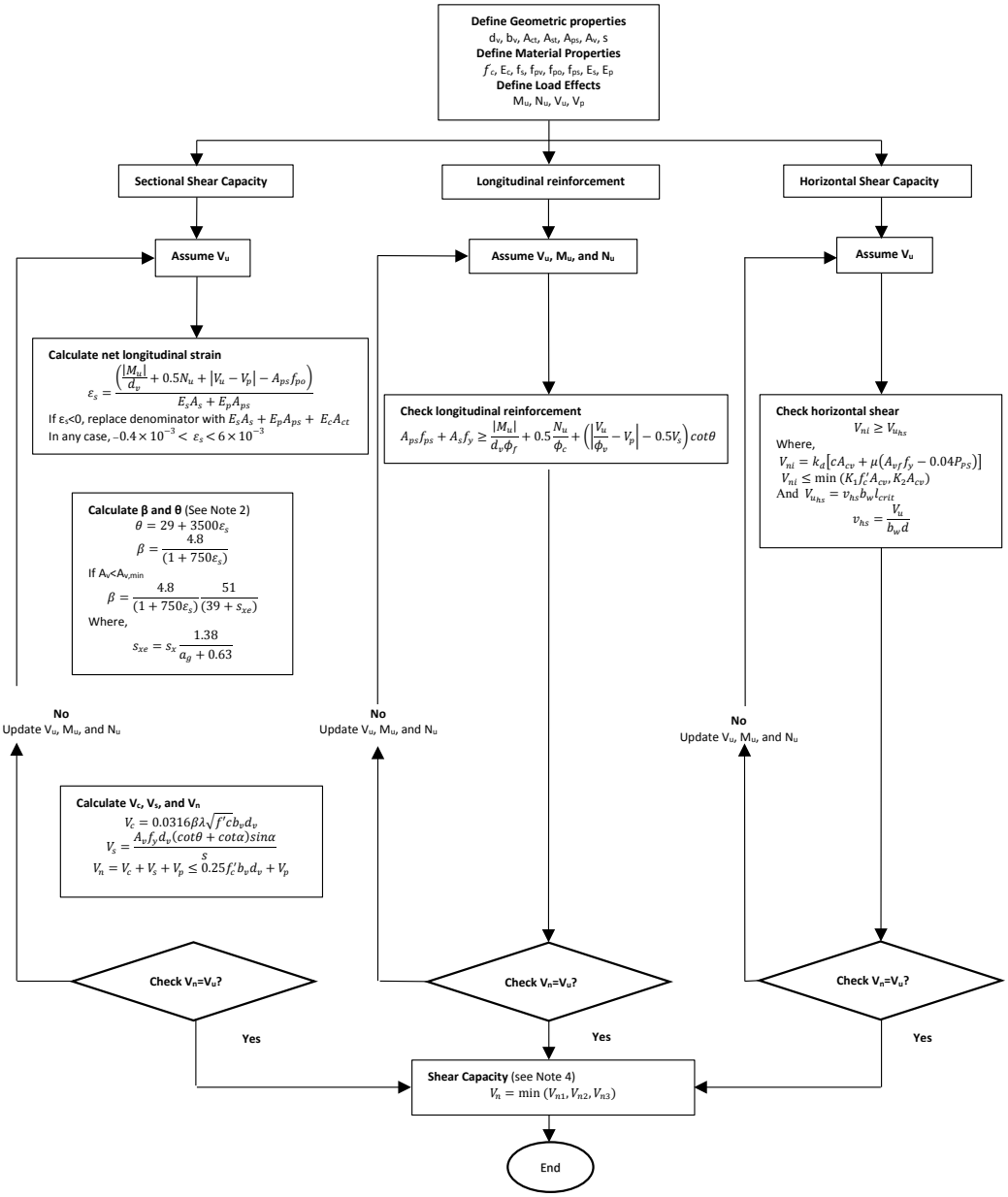

Note:

1. Use concurrent M_u and V_u in calculations.
2. Prestressing mitigates size effect, as shown in this document.
3. Longitudinal tie anchorage should be checked as per AASHTO LRFD (2017) in all cases.
4. V_{n1}, V_{n2}, and V_{n3} are shear capacity calculated by
   i. Sectional shear
   ii. Longitudinal tie anchorage, and
   iii. Horizontal shear, respectively
5. This flowchart is intended for use with the general procedure.
6. This flowchart can be used for reinforced and prestressed concrete members that may or may not meet the $A_{v,min}$ requirement of AASHTO LRFD.

Figure 8. Assessment of structural capacity of prestressed concrete members (Adapted from Choi et al. 2021)[5]

[5] Reprinted from Engineering Structures, Volume 242, Choi, J., Zaborac, J., Bayrak, O., Assessment of shear capacity of prestressed concrete members with insufficient web reinforcement using AASHTO LRFD general shear design method, 12, 2021, with permission from Elsevier.

3.2.3 Evaluating Members with Less Than Minimum Shear Reinforcement

The shear strength of reinforced and prestressed concrete members with insufficient web reinforcement typically decreases as the member depth increases, which is known as the size-effect in shear. To take this size effect into account in binding shear design provisions of AASHTO LRFD (2017), the β parameter is adjusted depending on the amount of web reinforcement provided in the section using the following equations

$$\beta = \frac{4.8}{(1+750\varepsilon_s)} \text{ if } A_v \geq A_{v,min} \quad \text{(Equation 5)}$$

$$\beta = \frac{4.8}{(1+750\varepsilon_s)} \frac{51}{(39+s_{xe})} \text{ if } A_v < A_{v,min} \quad \text{(Equation 6)}$$

where, s_{xe} is the crack spacing parameter as influenced by aggregate size;

$$s_{xe} = s_x \frac{1.38}{a_g + 0.63} \quad \text{(Equation 7)}$$

where, s_x is crack spacing parameter taken as the lesser of d_v and the maximum distance between layers of longitudinal crack control reinforcement, and a_g is the maximum aggregate size. Finally, the concrete contribution on the shear capacity can be obtained using Equation 8.

$$V_c = 0.0316\beta\lambda\sqrt{f_c'}\, b_v d_v, \text{ ksi} \quad \text{(Equation 8)}$$

Where, λ is concrete density modification factor, b_v is effective web width taken as the minimum web width within the shear depth d_v, and d_v is effective shear depth.

3.2.3.1 Database Evaluation

Results of the analyses performed in accordance with the procedure summarized in **Figure 8** are presented in **Figure 9**. The procedure shown in **Figure 8** safely neglects size effect, since prestressing force effectively mitigates this effect. In **Figure 8**, the plots on the left column, in each row, relate to calculations performed on test specimens with AASHTO-compliant details. This column serves to provide baseline information on statistical biases associated with MCFT-based sectional design procedure of AASHTO LRFD. Data reported in this column are not from the evaluation database (300 specimens) discussed above. Rather, this column includes other data from AASHTO-compliant test specimens. The middle column represents strict application of AASHTO LRFD sectional design provisions, as is. That is to say, appropriate β is calculated from Equation 6 for specimens with non-compliant AASHTO details and used in the calculations. The plots on the right column are based on calculation in which size effect, and the associated/reduced β calculation is neglected. Instead, β is calculated as if the minimum reinforcement specifications of AASHTO LRFD Bridge Design Specifications are met (Equation 5). The technical reason behind this is discussed further later in this document. In each plot a best-fit line in the form of $y = ax + b$ is drawn as a dotted line and the slope (a) is provided. A

zero slope would indicate no statistical bias for the parameter under consideration. An examination of **Figure 9** results in the following observations:

- AASHTO LRFD method has almost no statistical bias with respect to compressive strength of concrete: For specimens that are in full compliance with AASHTO LRFD, the accuracy and the overall safety of the calculations remains almost the same for all compressive strengths considered. The use of Equation 6 for prestressed concrete beams with non-compliant details introduces a bias. The low strength estimates obtained from the calculations resulting in augmented levels of safety increases with increasing compressive strengths. The use of Equation 5 reduces this bias significantly as can be observed with the slope of the trend line.

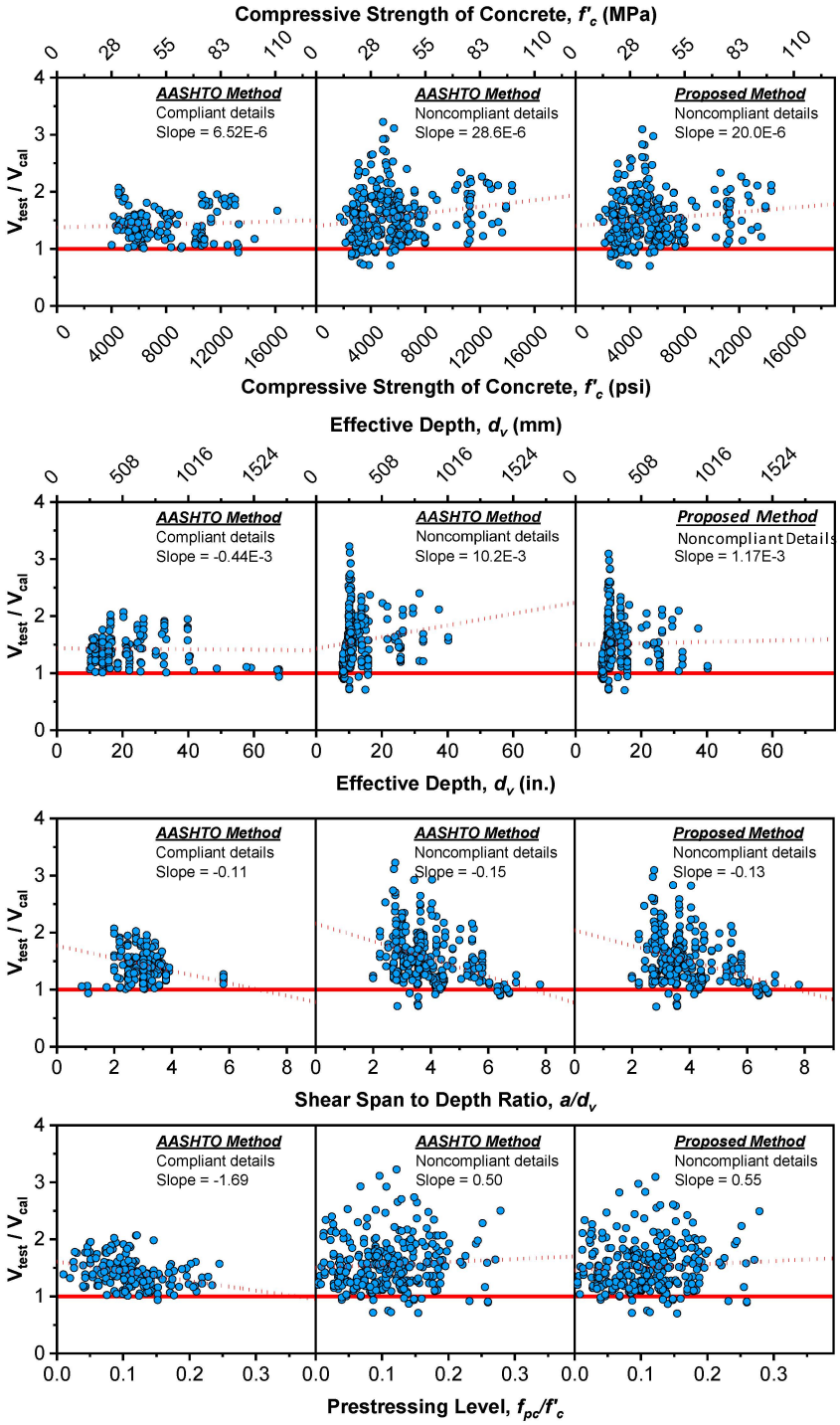

Figure 9. Influence on computed results (with/without size effect) of: (a) concrete compressive strength; (b) effective depth; (c) shear span-to-depth ratio; (d) prestress level (Adapted from Choi et al. 2021).[6]

[6] Reprinted from Engineering Structures, Volume 242, Choi, J., Zaborac, J., Bayrak, O., Assessment of shear capacity of prestressed concrete members with insufficient web reinforcement using AASHTO LRFD general shear design method, 12, 2021, with permission from Elsevier.

- MCFT-based sectional design provisions of AASHTO indicate no statistical bias with respect to specimen depth for Specimens with AASHTO-compliant details. This is not surprising since MCFT explicitly handles size effect and has a strong theoretical basis. The use of Equation 6 introduces a strong statistical bias with respect to member depth. Strength estimates for deeper beams become increasingly safer, on average. Use of Equation 5 removes this statistical bias almost entirely. Like the use of a "minimum quantity of transverse reinforcement" that clamps the shear cracks and mitigates size effect, a nominal quantity of prestressing force, provides a longitudinal clamping force and mitigates the size effect. This observation strongly supports using Equation 5 for calculating the shear strength of prestressed concrete beams with non-compliant details. By removing the statistical bias, and using MCFT with a strong theoretical basis, calculations made for members that are outside of the range of tests specimens considered herein, may also be justified.
- When the strength estimates are plotted against the shear span-to-depth ratio (a/d_v), a statistical bias is evident in all three sets of calculations. Focusing on specimens with AASHTO-compliant details, this bias can be explained by arching action that occurs for the short shear spans in the sectional shear range, an effect observed by Nakamura et al. (2013). With this theoretical background stated, it can be seen that the use of Equation 5 for specimens with non-compliant details brings the slope of the trend line closer to that observed for specimens with compliant details.

As the level of prestressing increases, the statistical bias that results from the use of Equation 5 is a little worse than that seen for Equation 6. This is viewed as a minor unintended consequence of using Equation 5 for all cases, in relation to major benefits discussed above.

3.2.3.2 Clamping Force from Prestressing

Minimum transverse reinforcement provisions of AASHTO LRFD, Equation 5.7.2.5-1, for concrete compressive strength of 5 ksi, would correspond to a quantity of reinforcement that provides a vertical clamping stress of about 70 psi (**Figure 10**). This magnitude of stress has been shown to mitigate the size effect and render the use of Equation 5 above appropriate. At the low end, the minimum level of prestressing included in the database evaluation discussed above is $f_{pc}/f_c' = 0.02$. For the same 5ksi compressive strength value discussed above, this would result in a longitudinal clamping stress (**Figure 10**) level of 100 psi. A typical shear crack in a prestressed concrete member would be about 27 to 32 degrees inclined from the horizontal axis. With this inclination, and by using simple equilibrium equations, it can be shown that the longitudinal clamping stress used to close a potential shear crack is higher than that for the vertical direction. As a result, the lower bound value of $f_{pc}/f_c' = 0.02$ seen in the database analysis is technically justified. Testing on realistically sized members out of compliance with minimum reinforcement provisions and with structural details that cover the common details, is suggested.

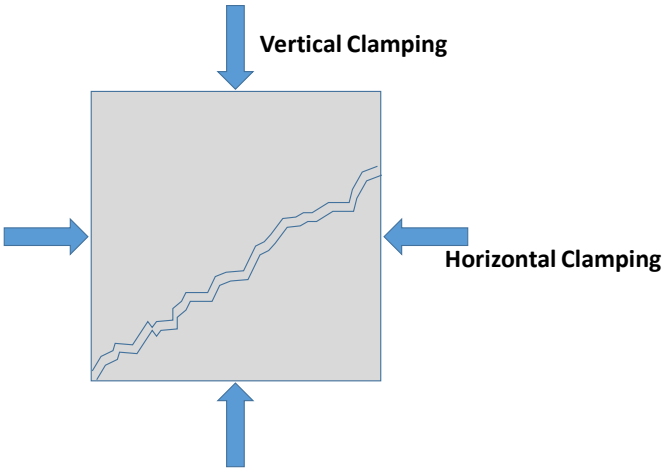

Source: Authors

Figure 10. Clamping forces acting on a typical shear crack.

3.2.4 Suggestions for Load Rating with MCFT

Based on the discussion above, the following important conclusions can be drawn:

3.2.4.1 Prestressed Concrete vs Minimum Shear Reinforcement

The prestressing force introduces a longitudinal clamping force on diagonal cracks, mitigating the size effect. This clamping force effectively qualifies all prestressed concrete beams (pretensioned and post-tensioned) as candidates for which Equation 5 can be used regardless of the quantity of transverse reinforcement.

3.2.4.2 Longitudinal Reinforcement Check

Longitudinal tie anchorage should be checked as per AASHTO LRFD (2017) in all cases, as shown in **Figure 8**. Regardless of meeting or not meeting the minimum shear reinforcement provisions, this check should be performed in accordance with Equations 5.7.3.5-1 and 5.7.3.5-2 of AASHTO LRFD Bridge Design Specifications. Failure to check longitudinal tie anchorage may result in over-estimation of structural capacity and therefore lead to unsafe load ratings of bridges.

3.2.4.3 Horizontal Shear Check

Horizontal shear failure should be checked when assessing the structural capacity of prestressed concrete beams, as shown in **Figure 8**, regardless of meeting or not meeting the minimum shear reinforcement specifications. For modern pretensioned girders with thin webs and large bottom flange widths, the capacity of the web-to-bottom flange interface may control the structural capacity. With that stated, for older bridges with pretensioned girders that are similar to standard AASHTO shapes, this failure mode is unlikely to govern the calculated structural capacity. However, for complete structural evaluation, all steps shown in **Figure 8** should be followed.

3.2.4.4 Iterations to Determine Shear Strength

To estimate the actual shear capacity of existing pretensioned girders, iterations are necessary to establish consistency between the load effects and capacities (Choi et al. 2021, Caprani and

Melhem 2019, Nakamura et al. 2013 and Hawkins et al. 2005). Both the design provisions for the general procedure of Section 5 of AASHTO LRFD Specifications and the original MCFT procedure described in Appendix B5 of the Specifications should be used in an iterative manner to evaluate the structural capacity of a member.

3.2.4.5 Considerations with Reinforced Concrete Members

Below a certain level of prestressing force, a prestressed concrete element effectively behaves as a reinforced concrete element. Equation 6 should be used if $A_v < A_{v,min}$ and $f_{pc} < 0.02f_c'$.

For reinforced concrete elements being evaluated by using MCFT, which is outside of the scope of the database analyses discussed herein, the size effect should be taken into account properly. Previous research over decades at the University of Toronto, University of Texas and elsewhere point to the presence of size effect. As a result, for reinforced concrete members with web reinforcement less than the minimum ($A_v < A_{v,min}$), Equation 6 should be used to calculate β. In other cases where the minimum specifications are met, Equation 5 should be used to calculate β since size effect is effectively mitigated by using a minimum quantity of web reinforcement.

3.2.4.6 Other Observations

The overall depth of the largest specimen that informed the database analyses is 44 inches. As can be observed in **Figure 9**, there are few specimens with effective depths greater than 30 inches that inform the conclusions/observations discussed in 3.2.4.1 through 3.2.4.5 above. Additional experiments conducted on prestressed concrete girders with effective depths greater than 30 inches, and with details that represent the older inventory of bridges, can prove to be very beneficial in confirming the findings reported herein –or expanding the range of applicability of these findings. The conclusions have been validated for members that are shallower than 4-ft. (i.e., 44 inches plus clear cover).

If the prestressed concrete element under consideration is not in compliance with the minimum longitudinal reinforcement specifications of AASHTO LRFD, it is highly likely that the shear strength of such a beam should not control the structural capacity. In such cases the inadequate flexural capacity ends up being a major concern. The shear strength of a member that fails to comply with both minimum and flexural and shear strength AASHTO specifications should be evaluated for both limit states. The procedures discussed within this Guide address the checks that relate to shear strength. In this context, it is important to recognize that AASHTO minimum flexural reinforcement has recently been examined by Sritharan et al. (2019).

CHAPTER 4. APPLICATION OF MCFT WITH LRFR

4.1 LOAD RATING CONCRETE IN SHEAR WITH LRFR

4.1.1 General

Some owners have their own requirements for when to load rate concrete elements in shear. Load raters should consult the bridge owner for any specific load rating requirements or limitations that supersede or complement the nonbinding AASHTO MBE. In accordance with the AASHTO MBE Article 6A.5.8 (nonbinding), a shear load rating should be performed for permit loads, and for design and legal loads if the member is displaying shear distress. **Figure 11** depicts a prestressed girder end with shear cracking; this would be a candidate for shear load rating. This girder end can still be load rated with MCFT, but the amount of web-shear cracking indicates that the concrete contribution to shear strength, V_c, has been exceeded. The angle of diagonal compression, θ, can be measured directly from the observed cracking. STM could also be used to evaluate this girder end. Repair may be warranted in cases such as these.

Source: Kenneth Ozuna

Figure 11. Shear cracks in a prestressed I-girder).

The AASHTO MBE suggests that load rating substructure is optional but the owner may desire a load rating if there is reason to believe it may govern the capacity of the bridge. For many substructure elements, such as deep beams or pile caps with small a/d_v ratios and large concentrated forces, Strut and Tie Modeling (STM) would be a better procedure for determining

a load rating. **Figure 12** shows a deep beam straddle bent with a large, concentrated reaction from a two-girder superstructure near the support with observed shear cracks.

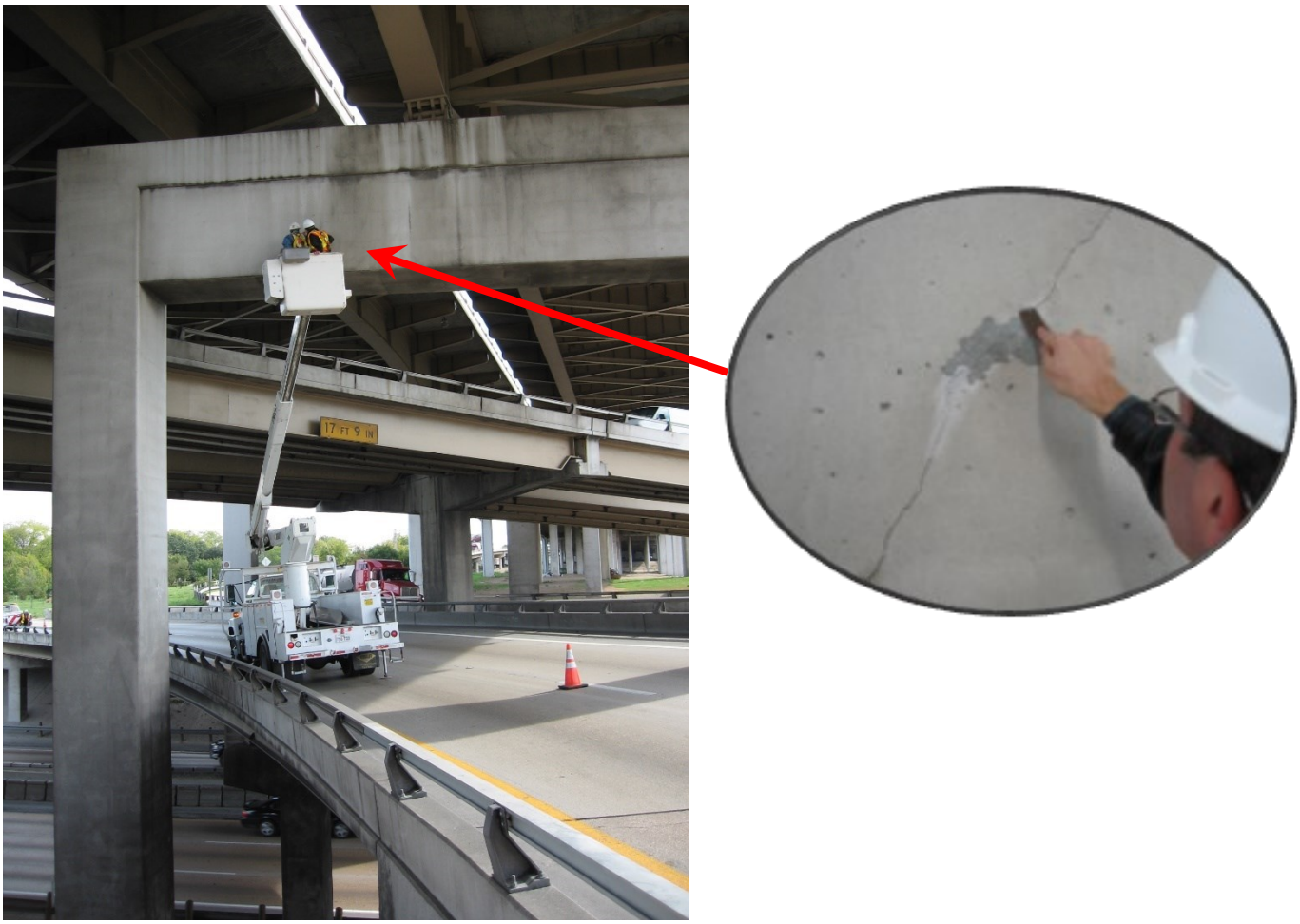

Source: Authors

Figure 12. Crack mapping and measuring shear crack width on straddle bent cap.

Load rating concrete in shear with LRFR is at the strength limit state for design, legal, and permit loads. The relevant load combinations and live load factors are provided in MBE Table 6A.4.2.2-1.

Segmental bridges are treated separately by the AASHTO MBE; per Article 6A.5.11.7, shear should be considered in load ratings for design, legal and permit loads regardless of condition.

4.1.2 Understanding Strain Leads to Focus Areas

As noted previously, the type and magnitude of strain at the member mid-depth is critical in evaluating shear strength with MCFT. Increasing tensile strain decreases shear strength; compressive strain benefits shear strength. Increasing amounts of tensile strain reduces the ability of the concrete to transmit shear between cracks (reflected in the factor, β) and increases the angle of diagonal cracking, θ, (measured from the longitudinal axis of the member) which

diminishes the strength contribution of shear reinforcement. **Figure 13** contrasts the differences between smaller and larger mid-depth tensile strain and the angle of diagonal cracking. Compressive strain, or even zero strain, at member mid-depth—often encountered with prestressed concrete—greatly improves the situation, with large values of β and low values of θ. In short, prestressed concrete out-performs reinforced concrete in shear strength due to a much more favorable state of strain at member mid-depth.

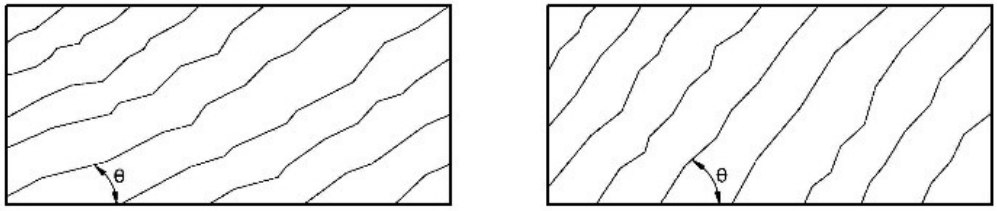

Source: Authors

Figure 13. Low θ/High β (left) vs High θ/Low β (right).

The MBE notes that not all cracking is from gravity loads; cracking can result from other sources such as a response to restraint from thermal forces. A locked-up bearing is an example of a condition that can result in large amounts of tension in a concrete superstructure. Likewise, compression introduced into a concrete element generally improves shear strength. A distinct advantage of MCFT over other shear strength methodologies is it directly addresses axial tension or compression in determining shear strength.

Since strain type and magnitude affect shear strength, areas of high moment, sources of direct tension, and the presence and size of cracking should be carefully considered when determining members and sections to evaluate for a shear load rating. They also point to expectations on shear strength, with prestressed concrete outperforming reinforced concrete.

For a concrete shear load rating to be as accurate as possible, it is important that the load rater is made aware of the type, size, and location of potential cracks in a concrete member. The source of the cracking is also useful information, but identifying the source is not always straightforward. Cracking in reinforced concrete from gravity loads is not uncommon, but it is with prestressed concrete. The ends of prestressed elements may display cracking from prestress transfer or anchorage zone stresses; these should not be confused with shear cracks. In pretensioned girders, these cracks begin at member ends and generally run diagonally from the top downwards toward the span or horizontally. See **Figure 14** for an example of cracking from prestress transfer. All cracks should be identified in an inspection report (crack widths, angle to the member if inclined, length and location along the member), and the load rater should evaluate their source and their impact on load rating. With the angle of inclined shear cracks known from observation and measurement, this can inform the load rater of the angle of diagonal compression, θ, to use in determining the V_s component of shear strength.

Source: Authors

Figure 14. Example of cracking related to prestress transfer.

4.1.3 Consideration of Year Built

Older bridges that were built during eras with less conservative amounts of shear reinforcement when compared to modern practice or did not address the influence of longitudinal reinforcement on shear capacity should be considered for design and legal load rating in addition to permit load rating. With potentially few stirrups to intercept a shear crack, the assumption that the lack of concrete cracking under service loads translates to acceptable levels of safety may be incorrect..

4.2 CROSS SECTION DIMENSIONS

4.2.1 Effective Shear Width

Member depth and width resisting shear is specified in AASHTO LRFD Article 5.7.2.8. (binding). AASHTO LRFD describes the effective web width, b_v, as the least width of the section between the tensile and compressive forces due to flexure, modified for the presence of any ungrouted ducts. The full ungrouted duct diameter is deducted from the section width in which it is located. If the ducts are grouted, no deduction in web width is taken. Current binding and past AASHTO LRFD suggest either one-half or one-fourth of a grouted duct diameter to be

deducted from the gross web width to obtain b_v. As more bridges are built with ungrouted tendons, incorporating the resulting web width reduction will be encountered more frequently in those States that implement ungrouted tendons.

In Chapter 5, which provides shear load rating examples, the duct size(s) was not specified in the as-built plans for the two-span continuous post-tensioned box girder (see Section 5.4). Had these tendons been ungrouted, shop drawings for the prestressing would be needed to account for duct size. Lacking those, field measurements may provide the duct size. The example in Section 5.4 uses the 8th Edition of LRFD when determining the effects of the duct on effective shear width and assumed the duct diameter to be 4 inches.

4.2.2 Effective Shear Depth

AASHTO LRFD describes the effective section depth resisting shear, d_v, as the distance between the resultants of the tensile and compressive forces due to flexure. AASHTO LRFD notes d_v need not be taken less than either $0.72h$ or $0.9d_e$, where h is total member depth and d_e is the depth to the center of gravity of tension reinforcing per AASHTO LRFD Equation 5.7.2.8-2 (binding). These limits will likely control for many continuous post-tensioned superstructures where the centroid of the tendon(s) is at approximate member mid-depth, as encountered near inflection points.

Only modest gains in strength are likely gained by refining d_v beyond the lower bound limits noted above, especially in precast member end regions with prestressed strand debonding or harping. If the load rating is very marginally low, a more refined d_v is suggested.

4.3 CRITICAL SECTIONS

Knowing the effects of mid-depth tensile strain, member regions subject to high shear, and especially those combined with high moment, are obvious critical locations that should be evaluated in shear. These locations are often near member supports.

4.3.1 Sections Near Supports

At member ends/supports, AASHTO LRFD identifies two potential critical sections—one is at the face of the support and the other is located d_v from the face of support. The further the critical section is from the face of the support, the lower the applied shear force in the rating equation.

AASHTO LRFD Article 5.7.3.2 (binding) allows the shear critical section to be located a distance d_v from the face of the support when the support reaction, in the direction of the applied shear, introduces compression into the member end region. This is permitted even when a concentrated load is located between the face of the support and a distance d_v from that support—when the reaction introduces compression into the member end region, which is a common situation for many superstructures with supports underneath the members and the members are top-loaded. Concentrated loads closer than dv directly strut into the support, as would be revealed in an STM.

If the supports do not introduce compression into the member end region in the direction of the applied shear, and there is a concentrated load between the face of support and d_v from the

support, as encountered with the applied loading below the top of the member such as an inverted tee cap beam, the shear critical section is to be taken at the face of the support. See **Figure 15** for an example of this condition.

Source: Authors

Figure 15. Example where support reactions do not introduce compression into the pier cap end regions in the direction of applied shear.

If there is any geometric, structural or load complexity to the member end region, an STM is a useful approach to ascertain the shear capacity. It is important to know that AASHTO LRFD Article 5.7.3.2 (binding) lowers the allowable shear stress from $0.25f'_c$ to $0.18\,f'_c$ when the member end is not built integrally with the support. This can be an issue with thin-webbed prestressed girders coupled with large, heavily prestressed flanges. This reduction can be avoided if an STM approach is employed to determine the strength of these end regions.

4.3.2 Other Points of Interest

AASHTO MBE Commentary C6A.5.8 notes that multiple sections should be evaluated for shear and suggests that be done at every 0.05L point along the span. For many concrete superstructures, 0.05L points will be relatively close to the superstructure depth. But span 20th

points could be excessive for a pier cap where the spans are typically short, so engineering judgment should be used in determining an appropriate interval. A common span location of interest is at the span quarter point as both the shear and moment are relatively large; evaluating shear at this point is suggested. Other points of interest include:

- regions adjacent to interior supports of simple span prestressed girders made continuous for live load
- locations at cross section changes (shear reinforcement spacing changes, locations near longitudinal bar terminations
- inflection regions of continuous girders where post-tensioning tendons are located near member mid-depth
- variable depth pier sections where the sloping component of the bottom flange contributes to shear demand, as illustrated in **Figure 16**
- any region of geometric, structural, or load complexity; these locations usually should be addressed with STM

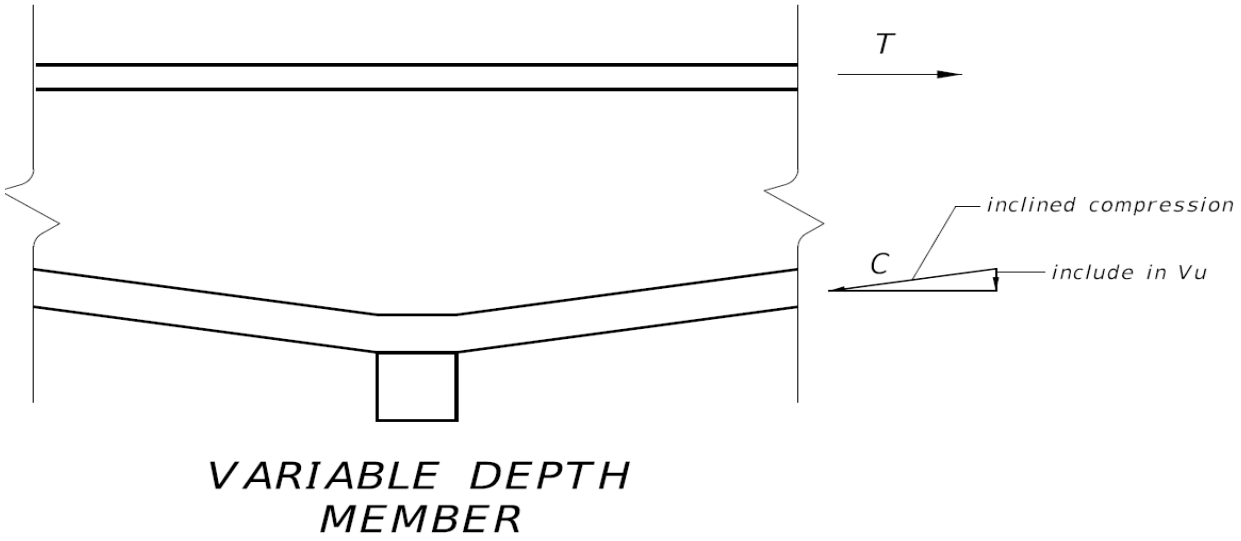

Source: Authors

Figure 16. Accounting for the vertical component of flange compression force with shear reinforcement.

4.3.3 Reinforcement Details and Anchorage

The as-built plans may indicate shear reinforcement, but the load rater should evaluate the details of the provided reinforcement to determine if the yield strength of the stirrup legs can be achieved. Shear reinforcement can be fully utilized up to its yield strength on the resistance side only if it is detailed to have adequate end anchorage, as specified in AASHTO LRFD Article 5.10.8.2.6. (binding). Just because a stirrup is provided does not mean it was adequately detailed to achieve full strength.

Engineering judgment should be applied when the stirrup detailing does not meet current specifications. In one instance, research demonstrated the adequacy of stirrup anchorage for a particular State DOT's prestressed beam details that do not meet current specification provisions (Mathys et al. 2014).

In Chapter 5, the as-built plans for the example load rating for the simple span prestressed girder indicates 90-degree hooks at the bottom of the vertical legs. These hooks are turned in-line with the prestressing strand and not hooked under the strands. Such a detail facilitates pretensioned girder fabrication but does not meet the AASHTO LRFD specifications for shear reinforcement anchorage. Load rating often involves application of engineering judgment and this is a good example. In the load rating example, the stirrups are assumed to be properly detailed to achieve yield.

Welded wire reinforcement (WWR) is often used for shear reinforcement. AASHTO LRFD specifications allow WWR legs to be fully developed without being hooked around longitudinal reinforcement. AASHTO LRFD Article 5.10.8.2.6c prescribes anchorage for WWR reinforcement.

Very deep members and some precast members will sometimes have stirrups comprised of two U-shapes that are lapped. AASHTO LRFD Article 5.10.8.2.6d lists minimum lap lengths for stirrups constructed in this manner.

4.3.4 Minimum Shear Reinforcement

The factor, β, for the concrete contribution to shear strength, V_c, is a function of whether the minimum shear reinforcement limits noted in Article 5.7.2.5 (binding) are met. As noted in Chapter 3, if the member is prestressed, meeting the minimum shear reinforcement limits of Article 5.7.2.5 (binding) may be waived in terms of β; Equation 5.7.3.4.2-1 for β can be used for prestressed concrete members regardless of satisfying Equation 5.7.2.5-1. This exception applies to prestressed concrete only—for all reinforced concrete members. Equation 5.7.3.4.2-2 should to be used in determining β if the minimum shear reinforcement limits of Article 5.7.2.5 is not met.

4.4 LOAD RATING EXPEDIENTS

Before initiating more complicated load rating calculations, and if the owner agrees, the load rater can perform an initial screening to see if the load rating is acceptable. These initial screenings will indicate a conservative shear strength but not necessarily establish the highest potential shear strength.

4.4.1 Simplified Procedure

The simplified procedure for nonprestressed sections in AASHTO LRFD Article 5.7.3.4.1 may be used to determine a shear strength using the equations for V_c and V_s that were widely used in the past. That procedure does not use an iterative approach. For design purposes, this equation is restricted to nonprestressed sections but can be used for prestressed sections for load rating as it will generally provide a quite conservative strength estimate for a prestressed section.

4.4.2 Use of Alternative Shear Design Procedure

For prestressed concrete members, the Alternative Shear Design Procedures for segmental bridges listed in AASHTO LRFD Article 5.12.5.3.8 (binding) can provide a quickly calculated shear strength. The superstructure does not have to be a segmental span for use of this procedure. However, note that if the section was not prestressed, the equations result in the same V_c and V_s as in the Simplified Procedure for nonprestressed sections.

4.4.3 Use of General Procedure, Design Approach

As will be outlined in the next section, and as shown in **Figure 8** in Chapter 3, an iterative approach is used to determine the actual shear strength for a given moment and shear combination. This is different from when designing with the General Procedure in AASHTO LRFD Article 5.7.3.4.2 (binding), where no iterations are used to determine a satisfactory shear design.

However, a load rater can treat the load rating problem as if it were a design problem. While using the General Procedure in the normal design approach, if the specified A_v/s is less than the provided A_v/s for the member in question, the member provides adequate strength. In this way, the designer knows the provided design is safe. Hence, this method will indicate if the member is safe but will not provide the peak member shear strength. The iterative approach in the next section is used to determine the strength for use in the rating factor equation.

4.4.4 Other Checks

The longitudinal reinforcement adequacy is still verified per the process in **Figure 8** when using these expedients. The horizontal shear may warrant an evaluation, too, as discussed in Section 4.7.

4.5 SHEAR STRENGTH, GENERAL PROCEDURE

The nominal shear resistance is the summation of the concrete contribution V_c, the reinforcement contribution V_s, and the prestressing contribution V_p (if present). There is a limiting value on nominal shear strength of 25 percent of the concrete strength times the effective shear area plus the prestressing contribution. This limit is higher than used in past practice so is unlikely to be an issue when load rating older bridges. Note that this limit is lowered to 18 percent of the concrete strength times the effective shear area when the member end is not built integrally with the support (reference AASHTO LRFD Article 5.7.3.2). **Figure 17** provides the shear load rating process with the General Method in a flow chart, as previously shown in **Figure 8**.

A more detailed procedure with MCFT is listed in AASHTO LRFD Appendix B5. Its use is suggested if a shear load rating is marginally low but using it does not guarantee a noticeable improvement in strength.

Many texts already describe each of the shear strength components in detail. This Guide provides a high-level view of each component to assist with a general understanding of each component's effect on the nominal shear strength.

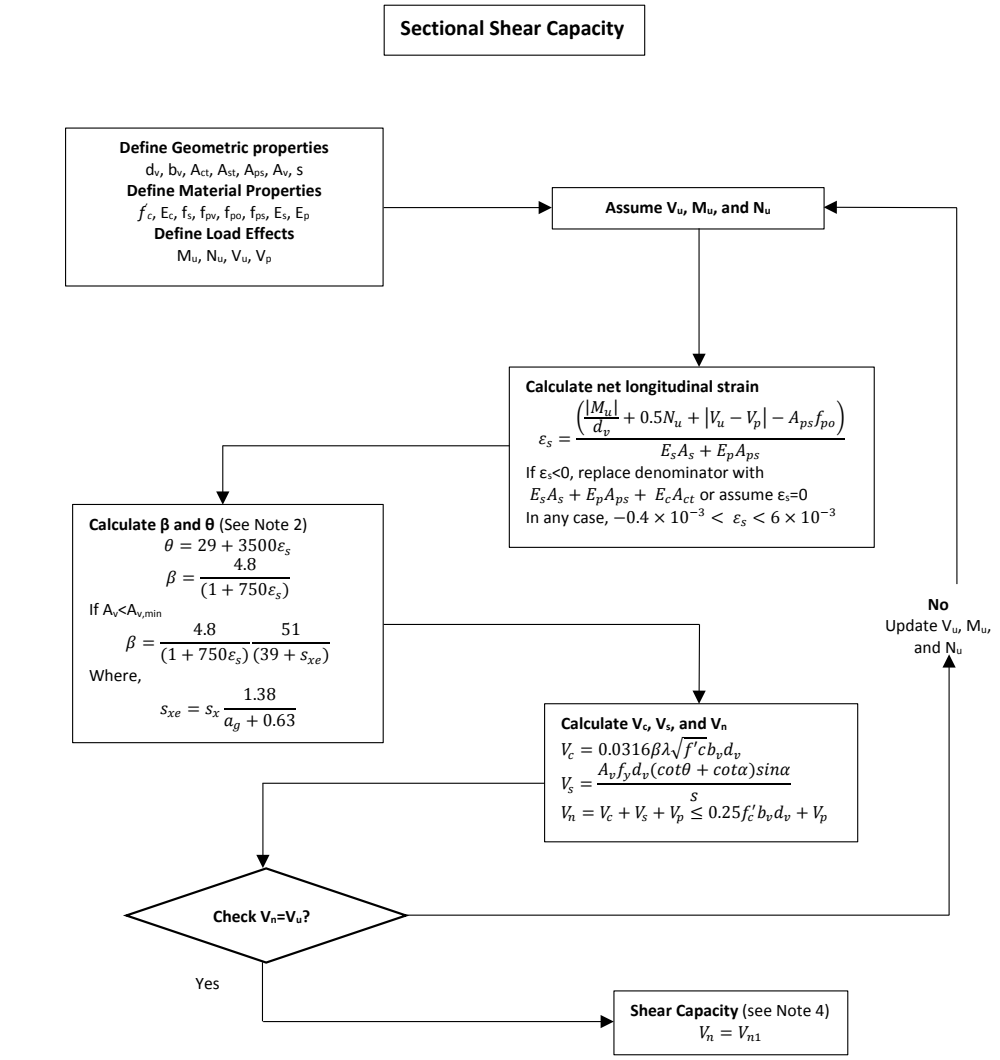

Note:

1. Use concurrent M_u and V_u in calculations.
2. Prestressing mitigates size effect, as shown in this document. Check for minimum reinforcement is therefore not required with prestressed members.
3. Longitudinal tie anchorage should be checked as per AASHTO LRFD (2017) in all cases.
4. V_{n1}, V_{n2}, and V_{n3} are shear capacity calculated by
   i. Sectional shear
   ii. Longitudinal tie anchorage, and
   iii. Horizontal shear, respectively
5. This flowchart is intended for use with the general procedure.
6. This flowchart can be used for reinforced and prestressed concrete members that may or may not meet the $A_{v,min}$ requirement of AASHTO LRFD.

Source: Authors

Figure 17. Flow chart for sectional shear using the general method.

4.5.1 Strain in Tension Reinforcement, ε_s

The first step is to calculate the strain at the centroid of the tensile reinforcement arising from the applied sectional forces V_u, M_u and N_u (if present). This strain will then be used to determine the

inclination of shear cracks, θ, and the factor, β, which are used in determining V_s and V_c, respectively. It is important to use concurrent factored force effects from discrete positions of live load. Using the maximum M_u and V_u values at a given point of interest, or from different live load positions, when determining strain may be unnecessarily conservative.

The strain at member mid-depth is the important value with MCFT. However, AASHTO LRFD Equation 5.7.3.4.2-4 (binding) generates the strain at the tensile reinforcement centroid and a simplifying assumption that the mid-depth strain is one-half the tensile reinforcement strain is made internally in the equations for the factors β and θ (AASHTO LRFD Equations 5.7.3.4.2-1 and 5.7.3.4.2-2).

AASHTO LRFD Equation 5.7.3.4.2-4 assumes the section is cracked. If the strain provided by this calculation is negative or if a separate calculation shows the section to be uncracked under the Strength Load combination, the load rater should assume the strain to be zero, or can go one step further by including the axial stiffness of the concrete in the flexural tension half of the member in the strain equation.

If using the General Procedure in AASHTO LRFD Appendix B5 (binding), the equations for strain are similar, but directly take one-half the strain in the tension reinforcement to obtain the mid-depth strain, $\varepsilon_{x.}$ Again, with MCFT, the strain at mid-depth is the goal. This is important because for some situations there are sources of beneficial strain—compressive strain—not accounted for in the strain equations for either General Method. AASHTO LRFD Commentary CB5.2 suggests that Equation CB5.2-1 be used in these cases to determine the mid-depth strain. The Commentary notes an example of where this would be useful is the ends of prestressed girders made continuous for live load, where the prestressing is largely in the flexural compression half of the member. Neglecting the beneficial compressive strain resulting from prestressing is overly conservative.

Determining mid-depth strain for continuous post-tensioned girders where the center of gravity of the tendons is at member mid-depth, sometimes even on the flexural compressive half of the member, may be a challenge when directly using the strain equations in AASHTO LRFD. The strain equations tend to neglect these tendons as they are not on the flexural tension half, which would be overly conservative. Another way to address these regions is to first calculate if the girder is cracked under the appropriate Strength Load combination using AASHTO LRFD Equation 5.6.3.3-1 (binding). The load rater may find in most, if not all cases, the section is not cracked as the post-tensioning provides large amounts of mid-depth compressive strain at flexural inflection points and the factored moments are very low. If this calculation indicates the section is uncracked, the load rater can assume the strain ε_s equals zero and proceed with calculating the factor β and the inclination of the shear cracks, θ. If this simple method does not work and the load rating is unsatisfactory, refined methods of determining mid-depth strain are warranted.

Note that if the load rater directly calculates a mid-depth strain and wishes to use Equations 5.7.3.4.2-1 through 5.7.3.4.2-3, the mid-depth strain is to be doubled to obtain an equivalent

strain at the level of the tension reinforcing, to be consistent with assumptions made in these equations.

4.5.2 Factor, β, and Inclination of Diagonal Cracks, θ

After determining ε_s, the factors β and θ can be determined. The β factor reflects the concrete's ability to carry tension between shear cracks. Two equations are provided, one if the minimum reinforcement limits of AASHTO LRFD Article 5.7.2.5 (binding) are met (Equation 5.7.3.4-1) (binding) and another if not met (Equation 5.7.3.4-2)(binding). Equation 5.7.3.4.2-2 (binding) lowers β to account for larger and more widely spaced cracks. Research conducted for this Guide and described in Chapter 3 indicates that with a prestressed section that does not meet the minimum shear reinforcement limit, it is appropriate to use AASHTO LRFD Equation 5.7.3.4.2-1 (minimum shear reinforcement met) (binding). This benefit is restricted to prestressed sections and not allowed with reinforced concrete where AASHTO LRFD Equation 5.7.3.4.2-2 (binding) is to be used for β if the section does not meet the minimum shear reinforcement limit. This equation lowers β to account for larger and more widely spaced cracks.

AASHTO LRFD Equation 5.7.3.4.1-3 provides for a direct calculation of θ. If the strain is assumed equal to zero, as is suggested if the section is not cracked under the Strength Load combination, θ becomes 29 degrees. Concrete Contribution, V_c

AASHTO LRFD Equation 5.7.3.3-3 provides the concrete contribution to shear strength. If shear cracks are observed in the member in question, it may indicate the member has experienced a demand greater than V_c. The angle of observed diagonal compression, θ, can be measured and used in the calculations for V_s. If exceptional cracking is encountered, engineering judgment is suggested to consider further action or investigation.

4.5.3 Steel Reinforcement Contribution, V_s

AASHTO LRFD Equation 5.7.3.3-4 provides the reinforcement contribution to shear strength.

4.5.4 Prestressing Contribution, V_p

For draped, or harped, pretensioning strands and sloping portions of post-tensioning tendons, there is a vertical component to the effective prestress force labeled V_p. In most cases, this vertical component of the effective prestress force benefits the shear strength. The load rater is responsible for recognizing situations where this is not the case and provide the proper sign for V_p. For sections being investigated near member ends, AASHTO LRFD notes the transfer length of pretensioning strands is be accounted for in determining V_p. See **Figure 18** for an illustration of V_p.

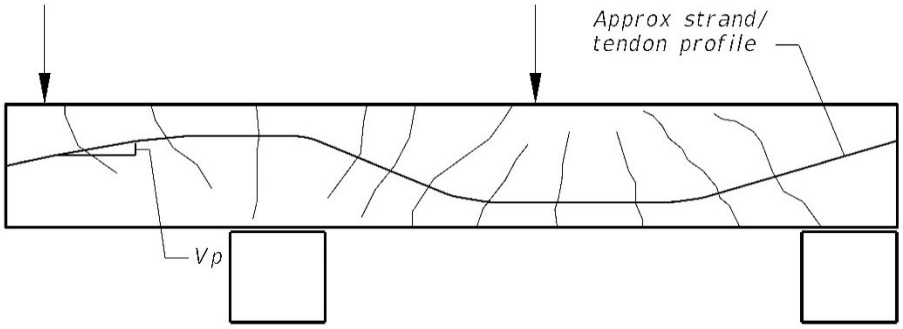

Source: Authors

Figure 18. Illustration of the vertical component of prestressing, V_p.

4.5.5 Iterations for Load Rating

As noted in Chapters 2 and 3, determining the shear strength for a load rating with MCFT General Procedure in AASHTO LRFD Article 5.7.3.4.2 (binding)is an iterative process due to the underlying differences in strain's role in determining shear capacity in design versus load rating. As stated in Caprani et al. (2019), with design, the longitudinal strain is directly calculated for the applied loading and a design directly follows. Load rating differs in that it seeks the loading that matches the section's ultimate shear strength, where the longitudinal strain at ultimate matches the applied strain. **Figure 17** provides a step-by-step process for iterating with the MCFT General Procedure.

Having determined ΦV_n by combining individual contributions of concrete, reinforcing and prestressing to shear strength and factoring with the appropriate strength resistance factor specified in AASHTO LRFD Article 5.5.4.2 (binding), this value is then compared to the applied V_u. If not equal, iterations should begin by updating V_u, M_u, and N_u, by proportionally increasing or decreasing the live load portion of these force effects. It is important that live load moment, shear and axial force are kept in proportion through the iteration process. Also, these force effects are to be concurrent with each other, i.e., from the same live load positioning.

Note that if the strain ε_s is zero, no iterations are necessary.

4.6 VERIFY ADEQUATE LONGITUDINAL REINFORCEMENT

After determining the web shear capacity, the flexural reinforcement's capacity to resist the longitudinal component of this web shear is to be verified using the provisions of AASHTO LRFD Article 5.7.3.5. In design, adding flexural reinforcement is the usual process to satisfy this load demand, but this is not possible in load rating.

If the longitudinal reinforcement is inadequate, then the applied V_u (and M_u and N_u) are reduced to reach equilibrium in LRFD Equation 5.7.3.5-1. An iterative process is used as θ and V_n are dependent on ε_s. **Figure 19** illustrates the steps to determine shear strength as controlled by the longitudinal reinforcement.

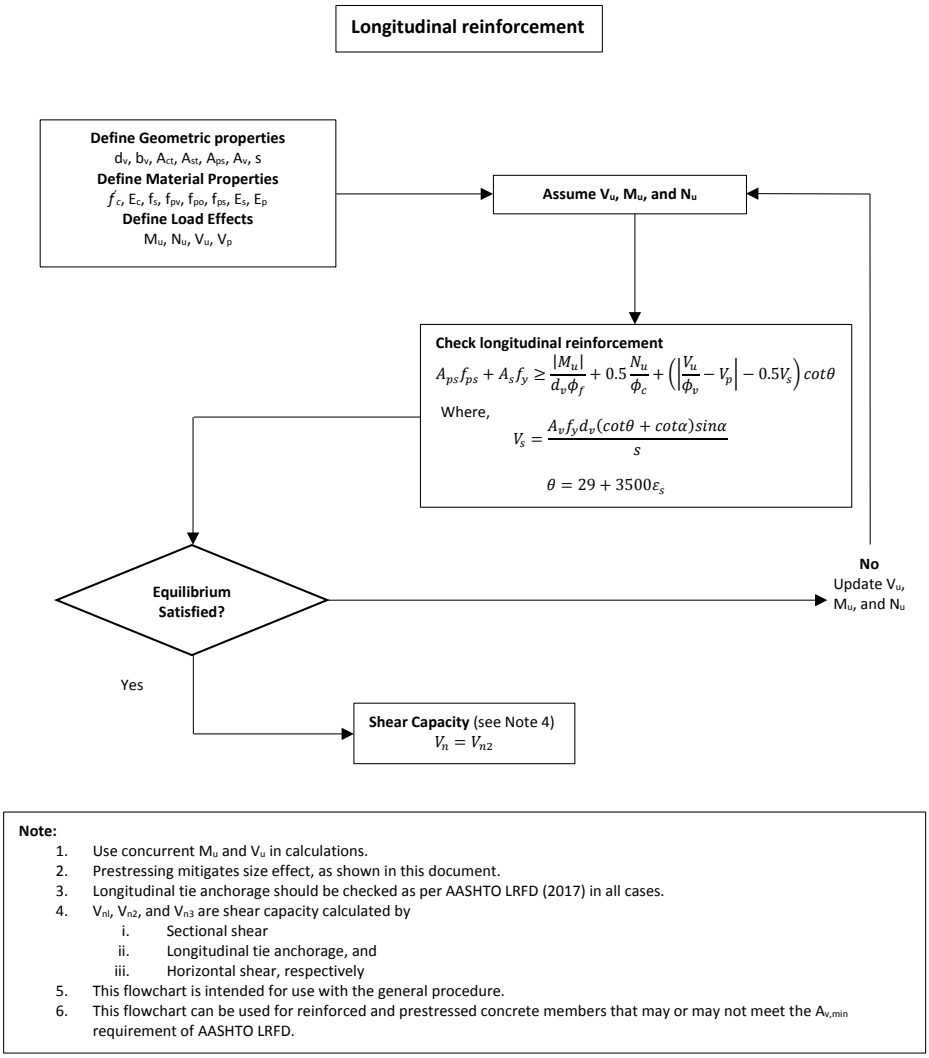

Source: Authors

Figure 19. Flow chart to determine shear capacity as controlled by longitudinal reinforcement.

The section's shear capacity is then the lower of the sectional shear capacity and the shear capacity as limited by the longitudinal reinforcement.

4.7 HORIZONTAL SHEAR STRENGTH AT WEB/BOTTOM FLANGE JUNCTION

Horizontal shear failures have been observed at the ends of prestressed girders in laboratory tests, especially in modern cross sections with thin webs and large flanges that provide optimal cross section efficiency for flexure, but not necessarily for shear (Hovell et al. 2013). The horizontal shear check listed in **Figure 8** is specifically intended for such members; engineering judgment can be used in determining if this check is necessary for older or less flexurally-

efficient prestressed concrete girder sections. This horizontal shear check is not expected to govern a reinforced concrete member; use engineering judgment when evaluating its applicability. The process to determine if horizontal shear resistance governs a section's capacity is illustrated in **Figure 20**.

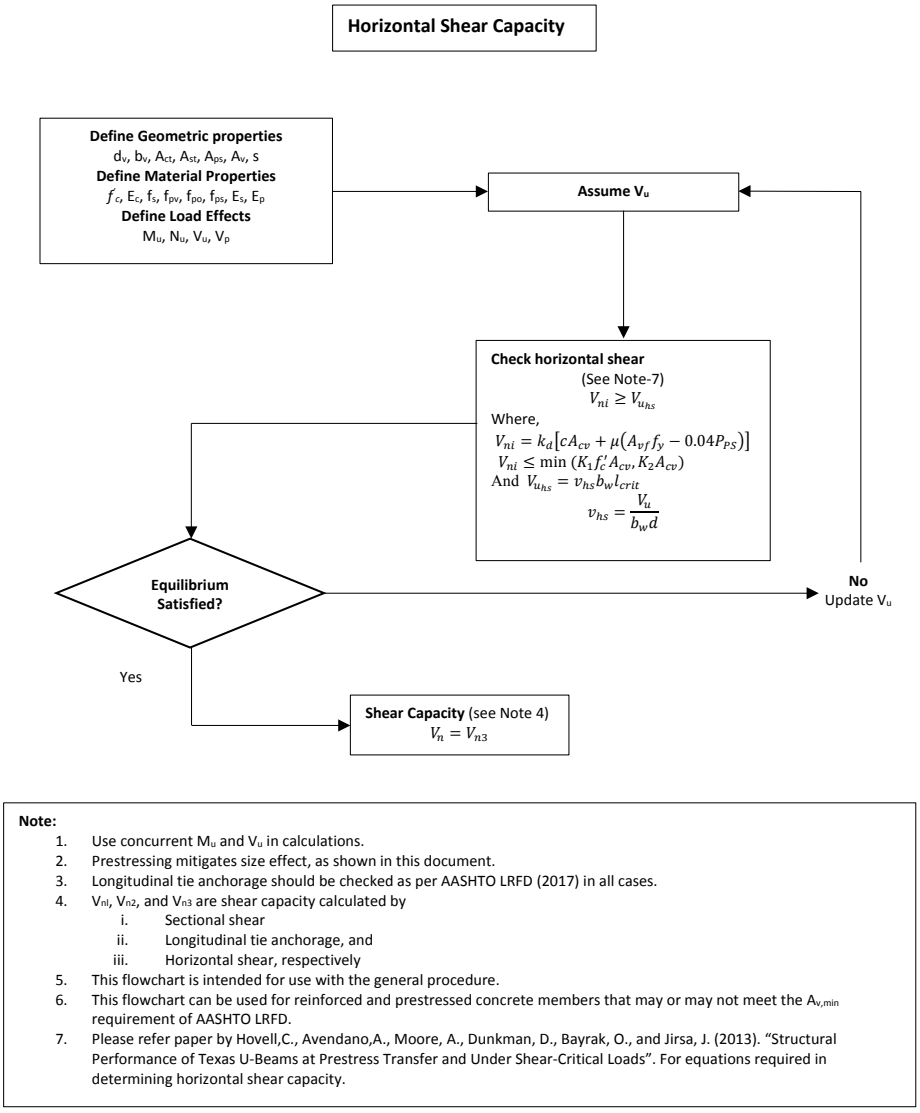

Source: Authors

Figure 20. Flow chart to determine shear strength as controlled by horizontal shear.

This check is not listed in AASHTO LRFD; however, Hovell et al. (2013) provides a methodology for determining both the load demand and horizontal shear strength at the interface between the web and bottom flange of a prestressed girder. **Figure 21** illustrates this horizontal shear mechanism at the bottom flange to web interface. The reader is directed to Hovell et al. (2013) for determining the applied loading and capacity for this check.

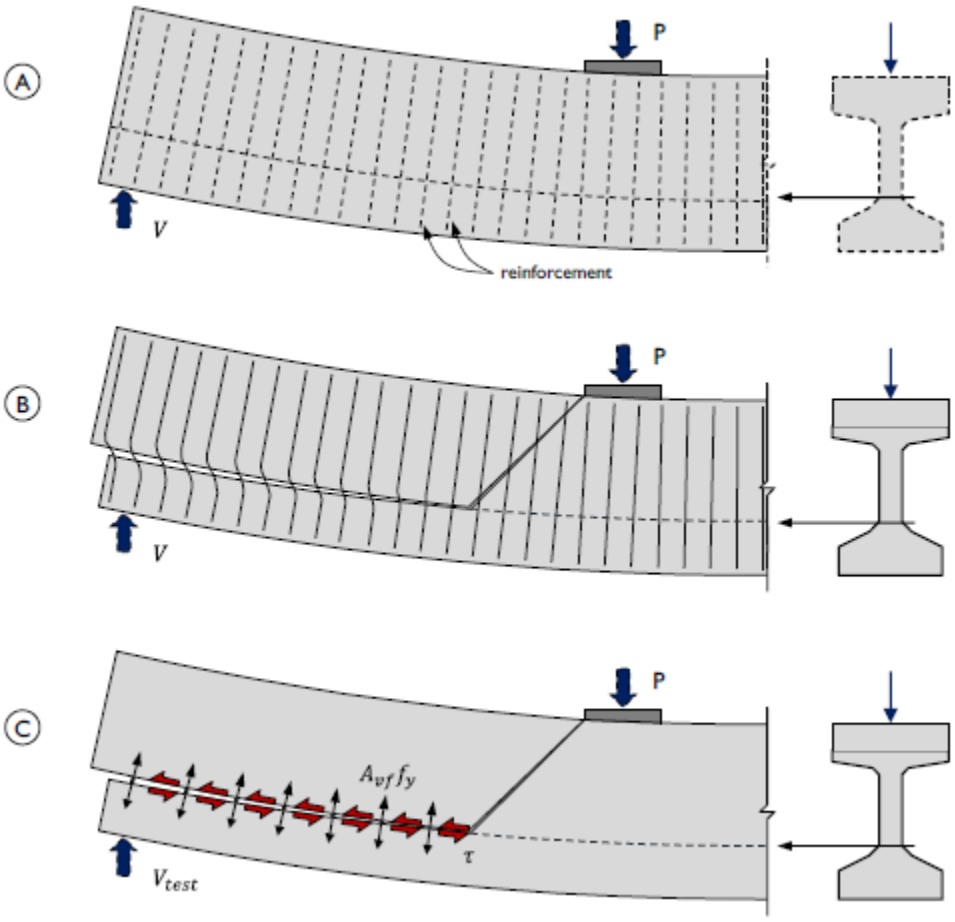

Figure 21. Bottom flange/web interface horizontal shear mechanism (Hovell et al. 2013).

CHAPTER 5. SHEAR LOAD RATING EXAMPLES WITH LRFR AND MCFT

Three bridges are load rated in this Chapter to demonstrate the use of MCFT in determining a design load rating in shear with LRFR, at both Inventory and Operating levels consistent with the provisions of AASHTO MBE Article 6A, for common bridge types. The examples are prepared assuming the reader is familiar with AASHTO LRFD and MBE and is already knowledgeable in determining moments and shears for specific load combinations, load factors and limit states appropriate for rating type, and live load distribution factors and section properties. The steps and calculations for these items are therefore not provided.

Provided example load ratings are at the strength limit state. Condition factors noted in AASHTO MBE Article 6A.4.2.3 are set to 1.0 for each example. Likewise, each example's system factor is taken as 1.0, consistent with the provisions of AASHTO MBE Article 6A.4.2.4 for shear load ratings at the strength limit state.

Section 5.1 illustrates the iterative processes for sectional shear (Section 5.1.2) and longitudinal reinforcement (Section 5.1.3). Both processes are used in and excerpted from the example load ratings in Sections 5.2 to 5.4.

Section 5.2 provides a shear design load rating example for a simple span, pretensioned girder bridge. An interior girder is load rated for shear at one critical section.

Section 5.3 provides a shear design load rating example for a three-span continuous reinforced concrete girder bridge. An interior girder is load rated for shear at two critical sections.

Lastly, Section 5.4 provides a shear design load rating example for a two-span continuous post-tensioned box girder bridge. An interior web is load rated for shear at three critical sections.

Calculations are prepared in a hand-calculation format. Simplifying assumptions, limiting decimal places of calculated values, etc., are made throughout these examples, where it is reasonable to expect a user to make similar assumptions to facilitate or expedite a hand calculation process. If software is used as a load rating tool, such simplifications are not expected.

5.1 EXAMPLE ITERATION PROCESSES

5.1.1 Common Data Needed for Iteration Processes

The material and geometrical data used to explain the iteration process is used from the load rating example in Section 5.4. Specifically, looking at the Maximum Moment Concurrent Shear Case: at critical section 2 (d_v from face of interior support) in Section 5.4.7.2.

Values established in the example and used in the iteration process are as follows:

$V_{u(DC)} + V_{u(PR)} = 212.3$ kip

$M_{u(DC)} + M_{u(PR)} = -50530$ kip-in

PR = Prestress restrain

$V_{um(inv)} = 92$ kip

$M_{um(inv)} = -30327$ kip-in

$V_u = 304$ kip

$M_u = -80858$ kip-in

$$\eta_{mm(inv)} = \frac{M_{um(inv)}}{V_{um(inv)}} = -329$$

$\eta_{mM(inv)}$ = factor to increase/decrease moment proportionally when iterating shear force

$M_{cr\text{-sec2}} = 75226$ kip-in

$V_p = 80$ kip

$d_v = 47.5$ in

$A_{ps} = 8.7$ in^2

$f_{po} = 189$ ksi

$E_{ps} = 28{,}500$ ksi

$E_s = 29{,}000$ ksi

$A_s = 7.6$ in^2

$f_{ps} = 221.4$ ksi

5.1.2 Iterations to Calculate Nominal Shear Resistance at Critical Section

5.1.2.1 Iteration 1

5.1.2.1.1 Step 1 – Check the section for cracking

If the factored strength bending moment due to HL-93 loading is less than the cracking moment, using AASHTO LRFD Equation 5.6.3.3-1 (binding), then the section is not cracked. The strain at the center of the girder can be assumed to be zero, as noted in AASHTO LRFD Article 5.7.3.4.2 (binding), and no iterations are necessary. If this were a reinforced concrete member, it can be assumed the section is cracked under the factored strength bending moment.

In this case, M_u exceeds M_{cr} (M_u=80858 k-in and M_{cr}=75051 k-in) and the following procedure should be followed. As the live load changes with each iteration, evaluating the section for cracking relative to applied loading should be made.

Since the section is prestressed, there is no need to check if minimum shear reinforcement is present as per AASHTO LRFD Article 5.7.2.5 (binding). If the section was not prestressed, minimum reinforcement check as per Article 5.7.2.5 (binding) would need to be made.

5.1.2.1.2 Step 2: Find strain at center of gravity (CG) of tensile reinforcement using the following equation

$$\varepsilon_s = \frac{\left(\frac{|M_u|}{d_v} + 0.5N_u + |V_u - V_p| - A_{ps}f_{po}\right)}{E_s A_s + E_p A_{ps}}$$

LRFD Design Eq. 5.7.3.4.2-4

If, ε_s is negative then:

$$\varepsilon_s = \frac{\left(\frac{|M_u|}{d_v} + 0.5N_u + |V_u - V_p| - A_{ps}f_{po}\right)}{E_s A_s + E_p A_{ps} + E_c A_{ct}}$$

LRFD Design Eq. B5.2-5

In the above, note that Eq B5.2.5 has been modified to determine the strain at the level of the tensile reinforcement, ε_s, to be consistent with the provisions of AASHTO LRFD Article 5.7.3.4.2.

To simplify the calculations, the equation can be modified as

$$\varepsilon_s = \frac{\left(\frac{\left| M_{u-DL} + V_{u-LL}\eta_{LL} \right|}{d_v} + 0.5N_u + \left| V_u - V_p \right| - A_{ps} f_{po} \right)}{E_s A_s + E_p A_{ps}}$$

Since,

$M_u = M_{u\text{-}DL} + M_{u\text{-}LL}$

and,

$$\eta_{LL} = \frac{M_{u-LL}}{V_{u-LL}}$$

$M_{u\text{-}LL} = V_{u\text{-}LL}\eta_{LL}$

It can be re-written as,

$M_u = M_{u\text{-}DL} + V_{u\text{-}LL}\eta_{LL}$

also,

$V_u = V_{u\text{-}DL} + V_{u\text{-}LL}$

There is no N_u applied to the section. By modifying the equation, the iteration process can be carried out by iterating only one value, which is V_u.

$V_u = V_{u(DC)} + V_{u(PR)} + V_{um(inv)} = 304$ kip

$\eta_{mS(inv)} = -329$

$\left| \frac{M_{u(DC)} + M_{u(PR)} + V_{um(inv)}\eta_{mm(inv)}}{d_v} \right| = 1701\text{kip}$, should be greater than, $|V_u - V_p| = 224$ kip

Adopt, $\left| \frac{M_{u(DC)} + M_{u(PR)} + V_{um(inv)}\eta_{mm(inv)}}{d_v} \right| = 1701\text{kip}$

$A_{ps} = 8.7$ in^2 (per web); $f_{po} = 0.7f_{pu} = 189$ ksi

$$\varepsilon_s = \frac{\left(1701 + \left|224\right| - 1643\right)}{29{,}000 \times 7.6 + 28{,}500 \times 8.7}$$
$$= 0.0006$$

$\theta = 29 + 3500\varepsilon_s = 29 + 3500 \times 0.0006 = 31.1°$

$$\beta = \frac{4.8}{1+750\varepsilon_s} = \frac{4.8}{1+750\times 0.0006}$$
$$= 3.3$$

5.1.2.1.3 Step 3 – Calculating shear capacity at the critical section
Shear strength of concrete:

$$V_c = 0.0316\beta\lambda\sqrt{f_c'}b_v d_v$$
$$= 0.0316\times 3.3\times 1\times\sqrt{3.5}\times 10.5\times 47.5$$
$$= 97.3\,\text{kip}$$

Shear strength of shear reinforcement:

$$V_s = \frac{A_v f_y d_v \cot(\theta)}{s}$$
$$= \frac{0.61\times 60\times 47.5\cot(31.1)}{12}$$
$$= 242\,\text{kip}$$

Total shear capacity of the section:

Minimum of

$V_c + V_s = 97.3 + 242 = 339.3$ kip

and

$0.25f'_c b_v d_v = 436.4$ kip

Therefore,

$V_n = 339.3 + V_p = 339.3 + 80 = 419.2$ kip

$\phi V_n = 0.9 \times 419.2 = 377.4$ kip $> V_u = 304$ kip

To demonstrate how the rating factor changes through the iterative process, the initial inventory level design rating factor after iteration 1 is calculated as

$\phi V_n = 377.4$ kip

$V_{u(DC)} = \gamma_{DC} \times V_{DC} = 213.4$ kip

$V_{u(PS)} = \gamma_{PS} \times V_{PS} = -1.1$ kip

$V_{um(inv)} = \gamma_{LL}(inv) \times V_m = 92.1$ kip

$M_{cr\text{-}sec2} = 75051$ k-in

Shear Load Rating Factor = $\dfrac{\phi V_n - V_{u(DC)} - V_{u(PS)}}{V_{um(inv)}} = \dfrac{377.4 - 212.3}{92.1} = 1.80$

Since the goal of iteration is to converge at a point where $V_u = \phi V_n$, perform a second iteration.

5.1.2.2 Iteration 2

Step 1, checking the section for cracking, is not necessary as this was addressed in Iteration 1 with lower applied loads; the applied M_u will be even higher for this iteration.

5.1.2.2.1 Step 2: Find strain at CG of tensile reinforcement using the following equation

Increasing V_u to get closer to $V_u = \phi V_n$

$V_u = V_{u(DC)} + V_{u(PR)} + V_{um(inv)} = 390$ kip

$\eta_{mS(inv)} = -329$

$\left|\dfrac{M_{u(DC)} + M_{u(PR)} + V_{um(inv)}\eta_{mm(inv)}}{d_v}\right| = 2294$ kip, should be greater than, $|V_u - V_p| = 310$ kip

Adopt, $\left|\dfrac{M_{u(DC)} + M_{u(PR)} + V_{um(inv)}\eta_{mm(inv)}}{d_v}\right| = 2294$ kip

$A_{ps} = 8.7$ in^2 (per web); $f_{po} = 0.7 f_{pu} = 189$ ksi

$$\varepsilon_s = \frac{\left(2294 + |310| - 1643\right)}{29{,}000 \times 7.6 + 28{,}500 \times 8.7} = 0.0021$$

$\theta = 29 + 3500\varepsilon_s = 29 + 3500 \times 0.0021 = 36.2°$

$$\beta = \frac{4.8}{1 + 750\varepsilon_s} = \frac{4.8}{1 + 750 \times 0.0021} = 1.9$$

5.1.2.2.2 Step 3 – Calculating shear capacity at the critical section

Shear strength of concrete:

$$V_c = 0.0316\beta\lambda\sqrt{f_c'}\,b_v d_v = 0.0316 \times 1.9 \times 1 \times \sqrt{3.5} \times 10.5 \times 47.5 = 56\,\text{kip}$$

Shear strength of shear reinforcement:

$$V_s = \frac{A_v f_y d_v \cot(\theta)}{s}$$
$$= \frac{0.61 \times 60 \times 47.5 \cot(36.2)}{12}$$
$$= 199 \text{ kip}$$

Total shear capacity of the section:

Minimum of

$V_c + V_s = 56 + 199 = 255$ kip

and

$0.25 f'_c b_v d_v = 436.4$ kip

Therefore,

$V_n = 255 + V_p = 255 + 80 = 335$ kip

$\phi V_n = 0.9 \times 335 = 301.5$ kip $< V_u = 390$ kip

Calculating the shear load rating factor for the second iteration.

$\phi V_n = 301.5$ kip

$V_{u(DC)} = \gamma_{DC} \times V_{DC} = 213.4$ kip

$V_{u(PS)} = \gamma_{PS} \times V_{PS} = -1.1$ kip

$V_{um(inv)} = \gamma_{LL}(inv) \times V_m = 92.1$ kip

$M_{cr\text{-}sec2} = 75051$ k-in

$$\text{Shear Load Rating Factor} = \frac{\phi V_n - V_{u(DC)} - V_{u(PS)}}{V_{um(inv)}} = \frac{301.5 - 212.3}{92.1} = 0.97$$

Since the goal of iteration is to converge where $V_u = \phi V_n$, performing third iteration.

5.1.2.3 Iteration 3

Step 1, checking the section for cracking, is not necessary as this was completed in Iteration 1.

5.1.2.3.1 Step 2: Find strain at CG of tensile reinforcement using the following equation.

Increasing V_u to get closer to $V_u = \phi V_n$

Decreasing $V_{un(inv)}$ to be 127 kip

$V_u = V_{u(DC)} + V_{u(PR)} + V_{um(inv)} = 339$ kip

$\eta_{mS(inv)}$ = -329

$\left|\frac{M_{u(DC)} + M_{u(PR)} + V_{um(inv)}\eta_{mm(inv)}}{d_v}\right|$ = 1944 kip, should be greater than, $|V_u - V_p|$ = 260 kip

Adopt, $\left|\frac{M_{u(DC)} + M_{u(PR)} + V_{um(inv)}\eta_{mm(inv)}}{d_v}\right|$ =1944

A_{ps} = 8.7 in^2 (per web); $f_{po} = 0.7f_{pu}$ = 189 ksi

$$\varepsilon_s = \frac{\left(1980 + |264| - 1643\right)}{29{,}000 \times 7.6 + 28{,}500 \times 8.7}$$
$$= 0.0012$$

$$\theta = 29 + 3500\varepsilon_s = 29 + 3500 \times 0.0012 = 33.17°$$

$$\beta = \frac{4.8}{1 + 750\varepsilon_s} = \frac{4.8}{1 + 750 \times 0.0012}$$
$$= 2.5$$

5.1.2.3.2 Step 3 – Calculating shear capacity at the critical section
Shear strength of concrete:

$$V_c = 0.0316\beta\lambda\sqrt{f_c'}b_v d_v$$
$$= 0.0316 \times 2.5 \times 1 \times \sqrt{3.5} \times 10.5 \times 47.5$$
$$= 75\,\text{kip}$$

Shear strength of shear reinforcement:

$$V_s = \frac{A_v f_y d_v \cot(\theta)}{s}$$
$$= \frac{0.61 \times 60 \times 47.5 \cot(33.5)}{12}$$
$$= 220\,\text{kip}$$

Total shear capacity of the section:

Minimum of

$V_c + V_s = 75 + 220 = 295$ kip

and

$0.25 f_c' b_v d_v = 436.4$ kip

Therefore,

$V_n = 295 + V_p = 295 + 80 = 375$ kip

$\phi V_n = 0.9 \times 375 = 338$ kip

Calculating the shear load rating factor for the second iteration.

$\phi V_n = 338$ kip

$V_{u(DC)} = \gamma_{DC} \times V_{DC} = 213.4$ kip

$V_{u(PS)} = \gamma_{PS} \times V_{PS} = -1.1$ kip

$V_{um(inv)} = \gamma_{LL}(inv) \times V_m = 92.1$ kip

$M_{cr\text{-}sec2} = 75051$ k-in

$$\text{Shear Load Rating Factor} = \frac{\phi V_n - V_{u(DC)} - V_{u(PS)}}{V_{um(inv)}} = \frac{338 - 212.3}{92.1} = 1.36$$

With RF=1.36, the factored M_u becomes -94200 k-in which exceeds the cracking moment and thus meets the initial consideration of the section being cracked.

Since the solution has converged to $V_u = \phi V_n$, the factored shear capacity of the section is determined to be 338 kips. To reduce the number of iterations, at the second iteration it is suggested to take the average of V_u at the beginning and end of the first iteration step. In this case, the average would be 341 kips (average of 304 kips and 377.4 kips), which is within 1 percent of the final value of 338 kips.

A summary of the RF at each iteration step is listed Table **2**. When the initial RF exceeds 1, iterating will lower the final RF closer to 1. When the initial RF is below1, iterating will increase the final RF closer to 1.

Table 2. Summary of Rating Factors at each Iteration Step

Iteration No	ϕV_n (kip)	Shear Load Rating Factor
1	377.4	1.80
2	301.5	0.97
3	338	1.36

5.1.3 Iteration to Determine Longitudinal Reinforcement Capacity

The example in the previous section is used here. Tensile capacity of the longitudinal reinforcement on the flexural tension side of the member should be proportioned to satisfy:

$$A_{ps}f_{ps} + A_s f_y \geq \frac{|M_u|}{d_v \phi_f} + 0.5\frac{N_u}{\phi_c} + \left(\left|\frac{V_u}{\phi_v} - V_p\right| - 0.5V_s\right)\cot\theta$$

$\phi_f = 1.0$ LRFD Design 5.7.3.5

$\phi_v = 0.9$

Since it uses an iterative process to determine the shear capacity as may be limited by the longitudinal reinforcement, the right-hand side (RHS) of the equation is modified to take account of the moments in the iterative process. Live load force effects are to be increased proportionally through the iteration steps. There is no axial force from live load or other loads in this example.

5.1.3.1 Iteration 1

5.1.3.1.1 Step 1 – Calculating strain and θ:

Strain can be calculated as

$$\varepsilon_s = \frac{\left(\frac{|M_{u-DL} + V_{u-LL}\eta_{LL}|}{d_v} + 0.5N_u + |V_u - V_p| - A_{ps}f_{po}\right)}{E_s A_s + E_p A_{ps}}$$ LRFD Design Eq. 5.7.3.4.2-4

Since,

$M_u = M_{u\text{-}DL} + M_{u\text{-}LL}$

and,

$$\eta_{LL} = \frac{M_{u-LL}}{V_{u-LL}}$$

$M_{u\text{-}LL} = V_{u\text{-}LL}\eta_{LL}$

It can be re-written as,

$M_u = M_{u\text{-}DL} + V_{u\text{-}LL}\eta_{LL}$

also,

$V_u = V_{u\text{-}DL} + V_{u\text{-}LL}$

Normally this evaluation would begin with the resistance determined in the previous section. If the amount of tension reinforcement is adequate for that resistance, no further evaluation may be necessary since the previously determined capacity will control. However, the process shown here will begin using the values from Section 5.1.1. Unlike the iteration process in the previous section, the iterations used for the longitudinal reinforcement evaluation are a trial-and-error process:

$V_u = V_{u(DC)} + V_{u(PR)} + V_{um(inv)} = 304$ kip

$\eta_{mS(inv)} = -329$

$\left|\frac{M_{u(DC)} + M_{u(PR)} + V_{um(inv)}\eta_{mm(inv)}}{d_v}\right| = 1701$ kip, should be greater than, $|V_u - V_p| = 224$ kip

Adopt, $\left|\frac{M_{u(DC)} + M_{u(PR)} + V_{um(inv)}\eta_{mm(inv)}}{d_v}\right| = 1701\text{kip}$

$A_{ps} = 8.7$ in^2 (per web); $f_{po} = 0.7f_{pu} = 189$ ksi

$$\varepsilon_s = \frac{\left(1701 + |224| - 1643\right)}{29{,}000 \times 7.6 + 28{,}500 \times 8.7} = 0.0006$$

$\theta = 29 + 3500\varepsilon_s = 29 + 3500 \times 0.0006 = 31.1°$

5.1.3.1.2 Step 2 – Determining both sides of LRFD Design Eq. 5.7.3.5-1:
Shear strength of shear reinforcement:

$$V_s = \frac{A_v f_y d_v \cot(\theta)}{s} = \frac{0.61 \times 60 \times 47.5 \cot(31.1)}{12} = 242\,\text{kip}$$

RHS of the LRFD Design Eq. 5.7.3.5-1

$$RHS = \frac{\left|M_{u(DC)} + M_{u(PR)} + V_{um(inv)}\eta_{LL}\right|}{d_v\phi_f} + 0.5\frac{N_u}{\phi_c} + \left(\left|\frac{V_u}{\phi_v} - V_p\right| - 0.5V_s\right)\cot\theta$$

$$= \frac{1701}{1} + \left(\left|\frac{304}{0.9} - 80\right| - 0.5 \times 242\right)\cot(31.1)$$

$$= 1928\,\text{kip}$$

Left hand side (LHS) of the LRFD Design Eq. 5.7.3.5-1

$LHS = A_{ps,top}f_{ps} + A_{s,top}f_y = 8.7 \times 221 + 7.6 \times 60 = 2379$ kip

Since LHS > RHS, iteration is used to determine the shear strength as controlled by longitudinal reinforcement. This is done by increasing V_u by increasing the live load shear force until the equilibrium is achieved. If flexural shear was lower, it would control and doing iterations with longitudinal reinforcement would not be necessary.

5.1.3.2 Iteration 2

5.1.3.2.1 Step 1 – Calculating strain and θ:

Increasing $V_{um(inv)}$ to 145 kip

$V_u = V_{u(DC)} + V_{u(PR)} + V_{um(inv)} = 358$ kip

$\eta_{mS(inv)} = -329$

$\left|\frac{M_{u(DC)} + M_{u(PR)} + V_{um(inv)}\eta_{mm(inv)}}{d_v}\right| = 2071\text{kip}$, should be greater than, $|V_u - V_p| = 277$ kip

Adopt, $\left|\frac{M_{u(DC)} + M_{u(PR)} + V_{um(inv)}\eta_{mm(inv)}}{d_v}\right| = 2071\text{kip}$

$A_{ps} = 8.7$ in^2 (per web); $f_{po} = 0.7f_{pu} = 189$ ksi

$$\varepsilon_s = \frac{\left(2071 + |277| - 1643\right)}{29{,}000 \times 7.6 + 28{,}500 \times 8.7} = 0.0015$$

$\theta = 29 + 3500\varepsilon_s = 29 + 3500 \times 0.0015 = 34.3°$

5.1.3.2.2 Step 2 – Determining both the sides of LRFD Design Eq. 5.7.3.5-1:

Shear strength of shear reinforcement:

$$V_s = \frac{A_v f_y d_v \cot(\theta)}{s} = \frac{0.61 \times 60 \times 47.5 \cot(34.3)}{12} = 214\text{kip}$$

RHS of the LRFD Design Eq. 5.7.3.5-1

$$RHS = \frac{\left|M_{u(DC)} + M_{u(PR)} + V_{um(inv)}\eta_{LL}\right|}{d_v\phi_f} + 0.5\frac{N_u}{\phi_c} + \left(\left|\frac{V_u}{\phi_v} - V_p\right| - 0.5V_s\right)\cot\theta$$

$$= \frac{2071}{1} + \left(\left|\frac{358}{0.9} - 80\right| - 0.5 \times 214\right)\cot(34.3) = 2379\text{kip}$$

LHS of the LRFD Design Eq. 5.7.3.5-1

$LHS = A_{ps,top}f_{ps} + A_{s,top}f_y = 8.7 \times 221 + 7.6 \times 60 = 2379$ kip

Since LHS = RHS, iterations have converged, and the shear load rating based on longitudinal reinforcement can be determined.

Calculating the shear load rating factor in this iteration:

ϕV_n = 358 kip

$V_{u(DC)} = \gamma_{DC} \times V_{DC}$ = 213.4 kip

$V_{u(PS)} = \gamma_{PS} \times V_{PS}$ = -1.1 kip

$V_{um(inv)} = \gamma_{LL}(inv) \times V_m$ = 92.1 kip

$M_{cr\text{-}sec2}$ = 75051 k-in

$$\text{Shear Load Rating Factor} = \frac{\phi V_n - V_{u(DC)} - V_{u(PS)}}{V_{um(inv)}} = \frac{358 - 212.3}{92.1} = 1.58$$

V_u obtained after iteration = 358 kip. Therefore, this is the factored shear capacity at the selected section to satisfy the LRFD Design Eq 5.7.3.5-1. Note that the factored resistance determined in Section 5.1.2 for sectional shear, 345 kips, governs at this section.

5.2 EXAMPLE RATING – SIMPLE SPAN PRESTRESSED I-GIRDER (INTERIOR)

This example is for a shear design load rating for an interior girder of a simple span, pretensioned girder. One section is evaluated, located at d_v from the end bearing. The end bearings have steel masonry plates with convex faces that react against a flat steel sole plate embedded in the beam to allow for rotation; using the centerline of bearing to measure the critical distance d_v from is appropriate in this instance. Had the bearing been a neoprene pad, the critical distance d_v could have been measured from the front edge of the pad.

The shear reinforcement anchorage at the bottom does not hook around the prestressed strands; it does not meet the anchorage specifications of AASHTO LRFD (2020). However, for this example, it will be assumed the stirrups are fully anchored to develop F_y.

A shear design load rating is also completed for the span quarter points. As the calculation steps for this section are identical, only the load rating results are reported.

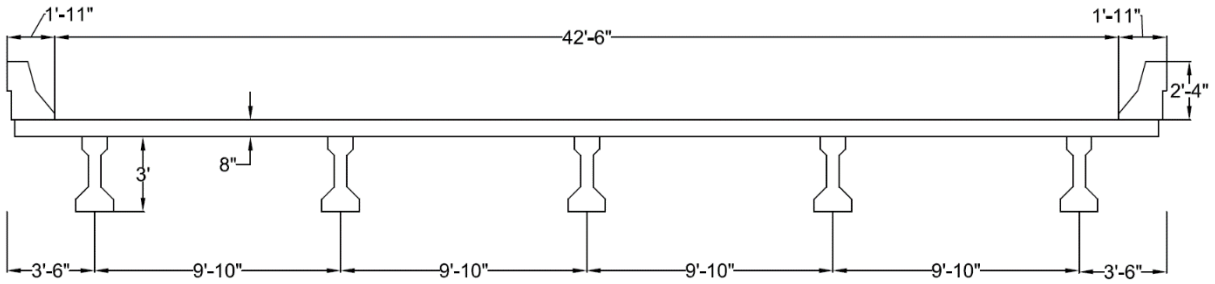

TRANSVERSE SECTION

Source: Authors

Figure 22. Transverse section.

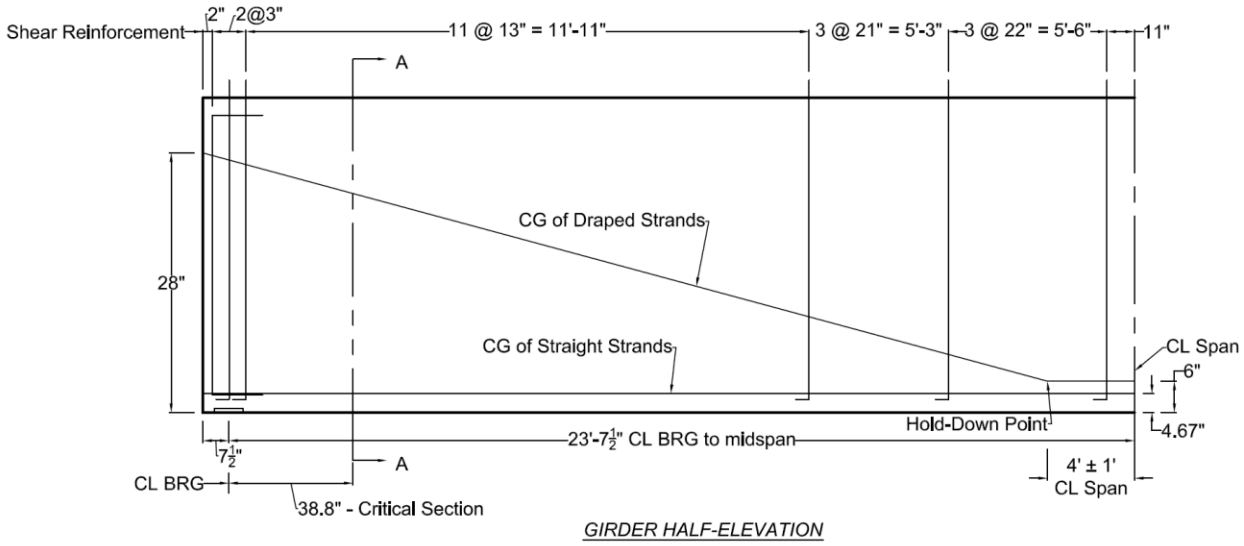

Source: Authors

Figure 23. Typical girder elevation.

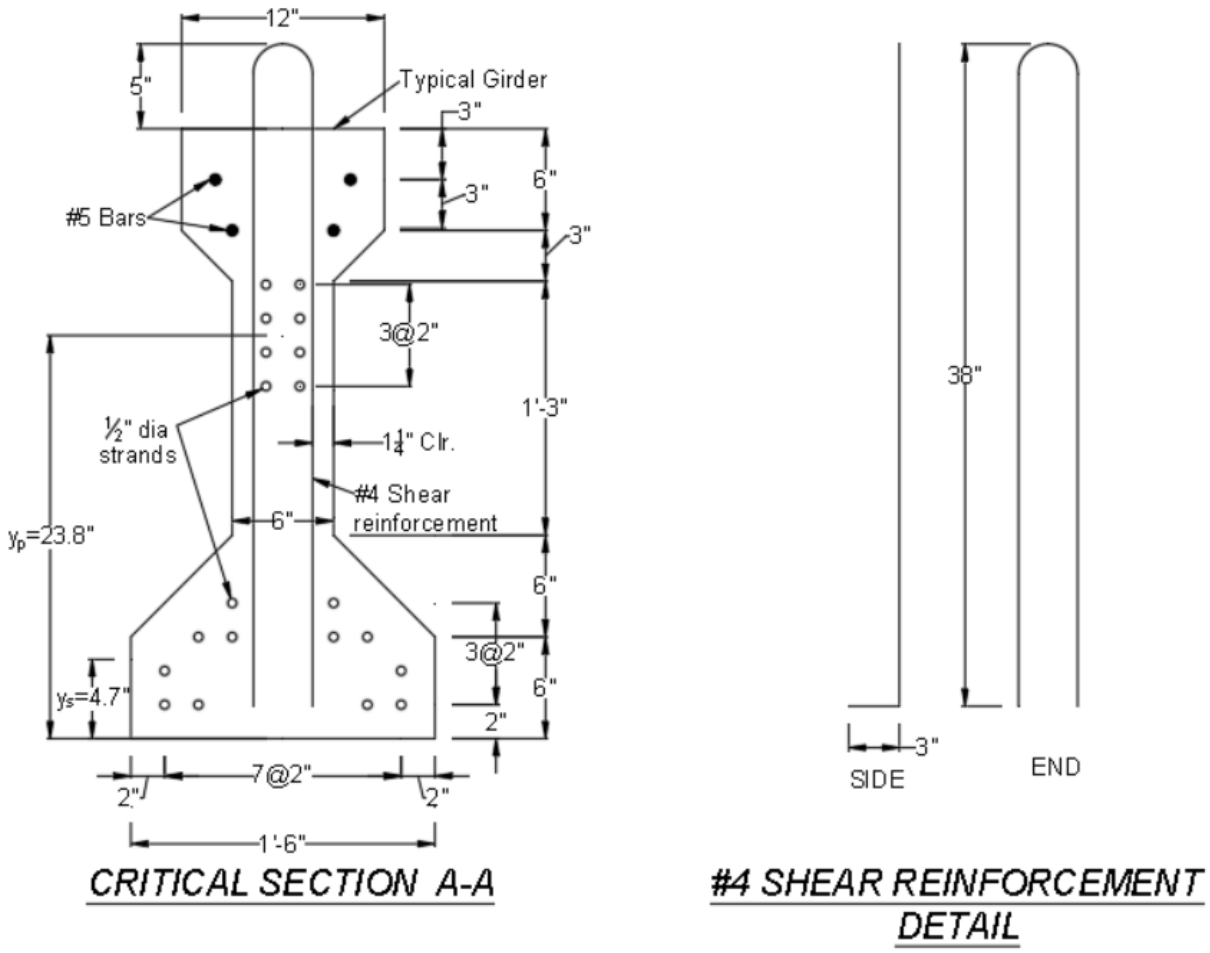

Source: Authors

Figure 24. Section A-A at critical section.

5.2.1 Bridge Data

Span: 47.25 ft

Year Built: 1972

Materials:

Concrete: f_c' = 4 ksi (Deck)

f_c' = 5 ksi (Girder)

f'_{ci} = 4.882 ksi (Girder at transfer)

Prestressing steel: ½ inch diameter, 270 ksi, stress relieved strands

A_{pr} = 0.153 in.^{2} per strand

20 prestressing strands; 12 straight strands 8 draped strands held down at 48 inches from midspan

Shear Stirrups: #4 stirrups. See **Figure 23** for spacing.

Compression steel: 4 - #5 Grade 40

Condition: Good

Riding surface: Not provided

ADTT: Not provided

Skew: 13.81°

Effective flange width, b_e, may be taken as the tributary width perpendicular to the axis of the member. LFRD Design 4.6.2.6.1

Effective flange width b_e= 108 in + 10 in = 118 in.

Modulus of elasticity of concrete: $Ec = 120{,}000\,K_1\,w_c^{2.0}\,f_c'^{0.33}$ LRFD Design Eq. 5.4.2.4-1

For deck, Ec = 120,000 x 1 x $(0.15)^{2.0}$ x $(4.0)^{0.33}$ = 4266 ksi

For girder, Ec = 120,000 x 1 x $(0.15)^{2.0}$ x $(5.0)^{0.33}$ = 4592 ksi

Modular Ratio, $n_i = \dfrac{E_{deck}}{E_{beam}} = \dfrac{4266\,\text{ksi}}{4592\,\text{ksi}} = 0.929$

Transformed width, b_{trans} = 118 in × 0.929 = 109.62 in

5.2.2 Summary of Section Properties

Girder properties:

$h = 36$ in.

$A = 369$ in.^{2}

$A_{ct} = 209$ in.^{2}

$I_g = 50{,}980$ in.^{4}

$Y_b = 15.83$ in.

Composite section properties

$h_c = h + t_{slab} = 36 + 8 = 44$ in.

$A_c = 1246$ in.^{2}

$y_{bot} = 32.84$ in.

$y_{top} = h_c - y_{bot} = 11.2$ in.

$I_{comp} = 207{,}384$ in.^{4}

$$S_b = \frac{I_{comp}}{y_{bot}} = 6315 \text{ in}^3$$

$$S_t = \frac{I_{comp}}{y_{top}} = 18516 \text{ in}^3$$

5.2.2.1 Determining Shear Depth of the Section at Critical Load Rating Section

It is difficult to determine the critical section based on the depth of the tensile reinforcement at the ends of pretensioned girders with harped, or draped, strands. To simplify the process without sacrificing much in terms of capacity, this example will use the lower bound value of $0.72h$ for the effective shear depth, as noted in AASHTO LRFD Article 5.7.2.8 (binding).

Therefore, effective shear depth is:

$0.72h = 0.72 \times 44$ in $= 31.7$ in

Shear reinforcement at critical section:

Shear Reinforcement Rebar = #4

Area of Shear Reinforcement = 0.4 in.^{2} (Two-Legged Stirrups)

Spacing of Shear Reinforcement = 13 in.

Prestressing steel in girder:

Draped strands:

Hold-down Point = 51 in. (from c/l of the girder)

Length of Beam = 582 in.

Critical Section for LR = 31.7 in.

Number of Draped Strands = 8

Strand Diameter = 0.5 in.

Strand Area = 0.153 in.^{2}

$A_{ps,draped}$ = 1.22in.^{2}

CG @ End of the Beam = 28 in.

CG @ c/l of the Beam = 6 in.

CG @ Critical Section = 24.4 in. (from bottom)

Depth of Draped Prestressing strands = $d_{p,draped}$ = 19.6 in.

$$\theta_{draped} = \tan\left(\frac{28-6}{240}\right) = 5.24°$$

Straight strands:

Critical Section for LR = 31.7 in.

Number of Straight Strands = 12

Strand Diameter = 0.5 in.

Strand Area = 0.153 in.^{2}

$A_{ps,straight}$ = 1.84 in.^{2}

CG @ Critical Section = 4.67 in. (from bottom)

Depth of Draped Prestressing strands = $d_{p,striaght}$ = 39.33 in.

Depth of combined prestressing strands:

$A_{ps,draped}d_{p,draped}$ = 0 (Since, it lies in the Compression zone)

$A_{ps} = A_{ps,draped} + A_{ps,straight}$ = 0 + 1.84 in.^{2} = 1.84 in.^{2}

($A_{ps,draped}$ = 0, Since it lies in the Compression zone)

$$d_p = \frac{A_{ps,draped}d_{p,draped} + A_{ps,straight}d_{p,straight}}{A_{ps}} = 39.33\,\text{in.}$$

5.2.3 Factored Loads at Critical Section

This is a design load rating; the live loads are calculated according to HL-93 loading. The live load moments and shears include the Dynamic Load Allowance, IM, from AASHTO LRFD Article 3.6.2(binding) and AASHTO MBE Article 6A.4.3.2 (nonbinding). Live loads are distributed to the girder using the provisions of AASHTO LRFD Article 4.6.2.2 (binding).

5.2.3.1 Strength-I Load Combination - Inventory Level
Load factors per Strength-I Load Combination

$\gamma_{DC} = 1.25$

$\gamma_{LL}(inv) = 1.75$

Factored shear forces and moments due to dead loads

$V_{u(DC)} = \gamma_{DC} \times V_{DC} = 39.7$ kip

$M_{u(DC)} = \gamma_{DC} \times M_{DC} = 1339$ kip-in

Inventory live load – Max Shear Concurrent Moment Case

$V_{us} = \gamma_{LL}(inv) \times V_s \times g_v = 146.1$ kip

$M_{us} = \gamma_{LL}(inv) \times M_s \times g_m = 3870$ kip-in

Inventory live load – Max Moment Concurrent Shear Case

$V_{um(inv)} = \gamma_{LL}(inv) \times V_m \times g_v = 146$ kip

$M_{um(inv)} = \gamma_{LL}(inv) \times M_m \times g_m = 3906$ kip-in

5.2.3.1.1 Inventory Ultimate Shear Force:
$V_{uS(inv)} = V_{u(DC)} + V_{us(inv)} = 185.9$ kip (Max Shear Case)

$V_{uM(inv)} = V_{u(DC)} + V_{um(inv)} = 185.8$ kip (Max Moment Case)

5.2.3.1.2 Inventory Ultimate Bending Moment:
$M_{uS(inv)} = M_{u(DC)} + M_{us(inv)} = 5209$ kip-in (Max Shear Case)

$M_{uM(inv)} = M_{u(DC)} + M_{um(inv)} = 5245$ kip-in (Max Moment Case)

5.2.4 Determine Effective Prestress Force, P_{pe}

$P_{pe} = A_{ps} f_{pe}$

Total Prestress Losses $\Delta f_{pT} = \Delta f_{pES} + \Delta f_{pLT}$ LRFD Design 5.9.3.1

$f_{pe} = f_{pi} - \Delta f_{pT}$

5.2.4.1 Prestress Loss due to Elastic Shortening

Initial Prestressing Force, P_i = 578 kip (provided in the as-built drawings)

Number of Prestressing Strands = 20

Area of a Prestressing Strand, a_{ps} = 0.153 in^2

Total Area of Strands, A_{ps} = $0.153 \times 20 = 3.06$ in^2

∴ Initial Prestress,

$$f_{pi} = \frac{P_i}{A_{ps}} = 189 \; ksi$$

Eccentricity of Strands, $e = y_b - y_{total} = 10.63$ inches

$$\Delta f_{pES} = \frac{E_p}{E_{ct}} f_{cgp}$$

$$f_{cgp} = \frac{P_i}{A} + \frac{P_i e^2}{I}$$

$$f_{cgp} = \frac{578}{369} + \frac{578 \times 10.63^2}{50980} = 2.8 \text{ ksi}$$ LRFD Design Eq. 5.9.3.2.3a-1

$E_{ps} = 28{,}500$ ksi

$E_c = 120{,}000 K_1 w_c^{2.0} f_c'^{0.33}$ LRFD Design Eq. 5.4.2.4-1

$E_{ci} = 120{,}000 \times 1 \times (0.15)^{2.0} \times (4.822)^{0.33} = 4556$ ksi

$$\Delta f_{pES} = \frac{28{,}500}{4{,}556} \times 2.8$$
$$= 18 \text{ ksi}$$

5.2.4.2 Approximate Lump Sum Estimate of Time-Dependent Losses, Δf_{pLT}

The approximate estimate of time dependent losses in AASHTO LRFD Article 5.9.3.3 are used even though the strands are stress relieved, not low relaxation, as the steel relaxation component of prestress losses is minor. The complexity of the refined estimate of time-dependent losses, as described in AASHTO LRFD Article 5.9.3.4, is not likely to change a load rating.

As an expedient, the estimated total losses in the AASHTO Standard Specifications (AASHTO 2002), Article 9.16.2.2 could be used. Doing so for this example would provide an estimate of total prestress loss of 45 ksi.

For precast, pretensioned girders, time dependent losses can be approximated by:

$$\Delta f_{pLT} = 10.0\frac{f_{pi}A_{ps}}{A_g}\gamma_h\gamma_{st} + 12.0\gamma_h\gamma_{st} + \Delta f_{pR}$$

LRFD Design Eq. 5.9.3.3-1

where $\gamma_h = 1.7 - 0.01H$

Assuming a relative humidity H ranging between 40 to 100 percent.

For this example, assume $H = 60$ percent or refer to LRFD Design Figure 5.4.2.3.3-1

$$\gamma_h = 1.7 - 0.01(60) = 1.1$$

and:

$$\gamma_{st} = \frac{5}{1 + f_{ci}'} = \frac{5}{1 + 4.88} = 0.85$$

and:

Δf_{pR} = an estimation of relaxation losses

$\Delta f_{pR} = 4$ ksi

and:

$f_{pi} = 189$ ksi

then:

$$\Delta f_{pLT} = 10.0 \times \frac{578}{369} \times 1.1 \times 0.85 + 12.0 \times 1.1 \times 0.85 + 4$$

$$\Delta f_{pLT} = 29.89 \text{ ksi}$$

$$\text{Using, } \Delta f_{pLT} = 30 \text{ ksi}$$

Total prestress losses:

$\Delta f_{pT} = 18 + 30 = 48$ ksi

Effective Prestress:

Δf_{pe} = Initial Prestress – Total Prestress Losses

= 189 – 48 = 141 ksi

Effective prestress force in straight strands:

$P_{straight} = 1.84 \times 141 = 260$ kip

Effective prestress force in draped strands:

$P_{draped} = 1.22 \times 141 = 172$ kip

5.2.5 Determining the Cracking Moment Capacity of the Critical Section

Critical section adopted for Shear Load Rating = d_v from the face of the support = 31.7 inches

Determining the Cracking Moment Capacity: LRFD Design Eq. 5.6.3.3.-1

$$M_{cr} = \gamma_3 \left[\left(\gamma_1 f_r + \gamma_2 f_{cpe} \right) S_c - M_{dnc} \left(\frac{S_c}{S_{nc} - 1} \right) \right]$$

$\gamma_1 = 1.0$

$\gamma_2 = 1.0$

$\gamma_3 = 1.0$

Non-Composite Section Modulus

$$S_{nc} = \frac{I_{nc}}{y_b} = \frac{50980}{15.83} = 3220\,\text{in}^3$$

Eccentricity of Strands from girder C.G.

$$e = y_b - \frac{12 \times y_{straight} + 8 \times y_{draped}}{20} = 15.83 - \frac{12 \times 4.67 + 8 \times 24.4}{20} =$$

$$= 3.268\,\text{in.}$$

Compressive stress in Concrete due to prestress only in tension zone

$$f_{cpe} = \frac{P}{A} + \frac{P \times e}{S_{nc}} = \frac{432^k}{369^{in^2}} + \frac{432^k \times 3.27^{in}}{3220.5^{in^3}} = 1.61\,\text{ksi}$$

Modulus of Rupture,

$$f_r = 0.24\sqrt{f_c'} = 0.24 \times \sqrt{5} = 0.54\ \text{ksi}$$

Composite Section Modulus

$$S_c = \frac{I_g}{y_{bc}} = \frac{207384\,\text{in}^4}{32.8\,\text{in}} = 6315\,\text{in}^3$$

Deal Load moment on Non-Composite Section at critical section

$$M_{dnc} = \frac{1.368^{k/ft} \times \left(47.25^{ft} \right)}{2} 2.64^{ft} - \frac{1.368^{k/ft} \times \left(2.64^{ft} \right)^2}{2} = 81\text{k-ft} = 966\ \text{k-in}$$

Therefore, cracking moment:

$$M_{cr} = 1.0\left[\left(1.0\times 0.54^{ksi} + 1.0\times 1.61^{ksi}\right)6315^{in^3} - 966^{k-in}\left(\frac{6315^{in^3}}{3220^{in^3}} - 1\right)\right]$$

= 12621 k-in

=1052 k-ft

5.2.6 Computing Nominal Shear Resistance at Critical Section

LRFD Design 5.7.3.4.2

Calculating strain at the centroid of the tension reinforcement at critical section:

$$\varepsilon_s = \frac{\left(\frac{|M_u|}{d_v} + 0.5N_u + |V_u - V_p| - A_{ps}f_{po}\right)}{E_s A_s + E_p A_{ps}}$$

LRFD Design Eq. 5.7.3.4.2-4

If, ε_s is negative then:

$$\varepsilon_s = \frac{\left(\frac{|M_u|}{d_v} + 0.5N_u + |V_u - V_p| - A_{ps}f_{po}\right)}{E_s A_s + E_p A_{ps} + E_c A_{ct}} \le 0.40\times 10^{-3}$$

LRFD Design Eq. B5.2-5

Since MCFT uses an iterative process of determining the shear capacity, the equation is modified to take account of the moment in the iterative process.

$$\varepsilon_s = \frac{\left(\frac{|M_{u-DL} + V_{u-LL}\eta_{LL}|}{d_v} + 0.5N_u + |V_u - V_p| - A_{ps}f_{po}\right)}{E_s A_s + E_p A_{ps}}$$

$N_u = 0$

Since,

$M_u = M_{u\text{-}DL} + M_{u\text{-}LL}$

and,

$$\eta_{LL} = \frac{M_{u-LL}}{V_{u-LL}}$$

$M_{u\text{-}LL} = V_{u\text{-}LL}\eta_{LL}$

It can be re-written as,

$M_u = M_{u\text{-}DL} + V_{u\text{-}LL}\eta_{LL}$

also,

$V_u = V_{u\text{-}DL} + V_{u\text{-}LL}$

Common input data for all load cases:

Dist. from abutment c/l = 31.7 in.

Shear depth, d_v = 31.7 in.

Web width, b_v = 6 in.

Flexural tension depth = 0.5h = 0.5 × 44 = 22 in.

Concrete area in tension, A_{ct} = 209 in.^{2}

Area of shear reinforcement, A_v = 0.4 in.^{2}

Spacing of shear reinforcement, s_v = 13 in.

$0.18f'_c b_v d_v$ = 171 kip (girder end not built integrally with support)

$E_c A_{ct}$ = 960236 in^2

Area of Top rebar = 1.23 in

$V_p = P_{draped} \times \sin(\theta_{draped})$ = 16 kip

$A_{ps,straight} f_{po}$ = 1.84 × 0.7 × 270 = 347.8 kip

5.2.6.1 Determining Shear Capacity for Inventory Level:

5.2.6.1.1 Maximum Shear Concurrent Moment Case:

As determined in Section 5.2.3,

$V_{uS(inv)} = V_{u(DC)} + V_{us(inv)}$ = 185.9 kip

$M_{uS(inv)} = M_{u(DC)} + M_{us(inv)}$ = 5206 kip-in

$$\eta_{ms(inv)} = \frac{M_{us(inv)}}{V_{us(inv)}} = \frac{3867}{146.1} = 26.5\left(\text{LL ratio}\right)$$

Determining the shear capacity at critical section after iterating V_u and M_u:

Since, $M_{uS} < M_{cr}$, iteration is not required, assuming strain at centroid of tension steel as zero

$\varepsilon_s = 0.0$

$\theta = 29 + 3500\varepsilon_s = 29 + 3500 \times 0.0 = 29°$

$$\beta = \frac{4.8}{1+750\varepsilon_s} = \frac{4.8}{1+750\times 0.0}$$
$$= 4.8$$

Shear strength of concrete:

$$V_c = 0.0316\beta\lambda\sqrt{f_c'}b_v d_v$$
$$= 0.0316\times 4.8\times 1\times\sqrt{5}\times 6\times 31.7$$
$$= 64.5\,\text{kip}$$

Shear strength of shear reinforcement:

$$V_s = \frac{A_v f_y d_v \cot(\theta)}{s}$$
$$= \frac{0.4\times 60\times 31.7\cot(29)}{13}$$
$$= 104\,\text{kip}$$

Total shear capacity of the section:

Minimum of

$V_c + V_s = 64.5 + 104 = 168.5$ kip

and

$V_n = 0.18f'_c b_v d = 171$ kip

Therefore,

$V_n = 168.5 + V_p = 168.5 + 16 = 184.5$ kip

$\phi V_n = 0.9 \times 184.5 = 166$ kip

5.2.6.1.2 Maximum Moment Concurrent Shear Case:
As determined in Section 5.2.3,

$V_{uM(inv)} = V_{u(DC)} + V_{um(inv)} = 185.8$ kip

$M_{uM(inv)} = M_{u(DC)} + M_{um(inv)} = 5242$ kip-in

$$\eta_{mm(inv)} = \frac{M_{um(inv)}}{V_{um(inv)}} = \frac{3904}{146} = 26.7\ (\text{LL ratio})$$

Determining the shear capacity at critical section after Iterating V_u and M_u:

Since, $M_{uM} < M_{cr}$, iteration is not required, assuming strain at centroid of tension steel as zero

$\varepsilon_s = 0.0$

$\theta = 29 + 3500\varepsilon_s = 29 + 3500 \times 0.0 = 29°$

$$\beta = \frac{4.8}{1 + 750\varepsilon_s} = \frac{4.8}{1 + 750 \times 0.0}$$
$$= 4.8$$

Shear Strength of Concrete:

$$V_c = 0.0316\beta\lambda\sqrt{f_c'}b_v d_v$$
$$= 0.0316 \times 4.8 \times 1 \times \sqrt{5} \times 6 \times 31.7$$
$$= 64.5\,\text{kip}$$

Shear Strength of Shear Reinforcement:

$$V_s = \frac{A_v f_y d_v \cot(\theta)}{s}$$
$$= \frac{0.4 \times 60 \times 31.7 \cot(29)}{13}$$
$$= 104\,\text{kip}$$

Total shear capacity of the section:

Minimum of

$V_c + V_s = 64.5 + 104 = 168.5$ kip

and

$V_n = 0.18 f'_c b_v d = 171$

Therefore,

$V_n = 168.5 + V_p = 168.5 + 16 = 184.5$ kip

$\phi V_n = 0.9 \times 184.5 = 166$ kip

5.2.7 Longitudinal Reinforcement Check at the Critical Section

Tensile capacity of the longitudinal reinforcement on the flexural tension side of the member is proportioned to satisfy:

$$A_{ps} f_{ps} + A_s f_y \geq \frac{|M_u|}{d_v \phi_f} + 0.5\frac{N_u}{\phi_c} + \left(\left|\frac{V_u}{\phi_v} - V_p\right| - 0.5V_s\right)\cot\theta$$

$\phi_f = 1.0$

$\phi_v = 0.9$ LRFD Design Eq. 5.7.3.5-1

$N_u = 0$

Since the Longitudinal Reinforcement Check uses an iterative process of determining the shear capacity corresponding to the longitudinal reinforcement, the RHS of the equation is modified to take account of the moments in the iterative process.

$$A_{ps}f_{ps} + A_s f_y \geq \frac{\left|M_{u-DL} + V_{u-LL}\eta_{LL}\right|}{d_v \phi_f} + 0.5\frac{N_u}{\phi_c} + \left(\left|\frac{V_u}{\phi_v} - V_p\right| - 0.5V_s\right)\cot\theta$$

Since,

$M_u = M_{u\text{-}DL} + M_{u\text{-}LL}$

and,

$$\eta_{LL} = \frac{M_{u-LL}}{V_{u-LL}}$$

$M_{u\text{-}LL} = V_{u\text{-}LL}\eta_{LL}$

It can be re-written as,

$M_u = M_{u\text{-}DL} + V_{u\text{-}LL}\eta_{LL}$

Transfer length = $60d_b$ (per 5.9.4.3.1)

= 30 inches

Critical section = 31.7 inches > 30 inches, hence, full f_{pe} can be used.

5.2.7.1 Determining Shear Strength Corresponding to Longitudinal Reinforcement :

5.2.7.1.1 Maximum Shear Concurrent Moment Case (Inventory Level):

As determined in Section 5.2.3,

$V_{uS(inv)} = V_{u(DC)} + V_{us(inv)} = 185.9$ kip

$M_{uS(inv)} = M_{u(DC)} + M_{us(inv)} = 5206$ kip-in

$$\eta_{ms(inv)} = \frac{3867}{146.1} = 26.5\left(\text{LL ratio}\right)$$

Determining the RHS of LRFD Design Eq. 5.7.3.5-1 by iterating V_u and M_u:

The iteration process is illustrated in Section 5.1.3. The end result after iterations is shown here.

$V_{us(inv)}$ after iteration = 91 kip (live load iterations only)

$V_u = V_{u(DC)} + V_{us(inv)} = 130.7$ kip

$\eta_{ms(inv)} = 26.5$

$\left|\frac{M_{u(DC)} + V_{us(inv)}\eta_{ms(inv)}}{d_v}\right| = 118.2$ kip, should be greater than $|V_u - V_p| = 114.9$ kip

Adopt, $\left|\frac{M_{u(DC)} + V_{us(inv)}\eta_{ms(inv)}}{d_v}\right| = 118.2$ kip

$$\varepsilon_s = \frac{\left(118.2 + \left|130.7 - 16\right| - 347.0\right)}{28,500 \times 1.84}$$
$$= -0.00217$$

Therefore, using Eq. B5.2-5

$E_c A_{ct} = 960235$ in^2

$$\varepsilon_s = \frac{\left(118.2 + \left|130.7 - 16\right| - 347.0\right)}{28,500 \times 1.84 + 960235}$$
$$= -0.00011$$

$\theta = 29 + 3500\varepsilon_s = 29 + 3500 \times -0.00011 = 28.6°$

Shear strength of shear reinforcement:

$$V_s = \frac{A_v f_y d_v \cot(\theta)}{s}$$
$$= \frac{0.4 \times 60 \times 31.7 \cot(28.6)}{13}$$
$$= 107 \text{ kip}$$

RHS of the LRFD Design Eq. 5.7.3.5-1

$$RHS = \frac{\left|M_{u(DC)} + V_{us(inv)}\eta_{LL}\right|}{d_v \phi_f} + \left(\left|\frac{V_u}{\phi_v} - V_p\right| - 0.5V_s\right)\cot\theta$$
$$= \frac{118.2}{1} + \left(\left|\frac{130.7}{0.9} - 16\right| - 0.5 \times 107\right)\cot(28.6)$$
$$= 259 \text{ kip}$$

LHS of the LRFD Design Eq. 5.7.3.5-1

$$LHS = A_{ps,straight} f_{pe}$$
$$= 1.84 \times 141$$
$$= 259\,\text{kip}$$

Since LHS=RHS, shear capacity corresponding to longitudinal reinforcement is

$$\phi_v V_n = 130.7\,\text{kip}$$

5.2.7.1.2 Maximum Moment Concurrent Shear Case (Inventory Level):
As determined in Section 5.2.3,

$V_{uM(inv)} = V_{u(DC)} + V_{um(inv)} = 185.8$ kip

$M_{uM(inv)} = M_{u(DC)} + M_{um(inv)} = 5242$ kip-in

$$\eta_{mm(inv)} = \frac{M_{um(inv)}}{V_{um(inv)}} = \frac{3904}{146} = 26.7\ (\text{LL ratio})$$

Determining the RHS of LRFD Design Eq. 5.7.3.5-1 by iterating V_u and M_u:

$V_{um(inv)}$ after iteration = 90.7 kip (live load iterations only)

$V_u = V_{u(DC)} + V_{us(inv)} = 130.4$ kip

$\eta_{ms(inv)} = 26.7$

$$\left|\frac{M_{u(DC)} + V_{um(inv)}\eta_{mm(inv)}}{d_v}\right| = 118.8\,\text{kip} < |V_u - V_p| = 115\text{ kip}$$

Adopt, $\left|\dfrac{M_{u(DC)} + V_{um(inv)}\eta_{mm(inv)}}{d_v}\right| = 118.8\,\text{kip}$

$$\varepsilon_s = \frac{\left(118.8 + |115| - 347.8\right)}{28{,}500 \times 1.84}$$
$$= -0.00217$$

Therefore, using Eq. B5.2-5

$E_c A_{ct} = 960235$ in^2

$$\varepsilon_s = \frac{\left(118.8 + |115| - 347.8\right)}{28{,}500 \times 1.84 + 960235}$$
$$= -0.00011$$

$\theta = 29 + 3500\varepsilon_s = 29 + 3500 \times \text{-}0.00011 = 28.6°$

Shear strength of shear reinforcement:

$$V_s = \frac{A_v f_y d_v \cot(\theta)}{s}$$
$$= \frac{0.39 \times 60 \times 31.7 \cot(28.6)}{13}$$
$$= 107 \text{ kip}$$

RHS of the LRFD Design Eq. 5.7.3.5-1

$$RHS = \frac{\left|M_{u(DC)} + V_{um(inv)}\eta_{LL}\right|}{d_v \phi_f} + \left(\left|\frac{V_u}{\phi_v} - V_p\right| - 0.5V_s\right)\cot\theta$$
$$= \frac{118.8}{1} + \left(\left|\frac{130.4}{0.9} - 16\right| - 0.5 \times 107\right)\cot(28.6)$$
$$= 259 \text{ kip}$$

LHS of the LRFD Design Eq. 5.7.3.5-1

$LHS = A_{ps,straigh} f_{pe} = 1.84 \times 141 = 259$ kip

Since LHS=RHS, shear capacity corresponding to longitudinal reinforcement is:

$$\phi_v V_n = 130.4 \text{ kip}$$

5.2.8 Horizontal Shear Check at Critical Section

The equations and variables used here are per Hovell et al. (2013).

Horizontal shear force is determined as follows:

Here total V_u is iterated instead of only live load V_{LL} since there is no use of corresponding bending moment in the calculations.

The change in live load shear can be calculated as $V_{LL} = V_u - V_{DC}$

Assuming $V_u = 2977$ kip

$b_w = 6$ in.

$d_{p,straight} = 39.3$ in.

$$v_{hs} = \frac{2977}{6 \times 39.3} = 12.615 \text{ksi}$$

$y_{crit} = 12$ in.

$l_{lp} = 10$ in.

h = 44 in.

$$l_{crit} = d_v - \frac{l_{lp}}{2} - h - y_{crit} = 2 \text{ in}$$

$V_{u,hs} = v_{hs} b_w l_{crit} = 12.615 \times 6 \times 2 = 151$ kip

Horizontal shear capacity can be determined by Eq. 7-14 from Hovell et al. (2013)

$V_{ni1} = k_d[cA_{cv} + \mu(A_{vf} f_y - 0.04 P_{PS})]$

where,

$k_d = 1.0$

$c = 0.4$ ksi

$A_{cv} = b_w d_v = 6 \times 31.7 = 190$ in^2

$\mu = 1.4$

$A_{vf} = 4 \times A_s = 4 \times 0.4 = 1.6$ in^2

$f_y = 60$ ksi

$P_{PS} = (A_{ps,\ draped} + A_{ps,straight}) \times f_{pe} = 3.06 \times 141 = 432$ kip

$K_1 = 0.25$

$K_2 = 1.5$ ksi

Therefore,

$V_{ni1} = 1[0.4 \times 190 + 1.4(1.6 \times 60 - 0.04 \times 432)]$

$V_{ni1} = 184$ kip

Horizontal shear capacity is the minimum of:

$\phi V_{ni} = \min(V_{n1}, K_1 f'_c A_{cv}, K_2 A_{cv}) \times 0.9 = \min(184, 238, 285) \times 0.9 = 165$ kip

5.2.9 Load Rating Factors

The Shear Capacity is the minimum of:

- Nominal shear resistance, 166 kips
- Shear resistance corresponding to longitudinal reinforcement, 130.7 kips
- Horizontal shear resistance, 165 kips

5.2.9.1 Max Shear Concurrent Moment Case (Inventory Level)
Shear Capacity for Inventory Level:

ϕV_n= 130.7 kip {min(166 kip, 130.7 kip, 165 kip)}

$V_{u(DC)} = \gamma_{DC} \times V_{DC}$ = 39.7 kip

$V_{us(inv)} = \gamma_{LL}(inv) \times V_s$ = 146.1 kip

$$\text{Shear Load Rating} = \frac{\phi V_n - V_{u(DC)}}{V_{us(inv)}} = 0.62$$

5.2.9.2 Max Moment Concurrent Shear Case (Inventory Level)
Shear Capacity for Inventory Level:

ϕV_n= 130.4 kip {min(166 kip, 130.4 kip, 165 kip)}

$V_{u(DC)} = \gamma_{DC} \times V_{DC}$ = 39.7 kip

$V_{um(inv)} = \gamma_{LL}(inv) \times V_m$ = 146 kip

$$\text{Shear Load Rating} = \frac{\phi V_n - V_{u(DC)}}{V_{um(inv)}} = 0.62$$

5.2.10 Load Rating at Span Quarter Point Summary

Although no calculations are provided in this example, an additional load rating is carried out at the quarter point of the simply supported span with results shown below:

5.2.10.1 *Max Shear Concurrent Moment Case (Inventory Level)*
Shear Capacity for Inventory Level:

ϕV_n= 82.9 kip

$V_{u(DC)} = \gamma_{DC} \times V_{DC}$ = 22 kip

$V_{us(inv)} = \gamma_{LL}(inv) \times V_s$ = 105 kip

$$\text{Shear Load Rating} = \frac{\phi V_n - V_{u(DC)}}{V_{us(inv)}} = 0.58$$

5.2.10.2 *Max Moment Concurrent Shear Case (Inventory Level)*
Shear Capacity for Inventory Level:

ϕV_n= 62.8 kip

$V_{u(DC)} = \gamma_{DC} \times V_{DC}$ = 22 kip

$V_{um(inv)} = \gamma_{LL}(inv) \times V_m$ = 68 kip

$$\text{Shear Load Rating} = \frac{\phi V_n - V_{u(DC)}}{V_{um(inv)}} = 0.60$$

5.3 EXAMPLE – CONTINUOUS REINFORCED CONCRETE GIRDER

This example is for a design load rating for shear, for an interior girder of a three-span continuous, CIP RC girder. The girders are built integrally with their interior supports and with CIP full-depth diaphragms at end supports. The details indicate the deck was placed after the girders were cast and cured, but with the girders shored during deck placement.

Two sections are evaluated:

- Section 1 is located at d_v from the end bearing
- Section 2 is located at d_v from the face of the interior support

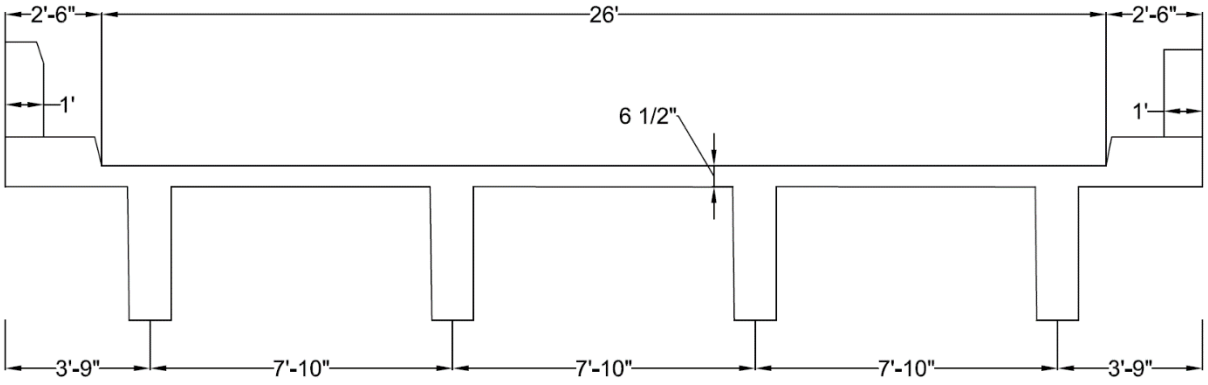

TRANSVERSE SECTION THRU DECK

- 45.4 Deg Right Forward Skew
- 9" thick integral diaphragms at each support and midspan

Source: Authors

Figure 25. Transverse section.

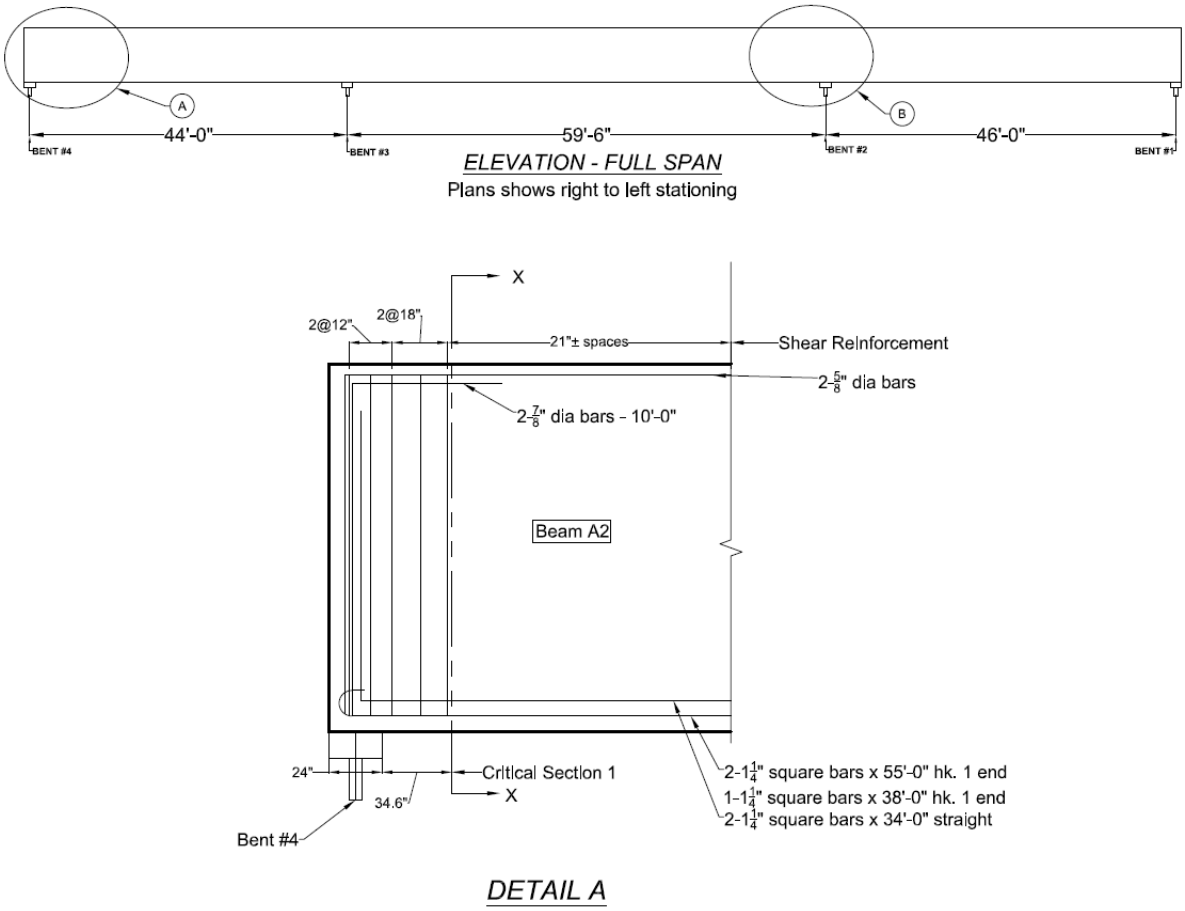

Source: Authors

Figure 26. Location of critical sections and part girder elevation at critical section 1.

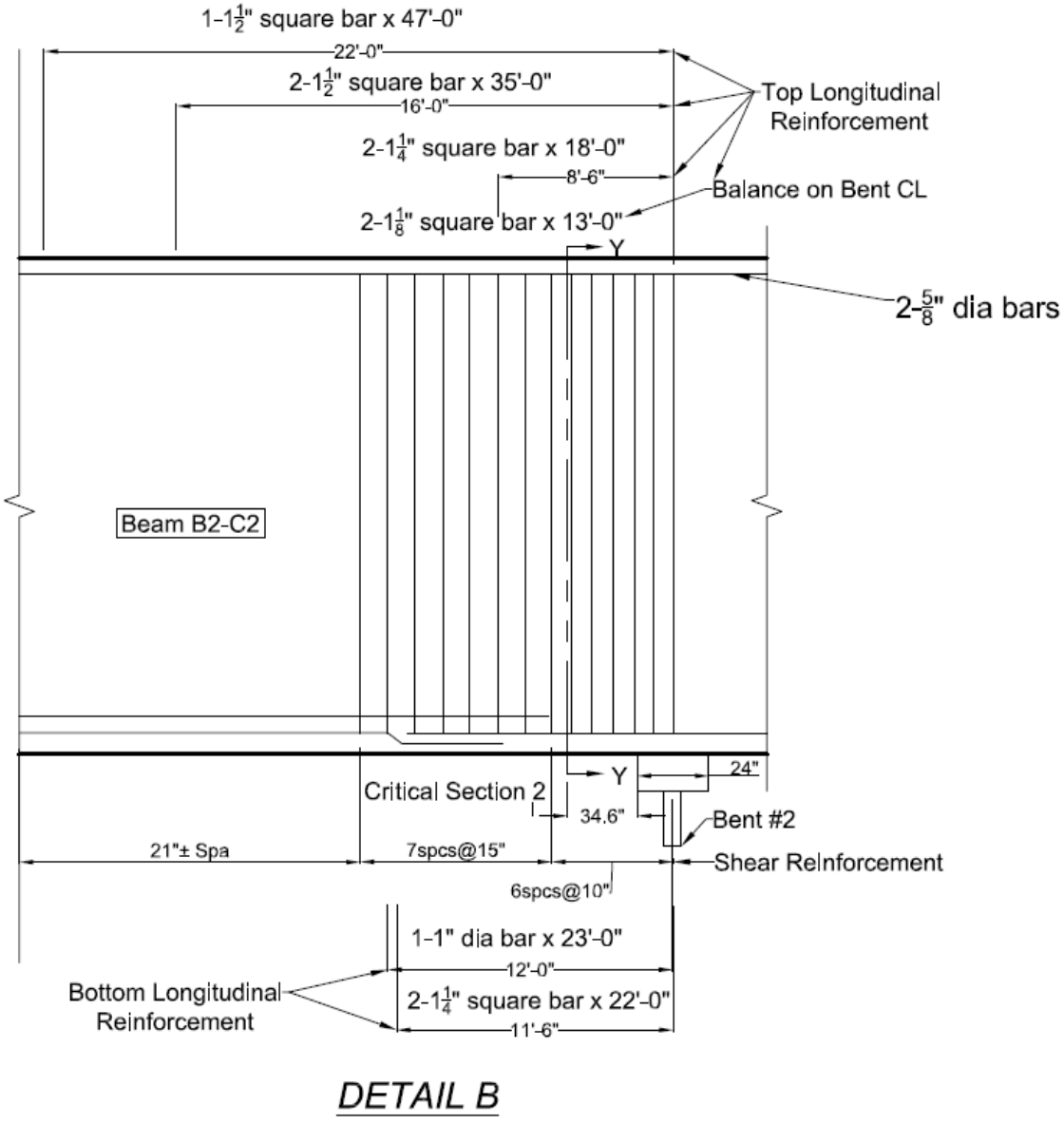

Source: Authors

Figure 27. Part girder elevation at critical section 2.

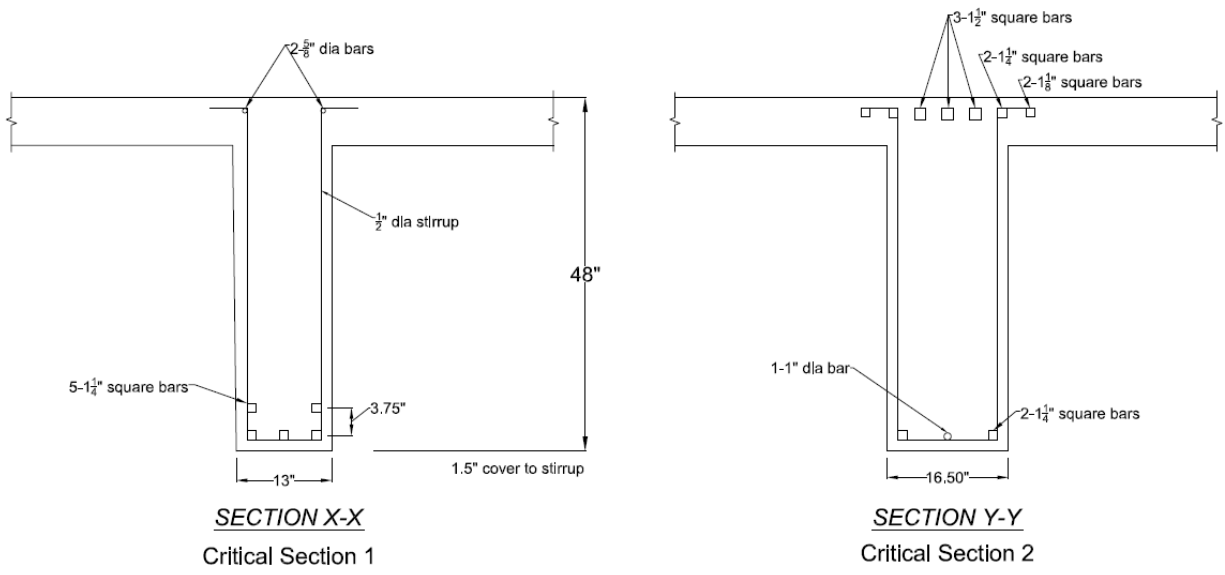

Source: Authors

Figure 28. Cross-section at critical sections.

5.3.1 Bridge Data

Span:	44 ft – 59.5 ft – 46 ft
Year Built:	1969
Materials:	
Concrete:	f_c' = 2.75 ksi (Deck & Beam)
Tension Steel Reinforcement:	5 – 1¼ in square bars (critical section 1)
	2 – 1⅛ in, 2 – 1¼ in & 3 – 1½ in square bars
	(critical section 2)
	Grade 40
Compression Steel:	2 – ⅝ inch diameter bars (critical section 1)
	1 – 1inch diameter & 2 – 1¼ in square bars
	Grade 40
Stirrups:	All spans with ½ inch diameter stirrups, refer to **Figure 26** and **Figure 27** for spacing
Condition:	Good
Riding Surface:	Not provided
ADTT:	Not provided
Skew:	45.4 °

Effective Flange Width b_e may be taken as the tributary width perpendicular to the axis of the member LFRD Design 4.6.2.6.1

Effective Flange Width $b_e = 84 \text{ in} + 10 \text{ in} = 94 \text{ in. (Spacing)}$

Modulus of Elasticity of Materials:

$Ec = 120{,}000\, K_1\, w_c^{2.0}\, f_c'^{0.33}$ LRFD Design Eq. 5.4.2.4-1

For Concrete,

$Ec = 120{,}000 \times 1 \times (0.15)^{2.0} \times (2.8)^{0.33} = 3770$ ksi

For Reinforcing Steel

E_s = 29,000 ksi

5.3.2 Summary of Section Properties

5.3.2.1 CIP – T-shaped Girder (Narrowest Section):

D = 48 in.

b_w = 13 in.

$b_f = s$ = 94 in.

t_f = 6.5 in.

$$I_{x-beam} = \frac{bd^3}{12} = \frac{13 \times (48 - 6.5)^3}{12} = 77430 \text{in}^3$$

Composite Section Properties

t_{slab} = 6 in.

A_{comp} = 1151 in.^{2}

y_{bot} = 33.5 in.

y_{top} = D – y_{bot} = 14.5 in.

I_{comp} = 244,695 in^4

$$S_b = \frac{I_{comp}}{y_{bot}} = 7304 in.^3$$

$$S_t = \frac{I_{comp}}{y_{bot}} = 16876 in.^3$$

Reinforcement Critical Section 1:

Rebars in tension zone:

Longitudinal Rebar = 5 – 1.25 in square bares

Total Area of the Rebar = A_s = 7.81 in.^{2}

Rebar CG from Top = 45.4 in.

Rebars in compression zone:

Longitudinal Rebar = 2 – 0.625 in square bars

Total Area of the Rebar = A'_s = 0.61 in.^{2}

Rebar CG from Top = 2.3 in.

Shear Reinforcement

Shear Reinforcement Rebar = #4

Area of Shear Reinforcement = 0.4 in.^{2} (Two-Legged Stirrups)

Spacing of Shear Reinforcement = 18 in.

Reinforcement Critical Section 2:

Rebars in Tension zone:

Longitudinal Rebar = 2 – 1.125 in, 2 - 1.25 in & 3 – 1.5 in square bars

Total Area of the Rebar = A_s = 12.41 in.^{2}

Rebar CG from Bottom = 45.3 in.

Rebars in Compression zone:

Longitudinal Rebar = 1 – 1 in. dia & 2 – 1.25 in square bars

Total Area of the Rebar = A'_s = 3.91 in.^{2}

Rebar CG from Bottom = 2.3 in.

Shear Reinforcement

Shear Reinforcement Rebar = #4

Area of Shear Reinforcement = 0.4 in.^{2} (Two-Legged Stirrups)

Spacing of Shear Reinforcement = 10 in.

5.3.2.2 Determining Shear Depth at Critical Load Rating Section

As a calculation expedient, the shear depth is taken as 0.72h as allowed by AASHTO LRFD Design Article 5.7.2.8 (binding).

Adopting effective shear depth as:

0.72h = 0.72 × 48 in = 34.6 in

5.3.3 Factored Loads

This is a design load rating; the live loads are calculated according to HL-93 loading. The live load moments and shears include the Dynamic Load Allowance, IM, from AASHTO LRFD Article 3.6.2 (binding) and AASHTO MBE Article 6A.4.3.2 (nonbinding). Live loads are distributed to the girder using the provisions of AASHTO LRFD Article 4.6.2.2 (binding).

5.3.3.1 Critical Section - 1

5.3.3.1.1 Strength-I Load Combination - Inventory Level

Load Factors per Strength-I Load Combination

$\gamma_{DC} = 1.25$

$\gamma_{LL}(inv) = 1.75$

Factored Shear Forces and Moments due to Dead Loads

$V_{u(DC)\text{-Sec1}} = \gamma_{DC} \times V_{Dc} = 24.0$ kip

$M_{u(DC)\text{-Sec1}} = \gamma_{DC} \times M_{DC} = 1296$ kip-in

Inventory Live Load – Max Shear Concurrent Moment Case

$V_{us(inv)} = \gamma_{LL}(inv) \times V_s \times g_v = 105.1$ kip

$M_{us(inv)} = \gamma_{LL}(inv) \times M_s \times g_m = 4264$ kip-in

Inventory Live Load – Max Moment Concurrent Shear Case

$V_{um(inv)} = \gamma_{LL}(inv) \times V_m \times g_v = 105.1$ kip

$M_{um(inv)} = \gamma_{LL}(inv) \times M_m \times g_m = 4264$ kip-in

Ultimate Shear Force:

$V_{uS(inv)} = V_{u(DC)} + V_{us(inv)} = 129$ kip (Max Shear Case)

$V_{uM(inv)} = V_{u(DC)} + V_{um(inv)} = 129$ kip (Max Moment Case)

Ultimate Bending Moment:

$M_{uS(inv)} = M_{u(DC)} + M_{us(inv)} = 5560$ kip-in (Max Shear Case)

$M_{uM(inv)} = M_{u(DC)} + M_{um(inv)} = 5560$ kip-in (Max Moment Case)

5.3.3.2 Critical Section - 2

5.3.3.2.1 Strength-I Load Combination - Inventory Level

Load Factors per Strength-I Load Combination

$\gamma_{DC} = 1.25$

$\gamma_{LL}(inv) = 1.75$

Factored Shear Forces and Moments due to Dead Loads

$V_{u(DC)\text{-Sec2}} = \gamma_{DC} \times V_{DC} = 52.6$ kip

$M_{u(DC)\text{-Sec2}} = \gamma_{DC} \times M_{DC} = -4320$ kip-in

Inventory Live Load – Max Shear Concurrent Moment Case

$V_{us(inv)} = \gamma_{LL}(inv) \times V_s \times g_v = 147.3$ kip

$M_{us(inv)} = \gamma_{LL}(inv) \times M_s \times g_m = -2102$ kip-in

Inventory Live Load – Max Moment Concurrent Shear Case

$V_{um(inv)} = \gamma_{LL}(inv) \times V_m \times g_v = 38.3$ kip

$M_{um(inv)} = \gamma_{LL}(inv) \times M_m \times g_m =$ -5678 kip-in

Ultimate Shear Force:

$V_{uS(inv)} = V_{u(DC)} + V_{us(inv)} = 200$ kip (Max Shear Case)

$V_{uM(inv)} = V_{u(DC)} + V_{um(inv)} = 91$ kip (Max Moment Case)

Ultimate Bending Moment:

$M_{uS(inv)} = M_{u(DC)} + M_{us(inv)} =$ -6422 kip-in (Max Shear Case)

$M_{uM(inv)} = M_{u(DC)} + M_{um(inv)} =$ -9998 kip-in (Max Moment Case)

5.3.4 Determining the Cracking Moment Capacity of the Critical Sections

Critical section adopted for Shear Load Rating = d_v from the face of the support = 34.6 inches

Determining the Cracking Moment Capacity: LRFD Design Eq. 5.6.3.3.-1

$$M_{cr} = \gamma_3 \left[\left(\gamma_1 f_r + \gamma_2 f_{cpe} \right) S_c - M_{dnc} \left(\frac{S_c}{S_{nc} - 1} \right) \right]$$

$\gamma_1 = 1$
$\gamma_2 = 1$
$\gamma_3 = 1$

Modulus of Rupture

$$f_r = 0.24\sqrt{f_c'} = 0.24 \times \sqrt{2.75} = 0.4 \text{ ksi}$$

Composite Section Modulus

$$S_{c-top} = \frac{I_g}{y_{top}} = \frac{244613 \text{in}^4}{14.5 \text{in}} = 16865 \text{in}^3$$

$$S_{c-bot} = \frac{I_g}{y_{bot}} = \frac{244613 \text{in}^4}{33.5 \text{in}} = 7303 \text{in}^3$$

Therefore, cracking moment:

$$M_{cr-top} = 1.0\left[\left(1.0 \times 0.4^{ksi} \right) 16865^{in^3} \right]$$

$= 6712$ k-in

$$M_{cr-bot} = 1.0\left[\left(1.0 \times 0.4^{ksi} \right) 7303^{in^3} \right]$$

$= 2906$ k-in

5.3.5 Computing Nominal Shear Resistance at Critical Sections

LRFD Design 5.7.3.4.2

Calculating strain at the centroid of the tension reinforcement at critical section:

$$\varepsilon_s = \frac{\left(\frac{|M_u|}{d_v} + 0.5N_u + |V_u - V_p| - A_{ps}f_{po}\right)}{E_s A_s + E_p A_{ps}}$$ LRFD Design Eq. 5.7.3.4.2-4

If, ε_s is negative then:

$$\varepsilon_s = \frac{\left(\frac{|M_u|}{d_v} + 0.5N_u + |V_u - V_p| - A_{ps}f_{po}\right)}{E_s A_s + E_p A_{ps} + E_c A_{ct}} \le 0.40\times10^{-3}$$ LRFD Design Eq. B5.2-5

Since MCFT uses an iterative process of determining the shear capacity the equation is modified to take account of the moment in the iterative process.

$$\varepsilon_s = \frac{\left(\frac{|M_{u-DL} + V_{u-LL}\eta_{LL}|}{d_v} + 0.5N_u + |V_u - V_p| - A_{ps}f_{po}\right)}{E_s A_s + E_p A_{ps}}$$

$N_u = 0$

Since,

$M_u = M_{u\text{-}DL} + M_{u\text{-}LL}$

and,

$$\eta_{LL} = \frac{M_{u-LL}}{V_{u-LL}}$$

$M_{u\text{-}LL} = V_{u\text{-}LL}\eta_{LL}$

It can be re-written as,

$M_u = M_{u\text{-}DL} + V_{u\text{-}LL}\eta_{LL}$

also,

$V_u = V_{u\text{-}DL} + V_{u\text{-}LL}$

5.3.5.1 *Minimum Shear Reinforcement Check:*
Determining maximum spacing allowed:

Rewriting LRFD Design Eq. 5.7.2.5-1

$$s \le \frac{A_v f_y}{0.0316 \lambda b_v \sqrt{f_c'}}$$

Therefore, maximum spacing allowed to maintain minimum reinforcement criteria is:

For critical section 1

$$s_{\max} \le \frac{0.4 \times 40}{0.0316 \times 1 \times 13 \times \sqrt{2.75}}$$
$$= 23.1\text{in} > 18\text{in (provided)}$$

$\lambda = 1.0$

Therefore, meets the minimum requirement.

For critical section 2

$$s_{\max} \le \frac{0.4 \times 40}{0.0316 \times 1 \times 16.7 \times \sqrt{2.75}}$$
$$= 18\text{in} > 10\text{in (provided)}$$

$\lambda = 1.0$

Therefore, meets the minimum requirement.

Since this is a reinforced concrete element, the equation for β depends on whether the minimum shear reinforcement specifications of AASHTO LRFD Article 5.7.2.5 (binding) are satisfied. If the minimum reinforcement specifications are not met, the following calculations to determine β are used:

β factor changes to:

$$\beta = \frac{4.8}{1 + 750\varepsilon_s} \frac{51}{(39 + s_{xe})}$$ LRFD Design Eq. 5.7.3.4.2-2

where,

$$s_{xe} = s_x \frac{1.38}{a_g + 0.63}$$

Had the shear reinforcement not met minimum values, a load rater could assume the maximum aggregate size, a_g, was 1.5 inches and the crack spacing parameter, s_x, would be governed by d_v, 34.6 inches. These provide a value for s_{xe} of 22.4 inches. The resulting reduction factor applied to β would be 0.83.

5.3.5.2 Determining Shear Capacity for Inventory Level (Critical Section–1):
Input data:

Dist. from abutment c/l = 12 + 34.6 = 46.6 in.

Shear depth, d_v = 34.6 in.

Web width, b_v = 13 in.

Flexural tension depth = 0.5D = 0.5 × 45 = 24 in.

Concrete area in tension, A_{ct} = 312 in.^{2}

Area of shear reinforcement, A_v = 0.4 in.^{2}

Spacing of shear reinforcement, s_v = 18 in.

$0.25f'_c b_v d_v$ = 309 kip

$E_c A_{ct}$ = 1176246 in^2

Area of Top rebar = 0.61 in^2

Area of Bottom rebar = 7.81 in^2

V_p = 0 kip

5.3.5.2.1 Maximum Shear Concurrent Moment Case:
As determined in Section 5.3.3,

$V_{uS(inv)} = V_{u(DC)} + V_{us(inv)}$ = 129 kip

$M_{uS(inv)} = M_{u(DC)} + M_{us(inv)}$ = 5560 kip-in

$$\eta_{ms(inv)} = \frac{M_{us(inv)}}{V_{us(inv)}} = \frac{4264}{105} = 40.6\left(\text{LL ratio}\right)$$

Determining the shear capacity at critical section after iterating V_u and M_u:

Since, $M_{uS} > M_{cr\text{-}bot}$, calculating strain at the CG of tensile steel reinforcement:

$V_{us(inv)}$ after iteration = 76.5 kip (live load iterations only)

$V_u = V_{u(DC)} + V_{us(inv)}$ = 100.5 kip

$\eta_{ms(inv)}$ = 40.6

$\left|\frac{M_{u(DC)} + V_{us(inv)}\eta_{ms(inv)}}{d_v}\right|$ = 127 kip, should be greater than $|V_u - V_p|$ = 100.5 kip

Adopt, $\left|\frac{M_{u(DC)} + V_{us(inv)}\eta_{ms(inv)}}{d_v}\right| = 127\,\text{kip}$

$$\varepsilon_s = \frac{\left(127 + |100.5|\right)}{29{,}000 \times 7.81}$$
$$= 0.00101$$

$\theta = 29 + 3500\varepsilon_s = 29 + 3500 \times 0.00101 = 32.5°$

$$\beta = \frac{4.8}{1 + 750\varepsilon_s} = \frac{4.8}{1 + 750 \times 0.00101}$$
$$= 2.7$$

Shear strength of concrete:

$$V_c = 0.0316\beta\lambda\sqrt{f_c'}\,b_v d_v$$
$$= 0.0316 \times 2.7 \times 1 \times \sqrt{2.75} \times 13 \times 34.6$$
$$= 64\,\text{kip}$$

Shear strength of shear reinforcement:

$$V_s = \frac{A_v f_y d_v \cot(\theta)}{s}$$
$$= \frac{0.39 \times 40 \times 34.6 \cot(32.5)}{18}$$
$$= 47.3\,\text{kip}$$

Total shear capacity of the section:

Minimum of

$V_n = V_c + V_s = 64 + 47.3 = 111.3$ kip

And

$V_n = 0.25 f'_c b_v d = 309$ kip

Therefore,

$V_n = 111.3$ kip

$\phi V_n = 0.9 \times 111.3 = 100.5$ kip

5.3.5.2.2 Maximum Moment Concurrent Shear Case:
As determined in Section 5.3.3,

$V_{uM(inv)} = V_{u(DC)} + V_{um(inv)} = 129$ kip

$M_{uM(inv)} = M_{u(DC)} + M_{um(inv)} = 5560$ kip-in

$$\eta_{mm(inv)} = \frac{M_{um(inv)}}{V_{um(inv)}} = \frac{4264}{105} = 40.6\left(\text{LL ratio}\right)$$

Determining the shear capacity at critical section after iterating V_u and M_u:

Since, $M_{uS} > M_{cr\text{-}bot}$, calculating strain at the CG of tensile steel reinforcement:

$V_{us(inv)}$ after iteration = 76.5 kip (live load iterations only)

$V_u = V_{u(DC)} + V_{us(inv)} = 100.5$ kip

$\eta_{ms(inv)} = 40.6$

$\left|\frac{M_{u(DC)} + V_{us(inv)}\eta_{ms(inv)}}{d_v}\right| = 127$ kip, should be greater than $|V_u - V_p| = 100.5$ kip

Adopt, $\left|\frac{M_{u(DC)} + V_{us(inv)}\eta_{ms(inv)}}{d_v}\right| = 127$ kip

Shear strength of concrete:

$$\begin{aligned} V_c &= 0.0316\beta\lambda\sqrt{f_c'}b_v d_v \\ &= 0.0316 \times 2.7 \times 1 \times \sqrt{2.75} \times 13 \times 34.6 \\ &= 64\,\text{kip} \end{aligned}$$

Shear strength of shear reinforcement:

$$\begin{aligned} V_s &= \frac{A_v f_y d_v \cot\left(\theta\right)}{s} \\ &= \frac{0.39 \times 40 \times 34.6 \cot\left(32.5\right)}{18} \\ &= 47.3\,\text{kip} \end{aligned}$$

Total shear capacity of the section:

$V_n = V_c + V_s = 64 + 47.3 = 111.3$ kip

And

$V_n = 0.25 f'_c b_v d = 309$ kip

Therefore,

$V_n = 111.3$ kip

$\phi V_n = 0.9 \times 111.3 = 100.5$ kip

5.3.5.3 Determining Shear Capacity for Inventory Level (Critical Section–2):
Input data:

Dist. from abutment c/l = 1195.4 in.

Shear depth, $d_v = 36.4$ in.

Web width, $b_v = 16.7$ in. (at critical section)

Flexural tension depth = 0.5h = 0.5×48 = 24 in.

Concrete area in tension, $A_{ct} = 903$ in.^{2}

Area of shear r/f, $A_v = 0.4$ in.^{2}

Spacing of shear r/f, $s_v = 10$ in.

$0.25f'_c b_v d_v = 397$ kip

$E_c A_{ct} = 3404670$ in^2

Area of Top rebar = 12.41 in^2

Area of Bottom rebar = 3.91 in^2

$V_p = 0$ kip

5.3.5.3.1 Maximum Shear Concurrent Moment Case:
As determined in Section 5.3.3,

$V_{uS(inv)} = V_{u(DC)} + V_{us(inv)} = 200$ kip

$M_{uS(inv)} = M_{u(DC)} + M_{us(inv)} = -6422$ kip-in

$$\eta_{ms(inv)} = \frac{M_{us(inv)}}{V_{us(inv)}} = \frac{-2102}{147} = -14.3\left(\text{LL ratio}\right)$$

Determining the shear capacity at critical section after iterating V_u and M_u:

Since, $M_{uS} < M_{cr\text{-}top}$, iteration is not required, assuming strain at the CG of tensile steel reinforcement equal to zero:

$\varepsilon_s = 0.00$

$\theta = 29 + 3500\varepsilon_s = 29 + 3500 \times 0.00 = 29.0°$

$$\beta = \frac{4.8}{1+750\varepsilon_s} = \frac{4.8}{1+750\times 0.00}$$
$$= 4.8$$

Shear strength of concrete:

$$V_c = 0.0316\beta\lambda\sqrt{f_c'}b_v d_v$$
$$= 0.0316\times 4.8\times 1\times\sqrt{2.75}\times 16.7\times 34.6$$
$$= 145\,\text{kip}$$

Shear strength of shear reinforcement:

$$V_s = \frac{A_v f_y d_v \cot(\theta)}{s}$$
$$= \frac{0.4\times 40\times 34.6\cot(29)}{10}$$
$$= 98\,\text{kip}$$

Total shear capacity of the section:

Total shear capacity of the section:

Minimum of

$V_n = V_c + V_n = 145 + 98 = 243$ kip

and

$V_n = 0.25f'_c b_v d = 397$ kip

Therefore,

$V_n = 243$ kip

$\phi V_n = 0.9 \times 243 = 218.7$ kip

The section was shown to be uncracked at Step 1. Note that the shear strength, 218.7 kips, is much larger than the applied shear, 147.3 kips. The ultimate moment associated with this shear will likewise increase, based on a proportional increase in live load. At this stage, the load rater should start the process over as the section is now shown to be cracked. However, as shown in the following calculations, the shear strength is governed by the maximum moment case, where the section is cracked, and the resulting shear strength is 129.5 kips. Since this governs the shear capacity at Section 2, revisiting the maximum shear case may be unnecessary.

5.3.5.3.2 Maximum Moment Concurrent Shear Case:
As determined in Section 5.3.3,

$V_{uM(inv)} = V_{u(DC)} + V_{um(inv)} = 91$ kip

$M_{uM(inv)} = M_{u(DC)} + M_{um(inv)} = -9998$ kip-in

$$\eta_{mm(inv)} = \frac{M_{um(inv)}}{V_{um(inv)}} = \frac{-5678}{38} = -148.3\left(\text{LL ratio}\right)$$

Determining the shear capacity at critical section after iterating V_u and M_u:

Since, $M_{uS} > M_{cr\text{-}bot}$, calculating strain at the CG of tensile steel reinforcement:
$V_{um(inv)}$ after iteration = 76.8 kip (live load iterations only)
$V_u = V_{u(DC)} + V_{um(inv)} = 129.5$ kip

$\eta_{mm(inv)} = -148.3$

$\left|\frac{M_{u(DC)} + V_{um(inv)}\eta_{mm(inv)}}{d_v}\right| = 455$ kip, should be greater than, $|V_u - V_p| = 129.5$ kip

Adopt, $\left|\frac{M_{u(DC)} + V_{um(inv)}\eta_{mm(inv)}}{d_v}\right| = 455\,\text{kip}$

$$\varepsilon_s = \frac{\left(455 + \left|129.5\right|\right)}{29{,}000 \times 12.41}$$
$$= 0.00162$$

$\theta = 29 + 3500\varepsilon_s = 29 + 3500 \times 0.00162 = 34.7°$

$$\beta = \frac{4.8}{1 + 750\varepsilon_s} = \frac{4.8}{1 + 750 \times 0.00162}$$
$$= 2.2$$

Shear strength of concrete:

$$V_c = 0.0316\beta\lambda\sqrt{f_c'}\,b_v d_v$$
$$= 0.0316 \times 2.2 \times 1 \times \sqrt{2.75} \times 16.7 \times 34.6$$
$$= 65.4\,\text{kip}$$

Shear strength of shear reinforcement:

$$V_s = \frac{A_v f_y d_v \cot(\theta)}{s}$$
$$= \frac{0.4 \times 40 \times 34.6 \cot(34.7)}{10}$$
$$= 78.4 \text{ kip}$$

Total shear capacity of the section:

Minimum of:

$V_n = V_c + V_n = 65.4 + 78.4 = 143.8$ kip

and

$V_n = 0.25 f'_c b_v d = 397$ kip

Therefore,

$V_n = 143.8$ kip

$\phi V_n = 0.9 \times 143.8 = 129.5$ kip

Since the resulting shear strength, 129.5 kips, exceeds the starting shear strength and the section was determined to be cracked at the beginning, the section remains cracked as the ultimate moment only increases from the original step.

5.3.6 Longitudinal Reinforcement Check at the Critical Sections

LRFD Design 5.7.3.5

Tensile capacity of the longitudinal reinforcement on the flexural tension side of the member should be proportioned to satisfy:

$$A_{ps} f_{ps} + A_s f_y \geq \frac{|M_u|}{d_v \phi_f} + 0.5 \frac{N_u}{\phi_c} + \left(\left| \frac{V_u}{\phi_v} - V_p \right| - 0.5 V_s \right) \cot\theta$$

$\phi_f = 0.9$

$\phi_v = 0.9$

$N_u = 0$

Since an iterative process is used to determine the shear capacity corresponding to the longitudinal reinforcement, the RHS of the equation is modified to take account of the moments in the iterative process.

$$A_{ps}f_{ps} + A_s f_y \geq \frac{\left|M_{u-DL} + V_{u-LL}m_{LL}\right|}{d_v\phi_f} + 0.5\frac{N_u}{\phi_c} + \left(\left|\frac{V_u}{\phi_v} - V_p\right| - 0.5V_s\right)\cot\theta$$

Since,

$M_u = M_{u\text{-}DL} + M_{u\text{-}LL}$

and,

$$\eta_{LL} = \frac{M_{u-LL}}{V_{u-LL}}$$

$M_{u\text{-}LL} = V_{u\text{-}LL}\eta_{LL}$

It can be re-written as,

$M_u = M_{u\text{-}DL} + V_{u\text{-}LL}\eta_{LL}$

5.3.6.1 Determining Shear Strength Corresponding to Longitudinal Reinforcement (Critical Section – 1):

5.3.6.1.1 Maximum Shear Concurrent Moment Case (Inventory Level):

As determined in Section 5.3.3,

$V_{uS(inv)} = V_{u(DC)} + V_{us(inv)} = 129$ kip

$M_{uS(inv)} = M_{u(DC)} + M_{us(inv)} = 5560$ kip-in

$$\eta_{ms(inv)} = \frac{M_{us(inv)}}{V_{us(inv)}} = \frac{4264}{105} = 40.6\left(\text{LL ratio}\right)$$

Determining the RHS of LRFD Design Eq. 5.7.3.5-1 by iterating V_u and M_u:

The iteration process is illustrated in Section 5.1.3, hence the end result after iterations is showcased here.

$V_{us(inv)}$ after iteration = 87.9 kip (live load iterations only)

$V_u = V_{u(DC)} + V_{us(inv)} = 111.9$ kip

$\eta_{ms(inv)} = 40.6$

$\left|\frac{M_{u(DC)} + V_{us(inv)}m_{ms(inv)}}{d_v}\right| = 141\text{kip}$, should be greater than, $|V_u - V_p| = 111.9$ kip

Therefore, $\left|\frac{M_{u(DC)} + V_{us(inv)}\eta_{ms(inv)}}{d_v}\right| = 141\text{kip}$

$$\varepsilon_s = \frac{\left(141 + \left|111.9\right|\right)}{29{,}000 \times 7.81}$$
$$= 0.00112$$

$\theta = 29 + 3500\varepsilon_s = 29 + 3500 \times 0.00112 = 32.9°$

The iteration process is illustrated in Section 5.1.3. The end result after iterations is showcased here.

Shear strength of shear reinforcement:

$$V_s = \frac{A_v f_y d_v \cot(\theta)}{s}$$
$$= \frac{0.4 \times 40 \times 34.6 \cot(32.9)}{18}$$
$$= 47\,\text{kip}$$

RHS of the LRFD Design Eq. 5.7.3.5-1

$$RHS = \frac{\left|M_{u(DC)} + V_{us(inv)}\eta_{LL}\right|}{d_v \phi_f} + \left(\left|\frac{V_u}{\phi_v} - V_p\right| - 0.5V_s\right)\cot\theta$$
$$= \frac{141}{0.9} + \left(\left|\frac{111.9}{0.9}\right| - 0.5 \times 47\right)\cot(32.9)$$
$$= 312.5\,\text{kip}$$

LHS of the LRFD Design Eq. 5.7.3.5-1

$LHS = A_s f_y = 7.81 \times 40 = 312.5$ kip

Since LHS=RHS, shear capacity corresponding to longitudinal reinforcement is:

$$\phi_v V_n = 111.9\,\text{kip}$$

5.3.6.1.2 Maximum Moment Concurrent Shear Case (Inventory Level):
As determined in Section 5.3.3,

$V_{uM(inv)} = V_{u(DC)} + V_{um(inv)} = 129$ kip

$M_{uM(inv)} = M_{u(DC)} + M_{um(inv)} = 5560$ kip-in

$$\eta_{mm(inv)} = \frac{M_{um(inv)}}{V_{um(inv)}} = \frac{4264}{105} = 40.6\left(\text{LL ratio}\right)$$

Determining the RHS of LRFD Design Eq. 5.7.3.5-1 by iterating V_u and M_u:

$V_{us(inv)}$ after iteration = 87.9 kip (live load iteration only)

$V_u = V_{u(DC)} + V_{us(inv)} = 111.9$ kip

$\eta_{ms(inv)} = 40.6$

$\left|\frac{M_{u(DC)} + V_{us(inv)}\eta_{ms(inv)}}{d_v}\right| = 141\text{kip}$, should be greater than $|V_u - V_p| = 111.9$ kip

Therefore, $\left|\frac{M_{u(DC)} + V_{us(inv)}\eta_{ms(inv)}}{d_v}\right| = 141\text{kip}$

$$\varepsilon_s = \frac{\left(141 + \left|111.9\right|\right)}{29{,}000 \times 7.81}$$
$$= 0.00112$$

$\theta = 29 + 3500\varepsilon_s = 29 + 3500 \times 0.00112 = 32.9°$

The iteration process is illustrated in Section 5.1.3. The end result after iterations is showcased here.

Shear strength of shear reinforcement:

$$V_s = \frac{A_v f_y d_v \cot\left(\theta\right)}{s}$$
$$= \frac{0.4 \times 40 \times 34.6 \cot\left(32.9\right)}{18}$$
$$= 47\,\text{kip}$$

RHS of the LRFD Design Eq. 5.7.3.5-1

$$RHS = \frac{\left|M_{u(DC)} + V_{us(inv)}\eta_{LL}\right|}{d_v\phi_f} + \left(\left|\frac{V_u}{\phi_v} - V_p\right| - 0.5V_s\right)\cot\theta$$
$$= \frac{141}{0.9} + \left(\left|\frac{111.9}{0.9}\right| - 0.5 \times 47\right)\cot\left(32.9\right)$$
$$= 312.5\,\text{kip}$$

LHS of the LRFD Design Eq. 5.7.3.5-1

$LHS = A_s f_y = 7.81 \times 40 = 312.5$ kip

Since LHS=RHS, shear capacity corresponding to longitudinal reinforcement is:

$$\phi_v V_n = 111.9 \text{kip}$$

5.3.6.2 Determining Shear Strength Corresponding to Longitudinal Reinforcement (Critical Section – 2):

5.3.6.2.1 Maximum Shear Concurrent Moment Case (Inventory Level):

As determined in Section 5.3.3,

$V_{uS(inv)} = V_{u(DC)} + V_{us(inv)} = 200$ kip

$M_{uS(inv)} = M_{u(DC)} + M_{us(inv)} = -6422$ kip-in

$$\eta_{ms(inv)} = \frac{M_{us(inv)}}{V_{us(inv)}} = \frac{-2102}{147} = -14.3\left(\text{LL ratio}\right)$$

Determining the RHS of LRFD Design Eq. 5.7.3.5-1 by iterating V_u and M_u:

The iteration process is illustrated in Section 5.1.3. The end result after iterations is showcased here.

$V_{us(inv)}$ after iteration = 145.6 kip (live load iterations only)

$V_u = V_{u(DC)} + V_{us(inv)} = 198.2$ kip

$\eta_{ms(inv)} = -14.3$

$\left|\frac{M_{u(DC)} + V_{us(inv)}\eta_{ms(inv)}}{d_v}\right| = 185.1\text{kip}$, should be greater than, $|V_u - V_p| = 198.2$ kip

Therefore, $\left|\frac{M_{u(DC)} + V_{us(inv)}\eta_{ms(inv)}}{d_v}\right| = 198.2\text{kip}$

$$\varepsilon_s = \frac{\left(198 + |198|\right)}{29{,}000 \times 12.4}$$
$$= 0.00110$$

$\theta = 29 + 3500\varepsilon_s = 29 + 3500 \times 0.00110 = 32.9°$

Shear strength of shear reinforcement:

$$V_s = \frac{A_v f_y d_v \cot(\theta)}{s}$$
$$= \frac{0.4 \times 40 \times 34.6 \cot(32.9)}{10}$$
$$= 84 \text{ kip}$$

RHS of the LRFD Design Eq. 5.7.3.5-1

$$RHS = \frac{\left|M_{u(DC)} + V_{us(inv)}\eta_{LL}\right|}{d_v \phi_f} + \left(\left|\frac{V_u}{\phi_v} - V_p\right| - 0.5V_s\right)\cot\theta$$
$$= \frac{198}{0.9} + \left(\left|\frac{198}{0.9}\right| - 0.5 \times 84\right)\cot(32.9)$$
$$= 496.25 \text{ kip}$$

LHS of the LRFD Design Eq. 5.7.3.5-1

$$LHS = A_s f_y$$
$$= 12.41 \times 40$$
$$= 496.25 \text{ kip}$$

Since LHS=RHS, shear capacity corresponding to longitudinal reinforcement is:

$$\phi_v V_n = 198.2 \text{ kip}$$

5.3.6.2.2 Maximum Moment Concurrent Shear Case (Inventory Level):
As determined in Section 5.3.3,

$V_{uM(inv)} = V_{u(DC)} + V_{um(inv)} = 91$ kip

$M_{uM(inv)} = M_{u(DC)} + M_{um(inv)} = -9998$ kip-in

$$\eta_{mm(inv)} = \frac{M_{um(inv)}}{V_{um(inv)}} = \frac{-5678}{38} = -148.3 \left(\text{LL ratio}\right)$$

Determining the RHS of LRFD Design Eq. 5.7.3.5-1 by iterating V_u and M_u:

$V_{us(inv)}$ after iteration = 51 kip (live load iterations only)

$V_u = V_{u(DC)} + V_{us(inv)} = 104$ kip

$\eta_{ms(inv)} = -148.3$

$\left|\frac{M_{u(DC)} + V_{us(inv)}\eta_{ms(inv)}}{d_v}\right| = 345\,\text{kip}$, should be greater than, $|V_u - V_p| = 104$ kip

Therefore, $\left|\frac{M_{u(DC)} + V_{us(inv)}\eta_{ms(inv)}}{d_v}\right| = 345\,\text{kip}$

$$\varepsilon_s = \frac{\left(345 + |104|\right)}{29{,}000 \times 12.4}$$
$$= 0.00125$$

$\theta = 29 + 3500\varepsilon_s = 29 + 3500 \times 0.00125 = 33.4°$

The iteration process is illustrated in Section 5.1.3. The end result after iterations is showcased here.

Shear strength of shear reinforcement:

$$V_s = \frac{A_v f_y d_v \cot(\theta)}{s}$$
$$= \frac{0.4 \times 40 \times 34.6 \cot(33.4)}{10}$$
$$= 82\,\text{kip}$$

RHS of the LRFD Design Eq. 5.7.3.5-1

$$RHS = \frac{\left|M_{u(DC)} + V_{us(inv)}\eta_{LL}\right|}{d_v\phi_f} + \left(\left|\frac{V_u}{\phi_v} - V_p\right| - 0.5V_s\right)\cot\theta$$
$$= \frac{345}{0.9} + \left(\left|\frac{104}{0.9}\right| - 0.5 \times 82\right)\cot(33.4)$$
$$= 496.25\,\text{kip}$$

LHS of the LRFD Design Eq. 5.7.3.5-1

$$LHS = A_s f_y$$
$$= 12.41 \times 40$$
$$= 496.25\,\text{kip}$$

Since LHS=RHS, shear capacity corresponding to longitudinal reinforcement is:

$\phi_v V_n = 104\,\text{kip}$

5.3.7 Load Rating Factors

The Shear Capacity is the minimum of:

- Nominal shear resistance
- Shear resistance corresponding to longitudinal reinforcement
- Horizontal shear resistance (check not necessary since girders are built integrally with supports and end diaphragms)

5.3.7.1 Critical Section – 1

5.3.7.1.1 Max Shear Concurrent Moment Case

Shear Capacity for Inventory Level:

ϕV_n = 100.5 kip {min(100.5 kip, 117.6 kip)}

$V_{u(DC)} = \gamma_{DC} \times V_{DC}$ = 24 kip

$V_{us(inv)} = \gamma_{LL}(inv) \times V_s$ = 105.1 kip

$$\text{Shear Load Rating} = \frac{\phi V_n - V_{u(DC)}}{V_{us(inv)}} = 0.73$$

5.3.7.1.2 Max Moment Concurrent Shear Case

Shear Capacity for Inventory Level:

ϕV_n = 100.5 kip {min(100.5 kip, 117.6 kip)}

$V_{u(DC)} = \gamma_{DC} \times V_{DC}$ = 24 kip

$V_{us(inv)} = \gamma_{LL}(inv) \times V_s$ = 105.1 kip

$$\text{Shear Load Rating} = \frac{\phi V_n - V_{u(DC)}}{V_{us(inv)}} = 0.73$$

5.3.7.2 Critical Section – 2

5.3.7.2.1 Max Shear Concurrent Moment Case

Shear Capacity for Inventory Level:

ϕV_n = 207 kip {min(218.7 kip, 207 kip)}

$V_{u(DC)} = \gamma_{DC} \times V_{DC}$ = 52.6 kip

$V_{us(inv)} = \gamma_{LL}(inv) \times V_s$ = 147.3 kip

$$\text{Shear Load Rating} = \frac{\phi V_n - V_{u(DC)}}{V_{us(inv)}} = 1.05$$

5.3.7.2.2 Max Moment Concurrent Shear Case
Shear Capacity for Inventory Level:

ϕV_n = 110.5 kip {min(129.5 kip, 110.5 kip)}

$V_{u(DC)} = \gamma_{DC} \times V_{DC}$ = 52.6 kip

$V_{us(inv)} = \gamma_{LL}(inv) \times V_s$ = 38.3 kip

$$\text{Shear Load Rating} = \frac{\phi V_n - V_{u(DC)}}{V_{us(inv)}} = 1.51$$

5.4 EXAMPLE – CONTINUOUS POST-TENSIONED CONCRETE BOX GIRDER

This example is for a design load rating for shear, for an interior web of a two-span continuous, CIP PT box girder. Three sections are evaluated:

- Section 1 is located at d_v from the face of the integral end support
- Section 2 is located at d_v from the face of the integral interior support
- Section 3 is located where the CG of the PT is at mid-depth

The end supports are built integral with the girder ends. Secondary effects from prestressing, as noted in AASHTO MBE Article 6A.5.9 (nonbinding) , are present due to continuity and are accounted for in the load rating.

This example uses the provisions in the 8th Edition of AASHTO LRFD Design (incorporated by reference at 23 CFR § 625.4(d)(1)(v)), which reduces web width based on post-tensioning duct diameter.

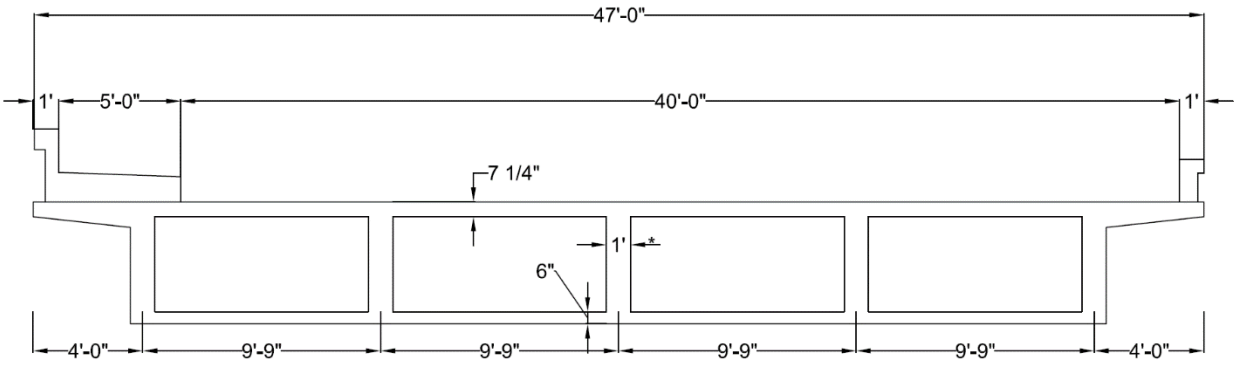

TRANSVERSE SECTION THRU DECK

* Usual, Varies

Source: Authors

Figure 29. Transverse section.

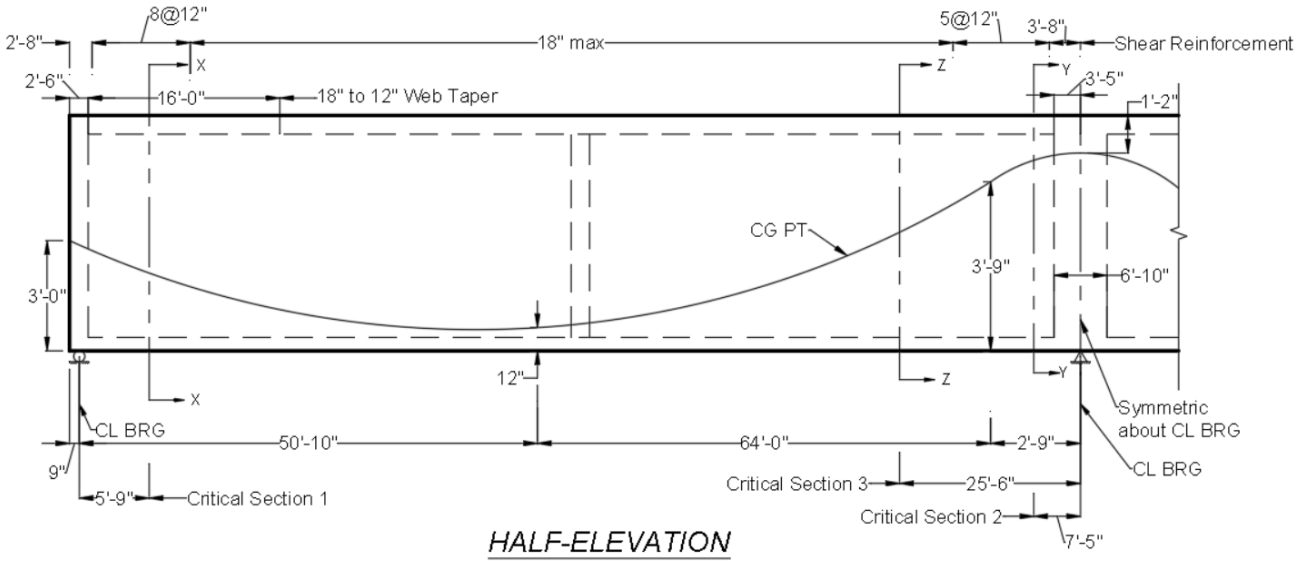

Source: Authors

Figure 30. Half girder elevation.

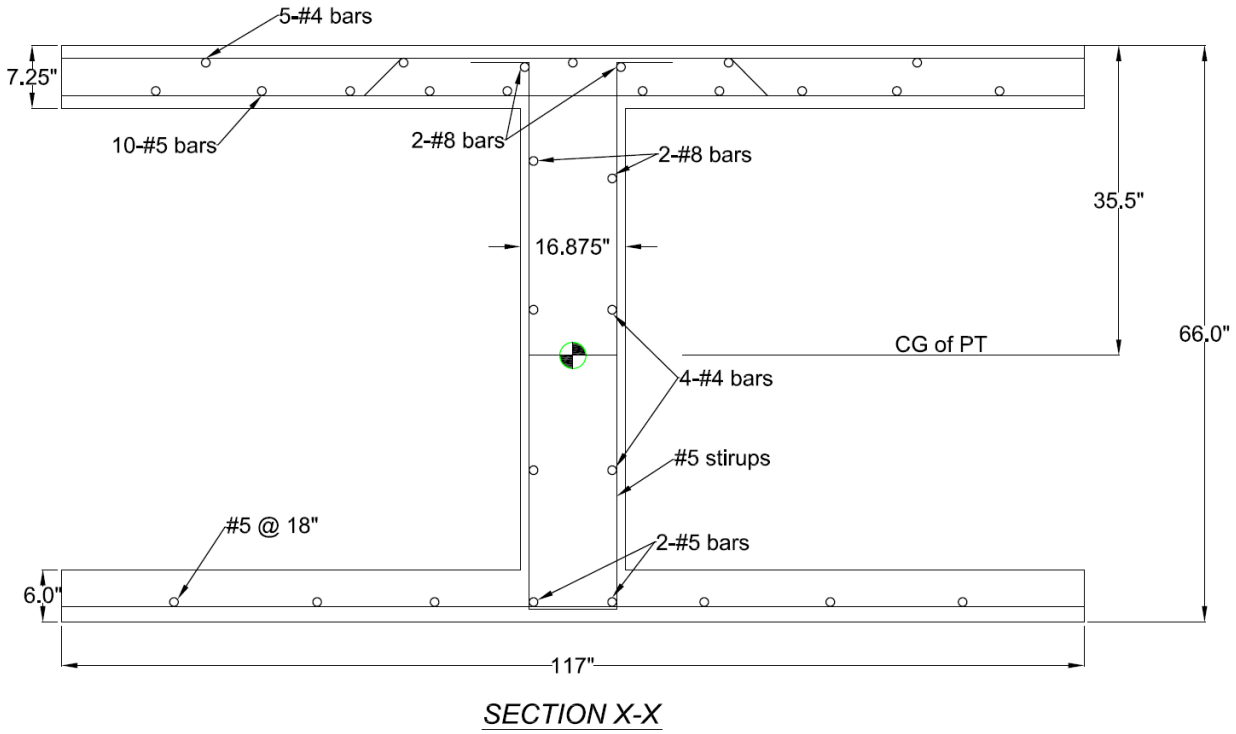

Source: Authors

Figure 31. Cross section at critical section 1.

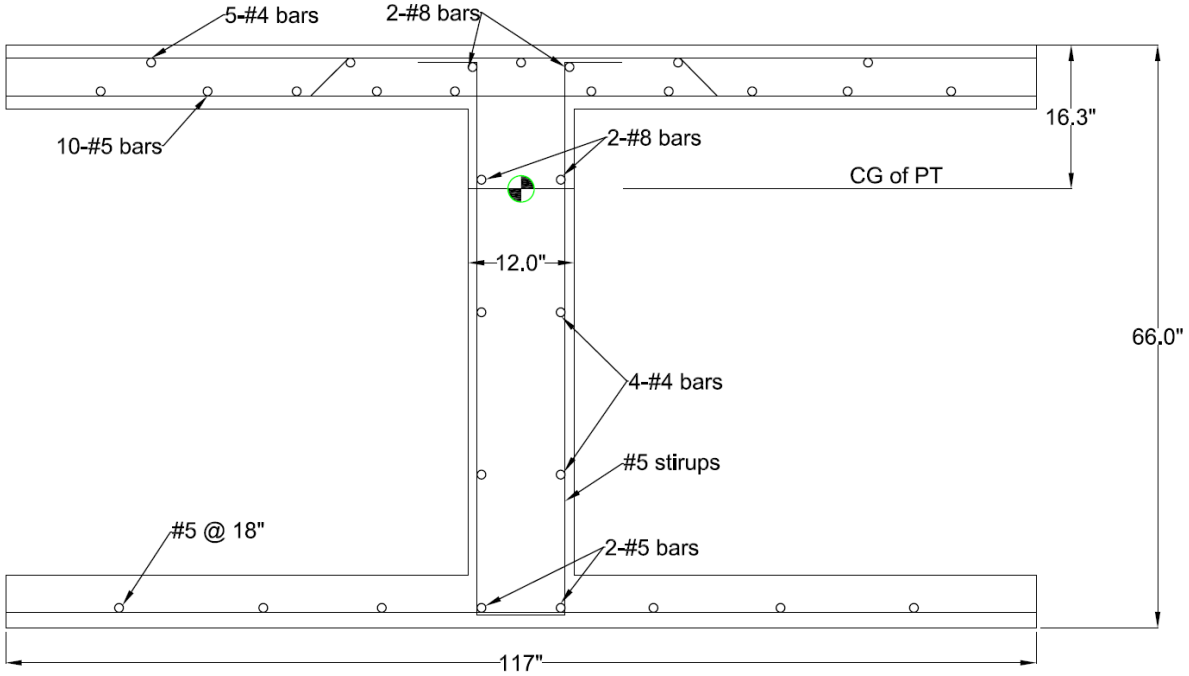

SECTION Y-Y

Source: Authors

Figure 32. Cross section at critical section 2

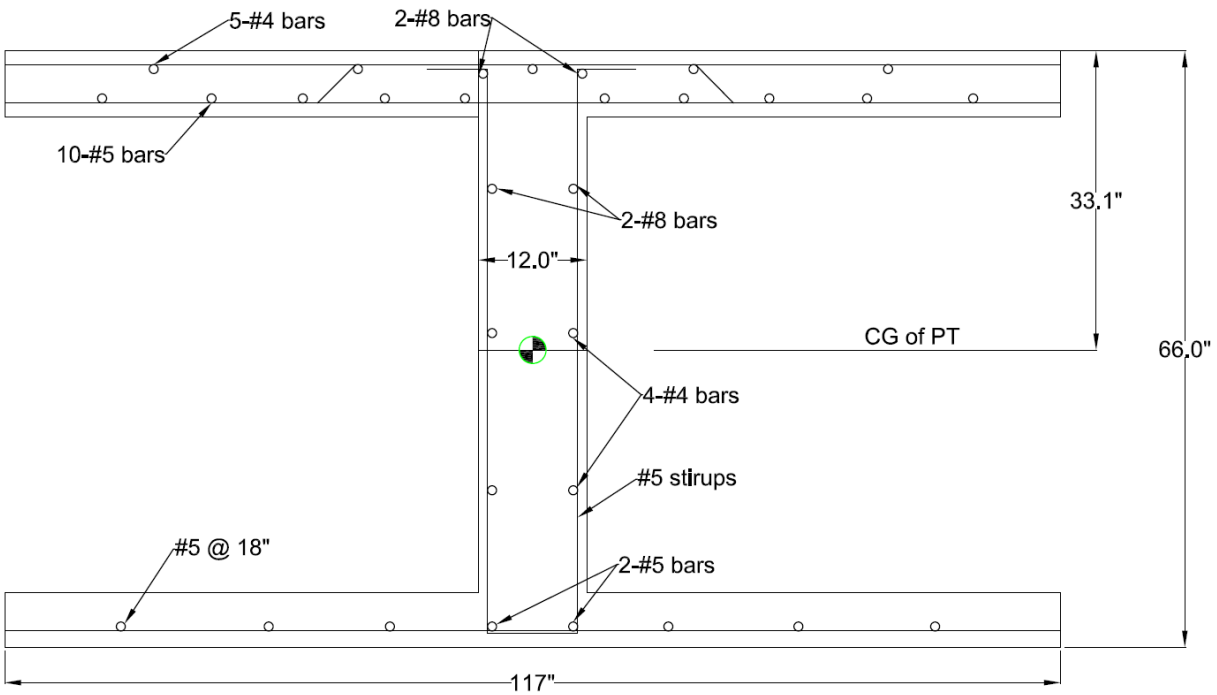

SECTION Z-Z

Source: Authors

Figure 33. Cross-section at critical section 3.

5.4.1 Bridge Data

Span:	128 ft – 128 ft
Year Built:	1969
Materials:	
Concrete:	f_c' = 3.5 ksi (deck & beam)
Top Steel Reinforcement:	6 – #4 bars (overhang slab-top rebar)
	8 – #5 bars (overhang slab-bottom rebar)
	20 – #4 bars (top slab-top rebar)
	40 – #5 bars (top slab-bottom rebar)
	20 – #8 bars (web/top slab rebar)
	10 – #4 bars (web top half rebar)
	Grade 60
Bottom Steel Reinforcement:	10 – #4 bars (web bottom half rebar)

	10 – #5 bars (web/bottom slab rebar)
	27 – #5 bars (bottom slab rebar)
	Grade 60
Post-tensioning Strands:	0.6-inch diameter, 270 ksi, stress relieved strands
	A_{ps} = 0.217 in.^{2} per strand
	40 post-tensioning strands per web; 200 strands for full box girder
Stirrups:	All #5 bars 2-legged stirrups, refer to **Figure 30** for spacing at critical sections
Condition:	Good
Riding Surface:	Not provided
ADDT:	Not provided
Skew:	0°

Effective Flange Width b_e may be taken as the tributary width perpendicular to the axis of the member LFRD Design 4.6.2.6.1

Effective Flange Width b_e=9.75 ft x 12 in =177 in. (Spacing)

Duct diameter = 3 inches (used for reduction in the width of web thickness). Duct size is assumed, based on three tendons, which would allow for 14 tendons per web if the post-tensioning supplier provided 3 approximately equal-size tendons. The duct size assumed also provides the minimum area noted in LRFD Article 5.4.6.2 (binding). The as-built plans only specified the final prestress force after losses. The post-tensioning shop drawings would be helpful in determining specific information and geometry that would assist the load rating process.

Modulus of Elasticity of Materials:

$E_c = 120{,}000\, K_1 w_c^{2.0} f_c'^{0.33}$ LRFD Design Eq. 5.4.2.4-1

For Concrete,

E_c = 120,000 x 1x $(0.15)^{2.0}$ x $(3.5)^{0.33}$ = 4082 ksi

For Reinforcing Steel

E_s = 29,000 ksi

For Post-tensioning Strands

E_{ps} = 28,500 ksi

5.4.2 Summary of Section Properties

5.4.2.1 CIP – Box Girder:

Computer aided design and drafting (CADD) software was used to calculate the section properties of the box girder due to its complexity.

$D = 66$ in.

$b_w = 12$ in.

$b_{f,top} = 564$ in.

$b_{f,bot} = 480$ in.

$t_{f,top} = 7.25$ in.

$t_{f,bot} = 6$ in.

$A_{box} = 10345$ in^2

$I_{box} = 6.88 \times 10^6$ in^4

Properties per web

$b_f = s = 117$ in.

$I_{each\ web} = 1.37 \times 10^6$ in^4

$y_{top} = 29.44$ in.

$y_{bot} = 36.56$ in.

$$S_{c,top} = \frac{I_{each\,web}}{y_{top}} = 46722\,\text{in}^3$$

$$S_{c,bot} = \frac{I_{each\,web}}{y_{bot}} = 37617\,\text{in}^3$$

5.4.2.2 Post-tensioning Strand Calculations

Only the prestress force at jacking is provided in the plans, leaving the strand size and number of tendons to the contractor. Assumptions are made in the strand size and number of tendons.

Data mentioned in the plans:

Jacking Force:

$P_j = 8800$ kip

The strands are stressed up to 75% of ultimate stress

$$A_{ps} = \frac{P_j}{0.75 \times f_{pu}} = \frac{8800}{0.75 \times 270} = 43.5\,\text{in}^2$$

Using 0.6" dia. strands

Total number of Strands:

$$\text{n} = \frac{43.5}{0.217} = 200$$

Reinforcement details at Critical Section 1:

Rebar in Tension zone:

Sum of Bottom Steel Reinforcement:

$A_s = 13.3\,\text{in}^2$

$d_s = 63\,\text{in.(from top)}$

Rebar in Compression zone:

Sum of Top Steel Reinforcement:

A'_s = 37.5 in.^{2}

Post-tensioning steel:

Assuming the area of post tensioning strands is spread across 10in deep for calculating of A_{ps} in flexural tension and compression side.

Number of Strands = 200

Strand Diameter = 0.6 in.

Strand Area = 0.217 in.^{2}

A_{ps} = 43.5 in.^{2}

Depth of strands = d_p = 35.5 in. (from top)

$A_{ps,top}$ = 10.9 in^2

$A_{ps,bot}$ = 32.6 in^2

Reinforcement details at Critical Section 2:

Rebar in Tension zone:

Sum of Top Steel Reinforcement:

A_s = 37.5 in^2

d_s = 62.4 in. (from bottom)

Rebar in Compression zone:

Sum of Bottom Steel Reinforcement:

A'$_s$ = 13.3 in.^{2}

Post-tensioning steel:

Assuming the area of post tensioning strands is spread across 10in deep for calculation of A_{ps} in flexural tension and compression side.

Number of Strands = 200

Strand Diameter = 0.6 in.

Strand Area = 0.217 in.^{2}

A_{ps} = 43.5 in.^{2}

Depth of strands = d_p = D – 16.3 in. = 66 – 16.3 = 49.7 in. (from bottom)

$A_{ps,top}$ = 43.5 in^2

$A_{ps,bot}$ = 0.00 in^2

Reinforcement details at Critical Section 3:

For positive moment case:

Rebars in Tension zone:

Sum of Bottom Steel Reinforcement:

A_s = 13.3 in^2

d_s = 63.0 in (from top)

Rebars in Compression zone:

Sum of Top Steel Reinforcement:

A'$_s$ = 37.5 in.^{2}

Post-tensioning steel:

Assuming the area of post tensioning strands is spread across 10 in deep for calculation of A_{ps} in flexural tension and compression side.

Number of Strands = 200

Strand Diameter = 0.6 in.

Strand Area = 0.217 in.^{2}

A_{ps} = 43.5 in.^{2}

Depth of strands = d_p = 33.1 in. (from top)

$A_{ps,top}$ = 21.3 in^2

$A_{ps,bot}$ = 22.2 in^2

For negative moment case:

Rebars in Tension zone:

Sum of Top Steel Reinforcement:

A_s = 37.5 in^2

d_s = 62.4 in (from bottom)

Rebars in Compression zone:

Sum of Bottom Steel Reinforcement:

A'_s = 13.3 in.^{2}

Post-tensioning steel:

Assuming the area of post tensioning strands is spread across 10 in deep for calculation of A_{ps} in flexural tension and compression side.

Number of Strands = 200

Strand Diameter = 0.6 in.

Strand Area = 0.217 in.^{2}

A_{ps} = 43.5 in.^{2}

Depth of strands = d_p = 66 in. - 33.1 in. = 32.9 in. (from top)

$A_{ps,top}$ = 21.3 in^2

$A_{ps,bot}$ = 22.2 in^2

5.4.2.3 Determining Shear Depth at Critical Load Rating Section

Shear Depth for Critical Sections 1, 2 & 3:

As per Article 5.7.2.8 of LRFD Bridge Design Specification (binding)

Adopting effective shear depth as:

$0.72D = 0.72 \times 66$ in. = 47.5 in.

Refining the effective shear depth may increase the final load rating, but draped tendon profiles complicate determination of locating d_v from face of support as d_v is constantly changing. Engineering judgment is suggested when reviewing the plans to determine if further refinement of the effective shear depth would be beneficial.

5.4.3 Factored Loads

This is a design load rating; the live loads are calculated according to HL-93 loading. The live load moments and shears include the Dynamic Load Allowance, IM, from AASHTO LRFD Article 3.6.2 (binding) and AASHTO MBE Article 6A.4.3.2 (nonbinding). Live loads are distributed to the girder using the provisions of AASHTO LRFD Article 4.6.2.2 (binding).

5.4.3.1 Critical Section - 1

5.4.3.1.1 Strength-I Load Combination - Inventory Level

Load Factors per Strength-I Load Combination

$\gamma_{DC} = 1.25$

$\gamma_{LL}(inv) = 1.75$

$\gamma_{PR} = 1.00$

Factored Shear Forces and Moments due to Dead Loads and Prestress Secondary Effects

$V_{u(DC)\text{-Sec1}} = \gamma_{DC} \times V_{DC\text{-sec1}} = 124.2$ kip

$M_{u(DC)\text{-Sec1}} = \gamma_{DC} \times M_{DC\text{-sec1}} = 9144$ kip-in

$V_{u(PR)\text{-Sec1}} = \gamma_{PR} \times V_{PR} = 1.1$ kip

$M_{u(PR)\text{-Sec1}} = \gamma_{PR} \times M_{PR} = 1.1 \times 69 = 75$ kip-in

Inventory Live Load – Max Shear Concurrent Moment Case

$V_{us(inv)} = \gamma_{LL}(inv) \times V_s \times g_v = 167.8$ kip

$M_{us(inv)} = \gamma_{LL}(inv) \times M_s \times g_m = 8858$ kip-in

Inventory Live Load – Max Moment Concurrent Shear Case

$V_{us(inv)} = \gamma_{LL}(inv) \times V_s \times g_v = 167.8$ kip

$M_{us(inv)} = \gamma_{LL}(inv) \times M_s \times g_m = 8858$ kip-in

Ultimate Shear Force:

$V_{uS(inv)} = V_{u(DC)} + V_{u(PR)} + V_{us(inv)} = 292$ kip (Max Shear Case)

$V_{uM(inv)} = V_{u(DC)} + V_{u(PR)} + V_{um(inv)} = 292$ kip (Max Shear Case)

Ultimate Bending Moment:

$M_{uS(inv)} = M_{u(DC)} + M_{u(PR)} + M_{us(inv)} = 18077$ kip-in (Max Shear Case)

$M_{uM(inv)} = M_{u(DC)} + M_{u(PR)} + M_{um(inv)} = 18077$ kip-in (Max Moment Case)

5.4.3.2 Critical Section - 2

5.4.3.2.1 Strength-I Load Combination - Inventory Level

Load Factors per Strength-I Load Combination

$\gamma_{DC} = 1.25$

$\gamma_{LL}(inv) = 1.75$

$\gamma_{PR} = 1.00$

Factored Shear Forces and Moments due to Dead Loads and Prestress Secondary Effects

$V_{u(DC)\text{-Sec2}} = \gamma_{DC} \times V_{DC\text{-sec2}} = 213.4$ kip

$M_{u(DC)\text{-Sec2}} = \gamma_{DC} \times M_{DC\text{-sec2}} = -52101$ kip-in

$V_{u(PR)\text{-Sec2}} = \gamma_{PR} \times V_{PR} = -1.1$ kip

$M_{u(PR)\text{-Sec2}} = \gamma_{PR} \times M_{PR} = 1.1 \times 1442 = 1571$ kip-in

Inventory Live Load – Max Shear Concurrent Moment Case

$V_{us(inv)} = \gamma_{LL}(inv) \times V_s \times g_v = 222.6$ kip

$M_{us(inv)} = \gamma_{LL}(inv) \times M_s \times g_m = -13863$ kip-in

Inventory Live Load – Max Moment Concurrent Shear Case

$V_{um(inv)} = \gamma_{LL}(inv) \times V_m = 92.1$ kip

$M_{um(inv)} = \gamma_{LL}(inv) \times M_m = -30327$ kip-in

Ultimate Shear Force:

$V_{uS(inv)} = V_{u(DC)} + V_{us(inv)} = 435$ kip (Max Shear Case)

$V_{uM(inv)} = V_{u(DC)} + V_{um(inv)} = 304$ kip (Max Moment Case)

Ultimate Bending Moment:

$M_{uS(inv)} = M_{u(DC)} + M_{us(inv)}$ = -64393 kip-in (Max Shear Case)

$M_{uM(inv)} = M_{u(DC)} + M_{um(inv)}$ = -80858 kip-in (Max Moment Case)

5.4.3.3 Critical Section - 3

5.4.3.3.1 Strength-I Load Combination - Inventory Level

There are many load combinations possible near contraflexure points. Engineering judgment is applied in refining the number of these combinations for evaluation.

Load Factors per Strength-I Load Combination

$\gamma_{DC} = 1.25$

$\gamma_{LL}(inv) = 1.75$

$\gamma_{PR} = 1.00$

Factored Shear Forces and Moments due to Dead Loads and Prestress Secondary Effects

$V_{u(DC)\text{-Sec3}} = \gamma_{DC} \times V_{DC\text{-sec3}}$ = 159.9 kip

$M_{u(DC)\text{-Sec3}} = \gamma_{DC} \times M_{DC\text{-sec3}}$ = -11505 kip-in

$V_{u(PR)\text{-Sec3}} = \gamma_{PR} \times V_{PR}$ = -1.1 kip

$M_{u(PR)\text{-Sec3}} = \gamma_{PR} \times M_{PR} = 1.1 \times 1225 = 1334.1$ kip-in

Inventory Live Load – Max Shear Concurrent Moment Case

$V_{us(inv)} = \gamma_{LL}(inv) \times V_s \times g_v$ = 186.0 kip

$M_{us(inv)} = \gamma_{LL}(inv) \times M_s \times g_m$ = 11134 kip-in

Inventory Live Load – Max Moment Concurrent Shear Case

$V_{um(inv)} = \gamma_{LL}(inv) \times V_m$ = 72.8 kip

$M_{um(inv)} = \gamma_{LL}(inv) \times M_m$ = -16844 kip-in

Ultimate Shear Force:

$V_{uS(inv)} = V_{u(DC)} + V_{us(inv)}$ = 345 kip (Max Shear Case)

$V_{uM(inv)} = V_{u(DC)} + V_{um(inv)}$ = 232 kip (Max Moment Case)

Ultimate Bending Moment:

$M_{uS(inv)} = M_{u(DC)} + M_{us(inv)}$ = 963 kip-in (Max Shear Case)

$M_{uM(inv)} = M_{u(DC)} + M_{um(inv)}$ = -27015 kip-in (Max Moment Case)

5.4.4 Determine Effective Prestress Force, P_{pe}

$P_{pe} = A_{ps} f_{pe}$

Total Prestress Losses $\Delta f_{pT} = \Delta f_{pF} + \Delta f_{pA} + \Delta f_{pES} + \Delta f_{pLT}$

$f_{pe} = f_{pi} - \Delta f_{pT}$

f_{pj} = 202.5 ksi (from plans)

5.4.4.1 Critical Section – 1

5.4.4.1.1 Calculating Prestress Loss due to Friction

Prestress loss due to friction can be estimated by:

$\Delta f_{pF} = f_{pj}\,[1-e^{-(Kx+\mu\alpha)}]$

Wobble coefficient, K = 0.0002 (noted in plans)
Friction factor, μ = 0.25
x = 69 inches
α = 0.0071

$$\Delta f_{pF} = f_{pj}\left[1-e^{-(Kx+\mu\alpha)}\right]$$
$$= 202.5\times\left[1-e^{-\left(0.0002\times\frac{69}{12}+0.25\times0.0071\right)}\right]$$
$$= 0.6\,\text{ksi}$$

5.4.4.1.2 Calculating Prestress Loss due to Anchorage set

Anchorage slip mentioned in drawings = Δ_s = 5/8 in = 0.052 ft

Wobble coefficient, K = 0.0002 (mentioned in plans)
Friction factor, μ = 0.25
x = 69 inches
α = 0.0071

$$l_{set} = \sqrt{\frac{E_{ps}\Delta_s}{f_{pj}\eta}}$$

$$\eta = \frac{\mu\alpha}{\frac{x}{12}+K}$$
$$= \frac{0.25\times0.0071}{\frac{69}{12}+0.0002}$$
$$= 0.000308$$

$$l_{set} = \sqrt{\frac{28{,}500 \times 0.052}{202.5 \times 0.000308}}$$
$$= 154.14 \text{ in.}$$

$\Delta P = 2\eta l_{set} P_j = 2 \times 0.000308 \times 154.14 \times 8800 = 835.6$ kip

$$\Delta f_{pA} = \frac{\Delta P}{A_{ps}} = \frac{835.6}{43.5}$$
$$= 19.6 \text{ ksi}$$

5.4.4.1.3 Calculating Prestress Loss Due to Elastic Shortening
Initial Prestressing Force, P_i:

$$P_i = \left(f_{pj} - \Delta f_{pF} - \Delta f_{pA}\right) A_{ps}$$
$$= \left(202.5 - 0.6 - 19.6\right) \times 43.5$$
$$= 7921 \text{ kip}$$

Eccentricity of Straight Strands, $e = y_b - y_{ps1}$

$$= 36.6 - 30.5$$
$$= 6.1 \text{ inches}$$

Number of post-tensioning instances = 2

$$\Delta f_{pES} = \frac{N-1}{2N}\left(\frac{E_p}{E_{ct}}\right) f_{cgp}$$

$$f_{cgp} = \frac{P_i}{A} + \frac{P_i e^2}{I} + \frac{M_{DC1} e}{I}$$

$$f_{cgp} = \frac{7921}{10345} + \frac{7921 \times 6.1^2}{6.88 \times 10^6} - \frac{32429 \times 6.1}{6.88 \times 10^6} = 0.8 \text{ ksi}$$ LRFD Design 5.9.3.2.3a

$$\Delta f_{pES} = \frac{2-1}{2 \times 2} \times \frac{28{,}500}{3815} \times 0.8$$
$$= 1.5 \text{ ksi}$$

5.4.4.1.4 Approximate Lump Sum Estimate of Time-Dependent Losses, Δf_{pLT}
Time-dependent losses include shrinkage of concrete, creep of concrete, and relaxation of steel.
For refined estimates: LRFD Design

$$\Delta f_{pLT} = \left(\Delta f_{pSR} + \Delta f_{pCR} + \Delta f_{pR1}\right)_{id} + \left(\Delta f_{pSD} + \Delta f_{pCD} + \Delta f_{pR2} - \Delta f_{pSS}\right)_{df}$$ Eq. 5.9.3.4.1-1

As noted in Example 1, the calculations for time dependent losses use the refined methods of AASHTO LRFD Article 5.9.3.4 (binding) . The approximate time dependent losses of AASHTO LRFD Article 5.9.3.3 (binding) are used instead even though this article does not extend to post-tensioned concrete. The plans note a time dependent loss of 25 ksi; this will be compared to the time dependent losses as determined by the approximate method as a cross check.

For I-Girders, time dependent losses can be approximated by: LRFD Design 5.9.3.3

$$\Delta f_{pLT} = 10.0\frac{f_{pi}A_{ps}}{A_g}\gamma_h\gamma_{st} + 12.0\gamma_h\gamma_{st} + \Delta f_{pR}$$ LRFD Design Eq. 5.9.3.3-1

where $\gamma_h = 1.7 - 0.01H$

Assuming a relative humidity H ranging between 40 to 100 percent.

For this example, assume $H = 70$ percent or refer to LRFD Design Figure 5.4.2.3.3-1

$$\gamma_h = 1.7 - 0.01(70) = 1.0$$

and:

$$\gamma_{st} = \frac{5}{1 + f_{ci}^{'}} = \frac{5}{1 + 3.5} = 1.11$$

and:

$\Delta f_{pR} =$ an estimation of relaxation losses

$\Delta f_{pR} = 1.9$ ksi

and:

$$f_{pi} = \left(f_{pj} - \Delta f_{pF} - \Delta f_{pA}\right)$$
$$= (202.5 - 0.6 - 19.6)$$
$$= 182.3 \text{ ksi}$$

then:

$$\Delta f_{pLT} = 10.0 \times \frac{182.3 \times 43.5}{10345} \times 1.0 \times 1.11 + 12.0 \times 1.0 \times 1.11 + 1.9$$

$$\Delta f_{pLT} = 23.7 \text{ ksi}$$

This compares very favorably with the losses of 25 ksi noted in the plans. Further calculations will proceed with 23.7 ksi losses at Critical Section 1.

Total Prestress Losses:

$\Delta f_{pT} = 21.67 + 23.7 = 45.37$ ksi

Effective Prestress:

Δf_{pe} = Prestress at Jacking – Total Prestress Losses

= 202.5 – 45.37 = 157.13 ksi

Effective Prestress Force in Strands:

$P_e = 43.5 \times 157.13 = 6835$ kip (Inclusive of all webs)

5.4.4.2 Critical Section – 2

5.4.4.2.1 Calculating Prestress Loss Due to Friction

Prestress loss due to friction can be estimated by:

$\Delta f_{pF} = f_{pj}\,[1\text{-}e^{-(Kx+\mu\alpha)}]$

Wobble coefficient, K = 0.0002 (mentioned in plans)
Friction factor, μ = 0.25
x = 1442 inches
α = -0.024

$$\Delta f_{pF} = f_{pj}\left[1 - e^{-(Kx+\mu\alpha)}\right]$$
$$= 202.5 \times \left[1 - e^{-\left(0.0002 \times \frac{1442}{12} + 0.25 \times -0.024\right)}\right]$$
$$= 3.57\,\text{ksi}$$

5.4.4.2.2 Calculating Prestress Loss due to Anchorage set

Anchorage slip does not affect at this section

$$\Delta f_{pA} = 0\,\text{ksi}$$

5.4.4.2.3 Calculating Prestress Loss due to Elastic Shortening

Initial Prestressing Force, P_i:

$$P_i = \left(f_{pj} - \Delta f_{pF} - \Delta f_{pA}\right) A_{ps}$$
$$= \left(202.5 - 3.6 - 0\right) \times 43.5$$
$$= 8645\,\text{kip}$$

Eccentricity of Straight Strands, $e = y_{ps1} - y_b$

= 49.7 – 36.6

$= 13.1$ inches.

Number of post-tensioning instances = 2

$$\Delta f_{pES} = \frac{N-1}{2N}\left(\frac{E_p}{E_{ct}}\right) f_{cgp}$$

$$f_{cgp} = \frac{P_i}{A} + \frac{P_i e^2}{I} + \frac{M_{DC1} e}{I}$$

$$f_{cgp} = \frac{8645}{10345} + \frac{8645 \times 13.1^2}{6.88 \times 10^6} - \frac{185137 \times 13.1}{6.88 \times 10^6} = 0.7 \text{ ksi}$$ LRFD Design 5.9.3.2.3a

$$\Delta f_{pES} = \frac{2-1}{2 \times 2} \times \frac{28,500}{3815} \times 0.7$$
$$= 1.31 \text{ ksi}$$

5.4.4.2.4 Approximate Lump Sum Estimate of Time-Dependent Losses, Δf_{pLT}

Time-dependent losses include shrinkage of concrete, creep of concrete, and relaxation of steel.

For refined estimates: LRFD Design

$$\Delta f_{pLT} = (\Delta f_{pSR} + \Delta f_{pCR} + \Delta f_{pR1})_{id} + (\Delta f_{pSD} + \Delta f_{pCD} + \Delta f_{pR2} - \Delta f_{pSS})_{df}$$ Eq. 5.9.3.4.1-1

For I-Girders, time dependent losses can be approximated by: LRFD Design 5.9.3.3

$$\Delta f_{pLT} = 10.0 \frac{f_{pi} A_{ps}}{A_g} \gamma_h \gamma_{st} + 12.0 \gamma_h \gamma_{st} + \Delta f_{pR}$$ LRFD Design Eq. 5.9.3.3-1

where $\gamma_h = 1.7 - 0.01H$

Assuming a relative humidity H ranging between 40 to 100 percent.

For this example, assume $H = 70\%$ or refer to LRFD Design Figure 5.4.2.3.3-1

$$\gamma_h = 1.7 - 0.01(70) = 1.0$$

and:

$$\gamma_{st} = \frac{5}{1 + f'_{ci}} = \frac{5}{1 + 3.5} = 1.11$$

and:

$\Delta f_{pR} =$ an estimation of relaxation losses

$\Delta f_{pR} = 1.9$ ksi

and:

$$f_{pi} = \left(f_{pj} - \Delta f_{pF} - \Delta f_{pA}\right)$$
$$= \left(202.5 - 3.57 - 0\right)$$
$$= 198.93\,\text{ksi}$$

then:

$$\Delta f_{pLT} = 10.0 \times \frac{198.93 \times 43.5}{10345} \times 1.0 \times 1.11 + 12.0 \times 1.0 \times 1.11 + 1.9$$

$$\Delta f_{pLT} = 24.5 \text{ ksi}$$

But by detailed calculations it was found to be

$$\Delta f_{pLT} = 23.3 \text{ ksi}$$

Both values compare very favorably with the losses of 25 ksi noted in the plans. Further calculations will proceed with 23.3 ksi losses at Critical Section 2.

Total Prestress Losses:

$\Delta f_{pT} = 4.87 + 23.3 = 28.17$ ksi

Effective Prestress:

Δf_{pe} = Prestress at Jacking – Total Prestress Losses

= 202.5 – 28.17 = 174.33 ksi

Effective Prestress Force in Strands:

$P_e = 43.5 \times 174.33 = 7583$ kip (Inclusive of all webs)

5.4.4.3 Critical Section – 3

5.4.4.3.1 Calculating Prestress Loss due to Friction

Prestress loss due to friction can be estimated by:

$\Delta f_{pF} = f_{pj}\,[1\text{-}e^{-(Kx+\mu\alpha)}]$

Wobble coefficient, K = 0.0002 (mentioned in plans)
Friction factor, μ = 0.25
x = 1225 inches
α = 0.0071

$$\Delta f_{pF} = f_{pj}\left[1 - e^{-(Kx+\mu\alpha)}\right]$$
$$= 202.5 \times \left[1 - e^{-\left(0.0002 \times \frac{1225}{12} + 0.25 \times 0.0071\right)}\right]$$
$$= 4.47\,\text{ksi}$$

5.4.4.3.2 Calculating Prestress Loss due to Anchorage set
Anchorage slip does not affect at this section

$$\Delta f_{pA} = 0\,\text{ksi}$$

5.4.4.3.3 Calculating Prestress Loss due to Elastic Shortening
Initial Prestressing Force, $P_{i:}$

$$P_i = \left(f_{pj} - \Delta f_{pF} - \Delta f_{pA}\right) A_{ps}$$
$$= \left(202.5 - 4.47 - 0\right) \times 43.5$$
$$= 8606\,\text{kip}$$

Eccentricity of Straight Strands, $e = y_b - y_{ps1}$

$$= 36.6 - 32.9$$
$$= 3.7 \text{ inches}$$

Number of post-tensioning instances = 2

$$\Delta f_{pES} = \frac{N-1}{2N}\left(\frac{E_p}{E_{ct}}\right) f_{cgp}$$

$$f_{cgp} = \frac{P_i}{A} + \frac{P_i e^2}{I} + \frac{M_{DC1} e}{I}$$

$$f_{cgp} = \frac{8606}{10345} + \frac{8606 \times 3.7^2}{6.88 \times 10^6} - \frac{40882 \times 3.7}{6.88 \times 10^6} = 0.9 \text{ ksi}$$ LRFD Design 5.9.3.2.3a

$$\Delta f_{pES} = \frac{2-1}{2 \times 2} \times \frac{28,500}{3815} \times 0.9$$
$$= 1.6 \text{ ksi}$$

5.4.4.3.4 Approximate Lump Sum Estimate of Time-Dependent Losses, Δf_{pLT}
Time-dependent losses include shrinkage of concrete, creep of concrete, and relaxation of steel.
For refined estimates: LRFD Design

$$\Delta f_{pLT} = \left(\Delta f_{pSR} + \Delta f_{pCR} + \Delta f_{pR1}\right)_{id} + \left(\Delta f_{pSD} + \Delta f_{pCD} + \Delta f_{pR2} - \Delta f_{pSS}\right)_{df}$$ Eq. 5.9.3.4.1-1

For I-Girders, time dependent losses can be approximated by: LRFD Design 5.9.3.3

$$\Delta f_{pLT} = 10.0\frac{f_{pi}A_{ps}}{A_g}\gamma_h\gamma_{st} + 12.0\gamma_h\gamma_{st} + \Delta f_{pR}$$ LRFD Design Eq. 5.9.3.3-1

where $\gamma_h = 1.7 - 0.01H$

Assuming a relative humidity H ranging between 40 to 100 percent.

For this example, assume $H = 70\%$ or refer to LRFD Design Figure 5.4.2.3.3-1

$$\gamma_h = 1.7 - 0.01(70) = 1.0$$

and:

$$\gamma_{st} = \frac{5}{1 + f_{ci}^{'}} = \frac{5}{1 + 3.5} = 1.11$$

and:

$\Delta f_{pR} =$ an estimation of relaxation losses

$\Delta f_{pR} = 2.4$ ksi

and:

$$f_{pi} = \left(f_{pj} - \Delta f_{pF} - \Delta f_{pA}\right)$$
$$= (202.5 - 4.47 - 0)$$
$$= 198.03 \text{ ksi}$$

then:

$$\Delta f_{pLT} = 10.0 \times \frac{198.03 \times 43.5}{10345} \times 1.0 \times 1.11 + 12.0 \times 1.0 \times 1.11 + 2.4$$

$$\Delta f_{pLT} = 25.2 \text{ ksi}$$

This compares very favorably with the losses of 25 ksi noted in the plans. Further calculations will proceed with 25.2 ksi losses at Critical Section 3.

Total Prestress Losses:

$\Delta f_{pT} = 6.07 + 25.2 = 31.27$ ksi

Effective Prestress:

Δf_{pe} = Prestress at Jacking – Total Prestress Losses

$= 202.5 - 31.27 = 171.2$ ksi

Effective Prestress force in Strands:

$P_e = 43.5 \times 171.2 = 7449$ kip (Inclusive of all webs)

5.4.5 Determining the Cracking Moment Capacity at the Critical Sections

5.4.5.1 Critical Section – 1

Determining the Cracking Moment Capacity: LRFD Design Eq. 5.6.3.3.-1

$$M_{cr} = \gamma_3 \left[\left(\gamma_1 f_r + \gamma_2 f_{cpe} \right) S_{c,bottom} - M_{dnc} \left(\frac{S_c}{S_{nc}} - 1 \right) \right]$$

$\gamma_1 = 1.0$

$\gamma_2 = 1.0$

$\gamma_3 = 1.0$

Eccentricity of Strands from girder C.G.

$e = y_{bot} - y_{ps} = 36.6 - 30.5 = 6.1$ in.

$$P = \frac{P_e}{5} = \frac{6835}{5} = 1367 \text{ kip } (\text{per girder})$$

$$A = \frac{10345}{5} = 2069 \text{ in}^2 \, (\text{per girder})$$

Compressive stress in Concrete due to prestress only in tension zone

$$f_{cpe} = \frac{P}{A} + \frac{P \times e}{S_{c,bottom}} = \frac{1367^k}{2069^{in^2}} + \frac{1367^k \times 6.1^{in}}{37617^{in^3}} = 0.88 \text{ ksi}$$

Modulus of Rupture

$$f_r = 0.24\sqrt{f_c'} = 0.24 \times \sqrt{3.5} = 0.45 \text{ ksi}$$

Therefore, cracking moment:

$M_{cr\text{-}sec1} = 1.0[(1.0 \times 0.45^{ksi} + 1.0 \times 0.88^{ksi}) 37617^{in^3}] = 50047$ kip-in

5.4.5.2 Critical Section – 2

Determining the Cracking Moment Capacity: LRFD Design Eq. 5.6.3.3.-1

$$M_{cr} = \gamma_3 \left[\left(\gamma_1 f_r + \gamma_2 f_{cpe} \right) S_{c,top} - M_{dnc} \left(\frac{S_c}{S_{nc}} - 1 \right) \right]$$

$\gamma_1 = 1.0$

$\gamma_2 = 1.0$

$\gamma_3 = 1.0$

Eccentricity of Strands from girder C.G.

$e = y_{ps} - y_{bot} = 49.7 - 36.6 = 13.1$ in.

$$P = \frac{P_e}{5} = \frac{7583}{5} = 1516 \text{ kip } (\text{per girder})$$

$$A = \frac{10345}{5} = 2069\,\text{in}^2\ (\text{per girder})$$

Compressive stress in Concrete due to prestress only in tension zone

$$f_{cpe} = \frac{P}{A} + \frac{P \times e}{S_{c,top}} = \frac{1516^{k}}{2069^{in^2}} + \frac{1516^{k} \times 13.1^{in}}{46722^{in^3}} = 1.16\,\text{ksi}$$

Modulus of Rupture,

$$f_r = 0.24\sqrt{f_c^{'}} = 0.24 \times \sqrt{3.5} = 0.45\ \text{ksi}$$

Therefore, cracking moment:

$M_{cr\text{-}sec2} = 1.0[(1.0 \times 0.45^{ksi} + 1.0 \times 1.16^{ksi})46722^{in3}] = 75051$ kip-in

5.4.5.3 Critical Section – 3

Determining the Cracking Moment Capacity

5.4.5.3.1 Positive Moment Case: LRFD *Design Eq. 5.6.3.3.*-1

$$M_{cr} = \gamma_3 \left[\left(\gamma_1 f_r + \gamma_2 f_{cpe} \right) S_{c,bottom} - M_{dnc} \left(\frac{S_c}{S_{nc}} - 1 \right) \right]$$

$\gamma_1 = 1.0$

$\gamma_2 = 1.0$

$\gamma_3 = 1.0$

Eccentricity of Strands from girder C.G.

$e = y_{bot} - y_{ps} = 36.6 - 32.9 = 3.7$ in.

$$P = \frac{P_e}{5} = \frac{7449}{5} = 1489\,\text{kip}\ (\text{per girder})$$

$$A = \frac{10345}{5} = 2069\,\text{in}^2\ (\text{per girder})$$

Compressive stress in Concrete due to prestress only in tension zone

$$f_{cpe} = \frac{P}{A} + \frac{P \times e}{S_{c,bottom}} = \frac{1489^{k}}{2069^{in^2}} - \frac{1489^{k} \times 3.7^{in}}{37617^{in^3}} = 0.57\,\text{ksi}$$

Modulus of Rupture,

$$f_r = 0.24\sqrt{f_c^{'}} = 0.24 \times \sqrt{3.5} = 0.45\ \text{ksi}$$

Therefore, cracking moment:

$M_{cr\text{-}sec3} = 1.0[(1.0 \times 0.45^{ksi} + 1.0 \times 0.57^{ksi})37617^{in3}] = 38434$ kip-in

5.4.5.3.2 Negative Moment Case: LRFD Design Eq. 5.6.3.3.-1

$$M_{cr} = \gamma_3 \left[\left(\gamma_1 f_r + \gamma_2 f_{cpe} \right) S_{c,bottom} - M_{dnc} \left(\frac{S_c}{S_{nc}} - 1 \right) \right]$$

$\gamma_1 = 1.0$

$\gamma_2 = 1.0$

$\gamma_3 = 1.0$

Eccentricity of Strands from girder C.G.

$e = y_{bot} - y_{ps} = 36.6 - 32.9 = 3.7$ in.

$$P = \frac{P_e}{5} = \frac{7449}{5} = 1489\,\text{kip (per girder)}$$

$$A = \frac{10345}{5} = 2069\,\text{in}^2\,\text{(per girder)}$$

Compressive stress in Concrete due to prestress only in tension zone

$$f_{cpe} = \frac{P}{A} + \frac{P \times e}{S_{c,bottom}} = \frac{1489^{k}}{2069^{in^2}} + \frac{1489^{k} \times 3.7^{in}}{46722^{in^3}} = 0.84\,\text{ksi}$$

Modulus of Rupture,

$$f_r = 0.24\sqrt{f_c'} = 0.24 \times \sqrt{3.5} = 0.45\ \text{ksi}$$

Therefore, cracking moment:

$M_{cr\text{-}sec3} = 1.0[(1.0 \times 0.45^{ksi} + 1.0 \times 0.84^{ksi})46722^{in3}] = 60077$ kip-in

5.4.6 Computing Nominal Shear Resistance at Critical Sections

LRFD Design 5.7.3.4.2

Calculating Strain at the centroid of the tension reinforcement at critical section:

$$\varepsilon_s = \frac{\left(\frac{|M_u|}{d_v} + 0.5N_u + |V_u - V_p| - A_{ps}f_{po}\right)}{E_s A_s + E_p A_{ps}}$$

LRFD Design Eq. 5.7.3.4.2-4

If, ε_s is negative then:

$$\varepsilon_s = \frac{\left(\frac{|M_u|}{d_v} + 0.5N_u + |V_u - V_p| - A_{ps}f_{po}\right)}{E_s A_s + E_p A_{ps} + E_c A_{ct}}$$

LRFD Design Eq. B5.2-5

Since MCFT uses an iterative process of determining the shear capacity the equation is modified to take account of the moment in the iterative process.

$$\varepsilon_s = \frac{\left(\frac{|M_{u-DL} + V_{u-LL}\eta_{LL}|}{d_v} + 0.5N_u + |V_u - V_p| - A_{ps}f_{po}\right)}{E_s A_s + E_p A_{ps}}$$

$N_u = 0$

Since,

$M_u = M_{u\text{-}DL} + M_{u\text{-}LL}$

and

$$\eta_{LL} = \frac{M_{u-LL}}{V_{u-LL}}$$

$M_{u\text{-}LL} = V_{u\text{-}LL}\eta_{LL}$

It can be re-written as,

$M_u = M_{u\text{-}DL} + V_{u\text{-}LL}\eta_{LL}$

also,

$V_u = V_{u\text{-}DL} + V_{u\text{-}LL}$

5.4.6.1 Determining Shear Capacity for Inventory Level (Critical Section–1):

Input data:

Dist. from abutment c/l = 69 in.

Shear web, d_v = 47.5 in.

Web width, b_v = 12 in.

Flexural tension depth = 0.5h = 0.5 × 66 = 33 in.

Concrete area in tension, $A_{ct} = \frac{h}{2} b_v + (S - b_v) t_{f,bot}$ =985.5 in.^{2}

Area of shear r/f, A_v = 0.61 in.^{2}

Spacing of shear r/f, s_v = 12 in.

$0.25f'_c b_v d_v$ = 436.3 kip

$E_c A_{ct}$ = 4188452 in^2

Area of Tensile rebar = 3.1 in^2

Area of Tensile Prestress steel = 6.52 in^2

$\frac{dy}{dx} = -0.06606$

$\phi = \tan^{-1}(-0.06606) = -3.78°$

$V_p = | P_e \sin(\phi) | = | 1366 \times \sin(-3.78) | = 90$ kip

5.4.6.1.1 Maximum Shear Concurrent Moment Case:

As determined in Section 5.4.3,

$V_{uS(inv)} = V_{u(DC)} + V_{u(PR)} + V_{us(inv)} = 293$ kip

$M_{uS(imv)} = M_{u(DC)} + M_{u(PR)} + M_{us(inv)} = 18077$ kip-in

$$\eta_{ms(inv)} = \frac{M_{us(inv)}}{V_{us(inv)}} = \frac{8858}{167.8} = 53\left(\text{LL ratio}\right)$$

Since, $M_{uS} < M_{cr\text{-}sec1}$, iteration is not required, assuming strain at the CG of tensile steel reinforcement equal to zero:

$\varepsilon_s = 0.00$

$\theta = 29 + 3500\varepsilon_s = 29 + 3500 \times 0.00 = 29.0°$

$$\beta = \frac{4.8}{1 + 750\varepsilon_s} = \frac{4.8}{1 + 750 \times 0.00}$$
$$= 4.8$$

Determining the shear capacity at critical section after iterating V_u and M_u:

Shear strength of concrete:

$$V_c = 0.0316\beta\lambda\sqrt{f_c'}b_v d_v$$
$$= 0.0316 \times 4.8 \times 1 \times \sqrt{3.5} \times 10.5 \times 47.5$$
$$= 142\,\text{kip}$$

Shear strength of shear reinforcement:

$$V_s = \frac{A_v f_y d_v \cot\left(\theta\right)}{s}$$
$$= \frac{0.61 \times 60 \times 47.5 \cot\left(29\right)}{12}$$
$$= 263\,\text{kip}$$

Total shear capacity of the section:

Minimum of

$V_c + V_s = 142 + 263 = 405$ kip

and

$0.25f'_c b_v d_v = 436.4$ kip

Therefore,

$V_n = 405 + V_p = 405 + 90 = 495$ kip

$\phi V_n = 0.9 \times 495 = 445.5$ kip

An inspection of the ultimate moment and shear at Step 1 and of the cracking moment, indicates the section remains uncracked with the resulting shear strength of 445.4 kips.

5.4.6.1.2 Maximum Moment Concurrent Shear Case:
As determined in Section 5.4.3,

$V_{uM(inv)} = V_{u(DC)} + V_{u(PR)} + V_{um(inv)} = 293$ kip

$M_{uM(inv)} = M_{u(DC)} + M_{u(PR)} + M_{um(inv)} = 18077$ kip-in

$$\eta_{mm(inv)} = \frac{M_{um(inv)}}{V_{um(inv)}} = \frac{8858}{167.8} = 53\left(\text{LL ratio}\right)$$

Determining the shear capacity at critical section after iterating V_u and M_u:

Since, $M_{uS} < M_{cr\text{-}bot}$, iteration is not required, assuming strain at the CG of tensile steel reinforcement equal to zero:

$\varepsilon_s = 0.00$

$\theta = 29 + 3500\varepsilon_s = 29 + 3500 \times 0.00 = 29.0°$

$$\beta = \frac{4.8}{1 + 750\varepsilon_s} = \frac{4.8}{1 + 750 \times 0.00}$$
$$= 4.8$$

Shear strength of concrete:

$$V_c = 0.0316\beta\lambda\sqrt{f_c'}b_v d_v$$
$$= 0.0316 \times 4.8 \times 1 \times \sqrt{3.5} \times 10.5 \times 47.5$$
$$= 142\,\text{kip}$$

Shear strength of shear reinforcement:

$$V_s = \frac{A_v f_y d_v \cot\left(\theta\right)}{s}$$
$$= \frac{0.61 \times 60 \times 47.5 \cot\left(29\right)}{12}$$
$$= 263\,\text{kip}$$

Total shear capacity of the section:

Minimum of

$V_c + V_s = 142 + 263 = 405$ kip

and

$0.25f'_c b_v d_v = 436.4$ kip

Therefore,

$V_n = 405 + V_p = 405 + 90 = 495$ kip

$\phi V_n = 0.9 \times 495 = 445.5$ kip

An inspection of the ultimate moment and shear at Step 1 and of the cracking moment, indicates the section remains uncracked with the resulting shear strength of 445.4 kips.

5.4.6.2 Determining Shear Capacity for Inventory Level (Critical Section–2):
Input data:

Dist. from abutment c/l = 1442 in.

Shear web, $d_v = 47.5$ in.

Web width, $b_v = 12$ in.

Flexural tension depth = $0.5h = 0.5 \times 66 = 33$ in.

Concrete area in tension, $A_{ct} = A_{ct} = \frac{h}{2} b_v + \left(S - b_v\right) t_{f,top} = 1119$ in.^{2}

Area of shear r/f, $A_v = 0.61$ in.^{2}

Spacing of shear r/f, $s_v = 12$ in.

$0.25f'_c b_v d_v = 436.4$ kip

$E_c A_{ct} = 4724256$ in^2

Area of Tensile rebar = 7.6 in^2

Area of Tensile Prestress steel = 8.69 in^2

$\frac{dy}{dx} = 0.05294$

$\phi = \tan^{-1}(0.05294) = 3.03°$

$V_p = | P_e \sin(\phi) | = | 1515 \times \sin(3.03) | = 80$ kip

5.4.6.2.1 Maximum Shear Concurrent Moment Case:
As determined in Section 5.4.3,

$V_{uS(inv)} = V_{u(DC)} + V_{u(PR)} + V_{us(inv)} = 435$ kip

$M_{uS(imv)} = M_{u(DC)} + M_{u(PR)} + M_{us(inv)} = -64393$ kip-in

$$\eta_{ms(inv)} = \frac{M_{us(inv)}}{V_{us(inv)}} = \frac{-13863}{223} = -62\left(\text{LL ratio}\right)$$

Since, $M_{uS} < M_{cr\text{-}sec1}$, iteration is not required, assuming strain at the CG of tensile steel reinforcement equal to zero:

$\varepsilon_s = 0.00$

$\theta = 29 + 3500\varepsilon_s = 29 + 3500 \times 0.00 = 29.0°$

$$\beta = \frac{4.8}{1 + 750\varepsilon_s} = \frac{4.8}{1 + 750 \times 0.00}$$
$$= 4.8$$

Determining the shear capacity at critical section after iterating V_u and M_u:

Shear strength of concrete:

$$V_c = 0.0316\beta\lambda\sqrt{f_c'}b_v d_v$$
$$= 0.0316 \times 4.8 \times 1 \times \sqrt{3.5} \times 10.5 \times 47.5$$
$$= 142\,\text{kip}$$

Shear strength of shear reinforcement:

$$V_s = \frac{A_v f_y d_v \cot\left(\theta\right)}{s}$$
$$= \frac{0.61 \times 60 \times 47.5 \cot\left(29\right)}{12}$$
$$= 263\,\text{kip}$$

Total Shear capacity of the section:

Minimum of

$V_c + V_s = 142 + 263 = 405$ kip

and

$0.25f'_c b_v d_v = 436.4$ kip

Therefore,

$V_n = 405 + V_p = 405 + 80 = 485$ kip

$\phi V_n = 0.9 \times 485 = 436.5$ kip

5.4.6.2.2 The initial check of the strength load combination moment versus the cracking moment is still valid based on inspection of the final shear strength. Maximum Moment Concurrent Shear Case:

As determined in Section 5.4.3,

$V_{uS(inv)} = V_{u(DC)} + V_{u(PR)} + V_{us(inv)} = 304$ kip

$M_{uS(imv)} = M_{u(DC)} + M_{u(PR)} + M_{us(inv)} = -80858$ kip-in

$$\eta_{ms(inv)} = \frac{M_{us(inv)}}{V_{us(inv)}} = \frac{-30327}{92} = -329\left(\text{LL ratio}\right)$$

Determining the shear capacity at critical section after iterating V_u and M_u:

Since, $M_{uS} > M_{cr\text{-}top}$, calculating strain at the CG of tensile steel reinforcement:

$V_{um(inv)}$ after iterating = 127 kip (live load iteration only)

$V_u = V_{u(DC)} + V_{u(PR)} + V_{um(inv)} = 339$ kip

$\eta_{mS(inv)} = -329$

$\left|\frac{M_{u(DC)} + M_{u(PR)} + V_{um(inv)}\eta_{mm(inv)}}{d_v}\right| = 1944\,\text{kip}$, should be greater than $|V_u - V_p| = 259$ kip

Adopt, $\left|\frac{M_{u(DC)} + M_{u(PR)} + V_{um(inv)}\eta_{mm(inv)}}{d_v}\right| = 1944\,\text{kip}$

$A_{ps} = 8.7$ in^2 (per web); $f_{po} = 0.7f_{pu} = 189$ ksi

$$\varepsilon_s = \frac{\left(1980 + |264| - 1643\right)}{29{,}000 \times 7.6 + 28{,}500 \times 8.7}$$
$$= 0.0012$$

$\theta = 29 + 3500\varepsilon_s = 29 + 3500 \times 0.0013 = 33.17°$

$$\beta = \frac{4.8}{1 + 750\varepsilon_s} = \frac{4.8}{1 + 750 \times 0.0013}$$
$$= 2.5$$

Shear strength of concrete:

$$V_c = 0.0316\beta\lambda\sqrt{f_c'}b_v d_v$$
$$= 0.0316 \times 2.5 \times 1 \times \sqrt{3.5} \times 10.5 \times 47.5$$
$$= 75\,\text{kip}$$

Shear strength of shear reinforcement:

$$V_s = \frac{A_v f_y d_v \cot(\theta)}{s}$$
$$= \frac{0.61 \times 60 \times 47.5 \cot(33.5)}{12}$$
$$= 220\,\text{kip}$$

Total shear capacity of the section:

Minimum of

$V_c + V_s = 75 + 220 = 295$ kip

and

$0.25f'_c b_v d_v = 436.4$ kip

Therefore,

$V_n = 295 + V_p = 302 + 80 = 375$ kip

$\phi V_n = 0.9 \times 385 = 338$ kip

By inspection of the final and initial shear strengths and associated moments, it is clear the section is still cracked, which is consistent with Step 1.

5.4.6.3 Determining Shear Capacity for Inventory Level (Critical Section–3)

5.4.6.3.1 Maximum Shear Concurrent Moment Case (Positive Moment Case):

Input data:

Dist. from abutment c/l = 1225 in.

Shear web, $d_v = 47.5$ in.

Web width, $b_v = 10.5$ in. (Reducing the web thickness by $0.5\phi_{Duct}$

Flexural tension depth = $0.5h = 0.5 \times 66 = 33$ in.

Concrete area in tension, $A_{ct} = A_{ct} = \frac{h}{2} b_v + (S - b_v) t_{f,bot} = 985.5$ in.^{2}

Area of shear r/f, $A_v = 0.61$ in.^{2}

Spacing of shear r/f, $s_v = 18$ in.

$0.25 f'_c b_v d_v = 436.4$ kip

$E_c A_{ct} = 4188452$ in^2

Area of Tensile rebar = 3.1 in^2

Area of Tensile Prestress steel = 4.43 in^2

$$\frac{dy}{dx} = 0.07020$$

$\phi = \tan^{-1}(0.07020) = 4.02°$

$V_p = | P_e \sin(\phi) | = | 1488 \times \sin(4.02) | = 104$ kip

As determined in Section 5.4.3,

$V_{uS(inv)} = V_{u(DC)} + V_{u(PR)} + V_{us(inv)} = 345$ kip

$M_{uS(imv)} = M_{u(DC)} + M_{u(PR)} + M_{us(inv)} = 963$ kip-in

$$\eta_{ms(inv)} = \frac{M_{us(inv)}}{V_{us(inv)}} = \frac{11134}{186} = 60(\text{LL ratio})$$

Determining the shear capacity at critical section after iterating V_u and M_u:

Since, $M_{uS} < M_{cr\text{-}sec1}$, iteration not required, assuming strain at the CG of tensile steel reinforcement equal to zero:

$\varepsilon_s = 0.00$

$\theta = 29 + 3500\varepsilon_s = 29 + 3500 \times 0.00 = 29°$

$$\beta = \frac{4.8}{1+750\varepsilon_s} = \frac{4.8}{1+750\times 0.00}$$
$$= 4.8$$

Shear strength of concrete:

$$V_c = 0.0316\beta\lambda\sqrt{f_c'}b_v d_v$$
$$= 0.0316\times 4.8\times 1\times\sqrt{3.5}\times 10.5\times 47.5$$
$$= 142\,\text{kip}$$

Shear strength of shear reinforcement:

$$V_s = \frac{A_v f_y d_v \cot(\theta)}{s}$$
$$= \frac{0.61\times 60\times 47.5\cot(29)}{18}$$
$$= 175\,\text{kip}$$

Total shear capacity of the section:

Minimum of

$V_c + V_s = 142 + 175 = 317$ kip

and

$0.25f'_c b_v d_v = 436.4$ kip

Therefore,

$V_n = 317 + V_p = 337 + 104 = 421$ kip

$\phi V_n = 0.9 \times 421 = 379$ kip

By inspection of the initial and final shear strengths, the assumption that the section is uncracked is still valid.

5.4.6.3.2 Maximum Moment Concurrent Shear Case (Negative Moment Case):
Input data:

Dist. from abutment c/l = 1225 in.

Shear web, $d_v = 47.5$ in.

Web width, $b_v = 10.5$ in. (Reducing the web thickness by $0.5\phi_{Duct}$)

Flexural tension depth = 0.5h = 0.5 × 66 = 33 in.

Concrete area in tension, $A_{ct} = \frac{h}{2} b_v + (S - b_v) t_{f,top} = 1119$ in.^{2}

Area of shear r/f, $A_v = 0.61$ in.^{2}

Spacing of shear r/f, $s_v = 18$ in.

$0.25 f'_c b_v d_v = 436.4$ kip

$E_c A_{ct} = 4724256$ in^2

Area of Tensile rebar = 7.6 in^2

Area of Tensile Prestress steel = 4.26 in^2

$$\frac{dy}{dx} = 0.07020$$

$$\phi = \tan^{-1}(0.07020) = 4.02^\circ$$

$$V_p = | P_e \sin(\phi) | = | 1488 \times \sin(4.02) | = 104 \text{ kip}$$

As determined in Section 5.4.3,

$V_{uS(inv)} = V_{u(DC)} + V_{u(PR)} + V_{us(inv)} = 292$ kip

$M_{uS(imv)} = M_{u(DC)} + M_{u(PR)} + M_{us(inv)} = -27015$ kip-in

$$\eta_{ms(inv)} = \frac{M_{us(inv)}}{V_{us(inv)}} = \frac{-16844}{73} = -231(\text{LL ratio})$$

Determining the shear capacity at critical section after iterating V_u and M_u:

Since, $M_{uS} < M_{cr-\sec 3}$, iteration not required, assuming strain at the CG of tensile steel reinforcement equal to zero:

$\varepsilon_s = 0.00$

$$\theta = 29 + 3500\varepsilon_s = 29 + 3500 \times 0.00$$
$$= 29°$$

$$\beta = \frac{4.8}{1 + 750\varepsilon_s} = \frac{4.8}{1 + 750 \times 0.00}$$
$$= 4.8$$

Shear strength of concrete:

$$V_c = 0.0316\beta\lambda\sqrt{f_c'}\, b_v d_v$$
$$= 0.0316 \times 4.8 \times 1 \times \sqrt{3.5} \times 10.5 \times 47.5$$
$$= 142\,\text{kip}$$

Shear strength of shear reinforcement:

$$V_s = \frac{A_v f_y d_v \cot(\theta)}{s}$$
$$= \frac{0.61 \times 60 \times 47.5 \cot(29)}{18}$$
$$= 175\,\text{kip}$$

Total Shear capacity of the section:

Minimum of

$V_c + V_s = 142 + 175 = 317$ kip

and

$0.25 f'_c b_v d_v = 436.4$ kip

Therefore,

$V_n = 337 + V_p = 317 + 104 = 421$ kip

$\phi V_n = 0.9 \times 421 = 379$ kip

By inspection of the initial and final shear strengths, the assumption that the section is uncracked is still valid.

5.4.7 Longitudinal Reinforcement Check at the Critical Sections

LRFD Design 5.7.3.5

Tensile capacity of the longitudinal reinforcement on the flexural tension side of the member shall be proportioned to satisfy:

$$A_{ps}f_{ps} + A_s f_y \geq \frac{|M_u|}{d_v \phi_f} + 0.5\frac{N_u}{\phi_c} + \left(\left|\frac{V_u}{\phi_v} - V_p\right| - 0.5V_s\right)\cot\theta$$

$\phi_f = 1.0$

$\phi_v = 0.9$

$N_u = 0$

Since it uses an iterative process of determining the shear capacity corresponding to the longitudinal reinforcement, the RHS of the equation is modified to take account of the moments in the iterative process.

$$A_{ps}f_{ps} + A_s f_y \geq \frac{|M_{u-DL} + V_{u-LL}\eta_{LL}|}{d_v \phi_f} + 0.5\frac{N_u}{\phi_c} + \left(\left|\frac{V_u}{\phi_v} - V_p\right| - 0.5V_s\right)\cot\theta$$

Since,

$M_u = M_{u\text{-}DL} + M_{u\text{-}LL}$

and,

$$\eta_{LL} = \frac{M_{u-LL}}{V_{u-LL}}$$

$M_{u\text{-}LL} = V_{u\text{-}LL}\eta_{LL}$

It can be re-written as,

$M_u = M_{u\text{-}DL} + V_{u\text{-}LL}\eta_{LL}$

5.4.7.1 Determining Shear Strength Corresponding to Longitudinal Reinforcement (Critical Section – 1):

5.4.7.1.1 Maximum Shear Concurrent Moment Case (Inventory Level):

As determined in Section 5.4.3,

$V_{uS(inv)} = V_{u(DC)} + V_{u(PR)} + V_{us(inv)} = 293$ kip

$M_{uS(imv)} = M_{u(DC)} + M_{u(PR)} + M_{us(inv)} = 18077$ kip-in

$$\eta_{ms(inv)} = \frac{M_{us(inv)}}{V_{us(inv)}} = \frac{8858}{167.8} = 53\left(\text{LL ratio}\right)$$

$V_{us(inv)}$ after iterating = 622 kip (live load iteration only)

$V_u = V_{u(DC)} + V_{u(PR)} + V_{us(inv)} = 748$ kip

$\eta_{mS(inv)} = 53$

$\left|\frac{M_{u(DC)} + M_{u(PR)} + V_{us(inv)}\eta_{ms(inv)}}{d_v}\right| = 885\,\text{kip}$, should be greater than, $|V_u - V_p| = 657$ kip

Adopt, $\left|\frac{M_{u(DC)} + M_{u(PR)} + V_{us(inv)}\eta_{ms(inv)}}{d_v}\right| = 885\,\text{kip}$

$A_{ps} = 6.52$ in^2 (per web); $f_{po} = 0.7f_{pu} = 189$ ksi

$$\varepsilon_s = \frac{\left(885 + |657| - 1232\right)}{29{,}000 \times 3.1 + 28{,}500 \times 6.52}$$
$$= 0.00113$$

$\theta = 29 + 3500\varepsilon_s = 29 + 3500 \times 0.00115 = 33.0°$

Shear strength of shear reinforcement:

$$V_s = \frac{A_v f_y d_v \cot\left(\theta\right)}{s}$$
$$= \frac{0.61 \times 60 \times 47.5 \cot\left(33.0\right)}{12}$$
$$= 225\,\text{kip}$$

Determining the RHS of LRFD Design Eq. 5.7.3.5-1 by iterating V_u and M_u:

$$RHS = \frac{\left|M_{u(DC)} + M_{u(PR)} + V_{us(inv)}\eta_{LL}\right|}{d_v\phi_f} + 0.5\frac{N_u}{\phi_c} + \left(\left|\frac{V_u}{\phi_v} - V_p\right| - 0.5V_s\right)\cot\theta$$
$$= \frac{885}{1} + \left(\left|\frac{748}{0.9} - 90\right| - 0.5 \times 225\right)\cot\left(33.0\right)$$
$$= 1854\,\text{kip}$$

LHS of the LRFD Design Eq. 5.7.3.5-1

$f_{ps} = 256$ ksi

$LHS = A_{ps,bot}f_{ps} + A_{s,bot}f_y = 6.52 \times 256 + 3.1 \times 60 = 1854$ kip

Since LHS=RHS, shear capacity corresponding to longitudinal reinforcement is:

$$\phi_v V_n = 748\,\text{kip}$$

5.4.7.1.2 Maximum Moment Concurrent Shear Case (Inventory Level):
As determined in Section 5.4.3,

$V_{uM(inv)} = V_{u(DC)} + V_{u(PR)} + V_{um(inv)} = 293$ kip

$M_{uM(imv)} = M_{u(DC)} + M_{u(PR)} + M_{um(inv)} = 18077$ kip-in

$$\eta_{mm(inv)} = \frac{M_{um(inv)}}{V_{um(inv)}} = \frac{8858}{167.8} = 53\left(\text{LL ratio}\right)$$

$V_{um(inv)}$ after iterating = 622 kip (live load iteration only)

$V_u = V_{u(DC)} + V_{u(PR)} + V_{um(inv)} = 748$ kip

$\eta_{mS(inv)} = 53$

$\left|\frac{M_{u(DC)} + M_{u(PR)} + V_{um(inv)}\eta_{mm(inv)}}{d_v}\right| = 885\,\text{kip}$, should be greater than, $|V_u - V_p| = 657$ kip

Adopt, $\left|\frac{M_{u(DC)} + M_{u(PR)} + V_{um(inv)}\eta_{mm(inv)}}{d_v}\right| = 885\,\text{kip}$

$A_{ps} = 6.52$ in^2 (per web); $f_{po} = 0.7 f_{pu} = 189$ ksi

$$\varepsilon_s = \frac{\left(885 + |657| - 1232\right)}{29{,}000 \times 3.1 + 28{,}500 \times 6.52}$$
$$= 0.00113$$

$\theta = 29 + 3500\varepsilon_s = 29 + 3500 \times 0.00115 = 33.0°$

Shear strength of shear reinforcement:

$$V_s = \frac{A_v f_y d_v \cot\left(\theta\right)}{s}$$
$$= \frac{0.61 \times 60 \times 47.5 \cot\left(33.0\right)}{12}$$
$$= 225\,\text{kip}$$

Determining the RHS of LRFD Design Eq. 5.7.3.5-1 by iterating V_u and M_u:

$$RHS = \frac{\left|M_{u(DC)} + M_{u(PR)} + V_{um(inv)}\eta_{LL}\right|}{d_v\phi_f} + 0.5\frac{N_u}{\phi_c} + \left(\left|\frac{V_u}{\phi_v} - V_p\right| - 0.5V_s\right)\cot\theta$$

$$= \frac{885}{1} + \left(\left|\frac{748}{0.9} - 90\right| - 0.5\times 225\right)\cot(33.0)$$

$$= 1854\,\text{kip}$$

LHS of the LRFD Design Eq. 5.7.3.5-1

f_{ps} = 256 ksi

$LHS = A_{ps,bot}f_{ps} + A_{s,bot}f_y = 6.52 \times 256 + 3.1 \times 60 = 1854$ kip

Since LHS=RHS, shear capacity corresponding to longitudinal reinforcement is:

$$\phi_v V_n = 748\,\text{kip}$$

5.4.7.2 Determining Shear Strength Corresponding to Longitudinal Reinforcement (Critical Section – 2):

5.4.7.2.1 Maximum Shear Concurrent Moment Case (Inventory Level):

As determined in Section 5.4.3,

$V_{uS(inv)} = V_{u(DC)} + V_{u(PR)} + V_{us(inv)} = 435$ kip

$M_{uS(imv)} = M_{u(DC)} + M_{u(PR)} + M_{us(inv)} = -64393$ kip-in

$$\eta_{ms(inv)} = \frac{M_{us(inv)}}{V_{us(inv)}} = \frac{-13863}{223} = -62\,(\text{LL ratio})$$

$V_{us(inv)}$ after iterating = 412 kip (live load iteration only)

$V_u = V_{u(DC)} + V_{u(PR)} + V_{us(inv)} = 624$ kip

$\eta_{mS(inv)} = -62$

$\left|\frac{M_{u(DC)} + M_{u(PR)} + V_{us(inv)}\eta_{ms(inv)}}{d_v}\right| = 1603\,\text{kip}$, should be greater than, $|V_u - V_p| = 544$ kip

Adopt, $\left|\frac{M_{u(DC)} + M_{u(PR)} + V_{us(inv)}\eta_{ms(inv)}}{d_v}\right| = 1603\,\text{kip}$

$A_{ps} = 8.69$ in^2 (per web); $f_{po} = 0.7f_{pu} = 189$ ksi

$$\varepsilon_s = \frac{\left(1603 + \left|544\right| - 1642\right)}{29{,}000 \times 7.6 + 28{,}500 \times 8.69}$$
$$= 0.0011$$

$\theta = 29 + 3500\varepsilon_s = 29 + 3500 \times 0.0011 = 32.8°$

Shear strength of shear reinforcement:

$$V_s = \frac{A_v f_y d_v \cot(\theta)}{s}$$
$$= \frac{0.61 \times 60 \times 47.5 \cot(32.8)}{12}$$
$$= 226\,\text{kip}$$

Determining the RHS of LRFD Design Eq. 5.7.3.5-1 by iterating V_u and M_u:

$$RHS = \frac{\left|M_{u(DC)} + M_{u(PR)} + V_{us(inv)}\eta_{LL}\right|}{d_v\phi_f} + 0.5\frac{N_u}{\phi_c} + \left(\left|\frac{V_u}{\phi_v} - V_p\right| - 0.5V_s\right)\cot\theta$$
$$= \frac{1603}{1} + \left(\left|\frac{624}{0.9} - 80\right| - 0.5 \times 226\right)\cot(32.8)$$
$$= 2379\,\text{kip}$$

LHS of the LRFD Design Eq. 5.7.3.5-1

$f_{ps} = 221$ ksi

$LHS = A_{ps,top}f_{ps} + A_{s,top}f_y = 8.69 \times 221 + 7.6 \times 60 = 2379$ kip

Since LHS=RHS, shear capacity corresponding to longitudinal reinforcement is:

$$\phi_v V_n = 624\,\text{kip}$$

5.4.7.2.2 Maximum Moment Concurrent Shear Case (Inventory Level):
As determined in Section 5.4.3,

$V_{uS(inv)} = V_{u(DC)} + V_{u(PR)} + V_{us(inv)} = 304$ kip

$M_{uS(imv)} = M_{u(DC)} + M_{u(PR)} + M_{us(inv)} = -80858$ kip-in

$$\eta_{ms(inv)} = \frac{M_{us(inv)}}{V_{us(inv)}} = \frac{-30327}{92} = -329\left(\text{LL ratio}\right)$$

$V_{um(inv)}$ after iterating = 145 kip (live load iteration only)

$V_u = V_{u(DC)} + V_{u(PR)} + V_{um(inv)} = 358$ kip

$\eta_{mS(inv)} = -329$

$\left|\frac{M_{u(DC)} + M_{u(PR)} + V_{um(inv)}\eta_{mm(inv)}}{d_v}\right| = 2071\text{kip}$, should be greater than, $|V_u - V_p| = 277$ kip

Adopt, $\left|\frac{M_{u(DC)} + M_{u(PR)} + V_{um(inv)}\eta_{mm(inv)}}{d_v}\right| = 2071\text{kip}$

$A_{ps} = 8.69$ in^2 (per web); $f_{po} = 0.7f_{pu} = 189$ ksi

$$\varepsilon_s = \frac{\left(2071 + |277| - 1642\right)}{29{,}000 \times 7.6 + 28{,}500 \times 8.69} = 0.0015$$

$\theta = 29 + 3500\varepsilon_s = 29 + 3500 \times 0.0015 = 34.3°$

Shear strength of shear reinforcement:

$$V_s = \frac{A_v f_y d_v \cot(\theta)}{s} = \frac{0.61 \times 60 \times 47.5 \cot(34.3)}{12} = 214\text{kip}$$

Determining the RHS of LRFD Design Eq. 5.7.3.5-1 by iterating V_u and M_u:

LHS of the LRFD Design Eq. 5.7.3.5-1

$f_{ps} = 221$ ksi

$LHS = A_{ps,top}f_{ps} + A_{s,top}f_y = 8.69 \times 221 + 7.6 \times 60 = 2379$ kip

Since LHS=RHS, shear capacity corresponding to longitudinal reinforcement is:

$\phi_v V_n = 358\text{kip}$

5.4.7.3 Determining Shear Strength Corresponding to Longitudinal Reinforcement (Critical Section – 3):

Engineering judgment is applied in refining the number of load combinations at Critical Section 3 for evaluation.

5.4.7.3.1 Maximum Shear Concurrent Moment Case (Inventory Level):
As determined in Section 5.4.3,

$V_{uS(inv)} = V_{u(DC)} + V_{u(PR)} + V_{us(inv)} = 345$ kip

$M_{uS(imv)} = M_{u(DC)} + M_{u(PR)} + M_{us(inv)} = 963$ kip-in

$$\eta_{ms(inv)} = \frac{M_{us(inv)}}{V_{us(inv)}} = \frac{11134}{186} = 60\left(\text{LL ratio}\right)$$

$V_{us(inv)}$ after iterating = 470 kip (live load iteration only)

$V_u = V_{u(DC)} + V_{u(PR)} + V_{us(inv)} = 629$ kip

$\eta_{mS(inv)} = 60$

$\left|\frac{M_{u(DC)} + M_{u(PR)} + V_{us(inv)}\eta_{ms(inv)}}{d_v}\right| = 378\,\text{kip}$, should be greater than, $|V_u - V_p| = 525$ kip

Adopt, $\left|\frac{M_{u(DC)} + M_{u(PR)} + V_{us(inv)}\eta_{ms(inv)}}{d_v}\right| = 525\,\text{kip}$

$A_{ps} = 4.43$ in^2 (per web); $f_{po} = 0.7f_{pu} = 189$ ksi

$$\varepsilon_s = \frac{\left(525 + |525| - 838\right)}{29{,}000 \times 3.1 + 28{,}500 \times 4.43} = 0.0010$$

$\theta = 29 + 3500\varepsilon_s = 29 + 3500 \times 0.0010 = 32.4°$

Shear strength of shear reinforcement:

$$V_s = \frac{A_v f_y d_v \cot\left(\theta\right)}{s} = \frac{0.61 \times 60 \times 47.5 \cot\left(32.4\right)}{18} = 153\,\text{kip}$$

Determining the RHS of LRFD Design Eq. 5.7.3.5-1 by iterating V_u and M_u:

$$RHS = \frac{\left|M_{u(DC)} + M_{u(PR)} + V_{us(inv)}\eta_{LL}\right|}{d_v\phi_f} + 0.5\frac{N_u}{\phi_c} + \left(\left|\frac{V_u}{\phi_v} - V_p\right| - 0.5V_s\right)\cot\theta$$

$$= \frac{525}{1} + \left(\left|\frac{629}{0.9} - 104.5\right| - 0.5\times 153\right)\cot(32.4)$$

$$= 1340\,\text{kip}$$

LHS of the LRFD Design Eq. 5.7.3.5-1

f_{ps} = 261 ksi

$LHS = A_{ps,bot}f_{ps} + A_{s,bot}f_y = 4.43 \times 261 + 3.1 \times 60 = 1340$ kip

Since LHS=RHS, shear capacity corresponding to longitudinal reinforcement is:

$$\phi_v V_n = 629\,\text{kip}$$

5.4.7.3.2 Maximum Moment Concurrent Shear Case (Inventory Level):
As determined in Section 5.4.3,

$V_{uS(inv)} = V_{u(DC)} + V_{u(PR)} + V_{us(inv)} = 292$ kip

$M_{uS(imv)} = M_{u(DC)} + M_{u(PR)} + M_{us(inv)} = -27015$ kip-in

$$\eta_{ms(inv)} = \frac{M_{us(inv)}}{V_{us(inv)}} = \frac{-16844}{73} = -231(\text{LL ratio})$$

$V_{um(inv)}$ after iterating = 204 kip (live load iteration only)

$V_u = V_{u(DC)} + V_{u(PR)} + V_{um(inv)} = 363$ kip

$\eta_{mm(inv)} = -231$

$\left|\frac{M_{u(DC)} + M_{u(PR)} + V_{um(inv)}\eta_{mm(inv)}}{d_v}\right| = 1209\,\text{kip}$, should be greater than, $|V_u - V_p| = 259$ kip

Adopt, $\left|\frac{M_{u(DC)} + M_{u(PR)} + V_{um(inv)}\eta_{mm(inv)}}{d_v}\right| = 1209\,\text{kip}$

$A_{ps} = 4.26$ in^2 (per web); $f_{po} = 0.7f_{pu} = 189$ ksi

$$\varepsilon_s = \frac{\left(1209 + |259| - 805\right)}{29{,}000\times 7.6 + 28{,}500\times 4.26}$$

$$= 0.0019$$

$\theta = 29 + 3500\varepsilon_s = 29 + 3500 \times 0.0019 = 35.8°$

Shear strength of shear reinforcement:

$$V_s = \frac{A_v f_y d_v \cot(\theta)}{s}$$
$$= \frac{0.61 \times 60 \times 47.5 \cot(35.8)}{18}$$
$$= 135 \text{ kip}$$

Determining the RHS of LRFD Design Eq. 5.7.3.5-1 by iterating V_u and M_u:

$$RHS = \frac{\left|M_{u(DC)} + M_{u(PR)} + V_{um(inv)}\eta_{LL}\right|}{d_v \phi_f} + 0.5\frac{N_u}{\phi_c} + \left(\left|\frac{V_u}{\phi_v} - V_p\right| - 0.5V_s\right)\cot\theta$$
$$= \frac{1209}{1} + \left(\left|\frac{363}{0.9} - 104\right| - 0.5 \times 135\right)\cot(35.8)$$
$$= 1530 \text{ kip}$$

LHS of the LRFD Design Eq. 5.7.3.5-1

f_{ps} = 252 ksi

$LHS = A_{ps,top} f_{ps} + A_{s,top} f_y = 4.26 \times 252 + 7.6 \times 60 = 1530$ kip

Since LHS=RHS, shear capacity corresponding to longitudinal reinforcement is:

$$\phi_v V_n = 363 \text{ kip}$$

5.4.8 Horizontal Shear Check at Critical Section

This check only applies at Critical Section 1.

Horizontal shear force is be determined as follows:

Assuming V_u = 2858 kip

b_w = 12 in

d_s = 35.5 in

$$v_{hs} = \frac{2858}{12 \times 35.5} = 6.71 \text{ksi}$$

y_{crit} = 6 in

$a + oh$ = 69 in

h = 66 in

l_{lp} (tire length) = 10 in

$$l_{crit} = a - \frac{l_{lp}}{2} - h + y_{crit} = 4\text{in}$$

$V_{u,hs} = v_{hs} b_w l_{crit} = 6.71 \times 12 \times 4 = 322.0$ kip

Horizontal Shear Capacity can be determined by Eq. 7-14 from Hovell et al. (2013)

$V_{ni1} = k_d [cA_{cv} + \mu(A_{vf} f_y - 0.04 P_{PS})]$

where,

k_d = 1.0

c = 0.4 ksi

$A_{cv} = b_w d_v = 12 \times 47.5 = 570.2$ in^2

μ = 1.4

$A_{vf} = 4 \times A_s = 4 \times 0.61 = 2.45$ in^2

f_y = 60 ksi

$$\mathrm{P}_{PS} = \left(A_{ps}\right) \times f_{pe} = \frac{43.46}{5} \times 157.1 = 1366\,\text{kip}$$

Therefore,

$V_{ni1} = 1\ [\ 0.4 \times 570.2 + 1.4(2.45 \times 60 - 0.04 \times 1366)]$

V_{ni1} = 357.8 kip

Horizontal Shear Capacity is the minimum of:

$\phi v_{ni} = \min(V_{n1}, K_1 f'c A_{cv}, K_2 A_{cv}) \times 0.9$

=min(357.8,499,855)×0.9

=322.0 kip

Since, $v_{u,hs} = \phi v_{ni}$,

ϕV_n = 2858 kip

5.4.9 Load Rating Factors

The Shear Capacity is the minimum of:

- Nominal shear resistance
- Shear resistance corresponding to longitudinal reinforcement
- Horizontal Shear Resistance (only at Critical Section - 1)

5.4.9.1 Critical Section – 1

5.4.9.1.1 Max Shear Concurrent Moment Case
Shear Capacity for Inventory Level:

ϕV_n = 445.5 kip {min(445.5 kip, 748 kip)}

$V_{u(DC)} = \gamma_{DC} \times V_{DC}$ = 124 kip

$V_{u(PS)} = \gamma_{PS} \times V_{PS}$ = 1.1 kip

$V_{us(inv)} = \gamma_{LL}(inv) \times V_s$ = 168 kip

$$\text{Shear Load Rating} = \frac{\phi V_n - V_{u(DC)} - V_{u(PS)}}{V_{us(inv)}} = 1.91$$

5.4.9.1.2 Max Moment Concurrent Shear Case
Shear Capacity for Inventory Level:

ϕV_n = 445.5 kip {min(445.5 kip, 748 kip)}

$V_{u(DC)} = \gamma_{DC} \times V_{DC}$ = 124 kip

$V_{u(PS)} = \gamma_{PS} \times V_{PS}$ = 1.1 kip

$V_{um(inv)} = \gamma_{LL}(inv) \times V_m$ = 168 kip

$$\text{Shear Load Rating} = \frac{\phi V_n - V_{u(DC)} - V_{u(PS)}}{V_{um(inv)}} = 1.91$$

5.4.9.2 Critical Section – 2

5.4.9.2.1 Max Shear Concurrent Moment Case
Shear Capacity for Inventory Level:

ϕV_n = 436.5 kip {min(436.5 kip, 624 kip)}

$V_{u(DC)} = \gamma_{DC} \times V_{DC}$ = 213 kip

$V_{u(PS)} = \gamma_{PS} \times V_{PS}$ = -1.1 kip

$V_{us(inv)} = \gamma_{LL}(inv) \times V_s$ = 223 kip

$$\text{Shear Load Rating} = \frac{\phi V_n - V_{u(DC)} - V_{u(PS)}}{V_{us(inv)}} = 1.00$$

5.4.9.2.2 Max Moment Concurrent Shear Case
Shear Capacity for Inventory Level:

ϕV_n = 338 kip {min(338 kip, 358 kip)}

$V_{u(DC)} = \gamma_{DC} \times V_{DC}$ = 213 kip

$V_{u(PS)} = \gamma_{PS} \times V_{PS}$ = -1.1 kip

$V_{um(inv)} = \gamma_{LL}(inv) \times V_m$ = 92 kip

$$\text{Shear Load Rating} = \frac{\phi V_n - V_{u(DC)} - V_{u(PS)}}{V_{um(inv)}} = 1.37$$

5.4.9.3 Critical Section – 3

5.4.9.3.1 Max Shear Concurrent Moment Case
Shear Capacity for Inventory Level:

ϕV_n = 379 kip {min(379 kip, 629 kip)}

$V_{u(DC)} = \gamma_{DC} \times V_{DC}$ = 160 kip

$V_{u(PS)} = \gamma_{PS} \times V_{PS}$ = 1.1 kip

$V_{us(inv)} = \gamma_{LL}(inv) \times V_s$ = 186 kip

$$\text{Shear Load Rating} = \frac{\phi V_n - V_{u(DC)} - V_{u(PS)}}{V_{us(inv)}} = 1.17$$

5.4.9.3.2 Max Moment Concurrent Shear Case
Shear Capacity for Inventory Level:

ϕV_n = 363 kip {min(379 kip, 363 kip)}

$V_{u(DC)} = \gamma_{DC} \times V_{DC}$ = 160 kip

$V_{u(PS)} = \gamma_{PS} \times V_{PS}$ = 1.1 kip

$V_{um(inv)} = \gamma_{LL}(inv) \times V_m$ = 73 kip

$$\text{Shear Load Rating} = \frac{\phi V_n - V_{u(DC)} - V_{u(PS)}}{V_{um(inv)}} = 2.78$$

CHAPTER 6. SUMMARY

Chapters 2 and 3 showed the Modified Compression Field Theory to provide the most accurate methodology for predicting the shear strength of concrete bridge members. MCFT is also the concrete shear strength methodology provided in the binding AASHTO LRFD Bridge Design Specifications, 8th Edition (2017). In addition to its accuracy, it has the ability to account for axial loads, an advantage over other shear strength prediction methods.

For design, use of MCFT is straightforward with the General Method listed in AASHTO LRFD. Application of MCFT with load rating is less simple. This Guide has shown that using MCFT for load rating needs an iterative process to determine a member's shear strength, as the strength is dependent on the loading. The trend identified is that if the load rating factor exceeds 1 for the initial step, the final rating factor will be closer to 1 than the RF obtained with the first step. If the RF is lower than 1, the final RF will be closer to 1 than the first RF obtained.

Research performed during the preparation of this Guide has shown that for prestressed concrete members, the more liberal β value—used to determine V_c—provided for members that have the minimum amount of shear reinforcement can be used safely even when the provided shear reinforcement does not meet the minimum specified amounts in AASHTO LRFD. This only applies to prestressed concrete; reinforced concrete members cannot take advantage of this.

MCFT differs from the shear design methods from the AASHTO Standard Specifications in that there is an additional check to ensure the longitudinal tension flexural reinforcement is adequate to achieve the predicted shear strength. With design, this is straightforward to apply but as with flexural shear, it needs an iterative process with load rating to establish a member's shear strength as controlled by the amount of provided flexural reinforcement.

This Guide introduces a third check when load rating concrete members for shear, and that is to ensure the horizontal shear capacity between a webbed member and a bottom flange is adequate to achieve the predicted shear strength. This third check is not currently in AASHTO LRFD but was identified in the literature as a potential limit on the shear strength of concrete girders.

Shear strength and load rating provisions in AASHTO LRFD and MBE have evolved over the years and it is anticipated they will continue to evolve as research reveals improved ways to predict shear strength.

REFERENCES

AASHTO. (2002). *AASHTO Standard Specifications for Highway Bridge*s., 17th Edition. American Associations of State Highway and Transportation Officials, Washington, DC.

AASHTO. (2007). *AASHTO LRFD Bridge Design Specification*s., 4th Edition. American Association of State Highway and Transportation Officials. Washington, DC.

AASHTO. (2010). *AASHTO LRFD Bridge Design Specification*s., 5th Edition. American Association of State Highway and Transportation Officials. Washington, DC.

AASHTO. (2017). *AASHTO LRFD Bridge Design Specifications*., 8th Edition. American Association of State Highway and Transportation Officials, Washington, DC.

AASHTO. (2018). *Manual for Bridge Evaluation*., 3rd Edition. American Association of State Highway and Transportation Officials, Washington, DC.

ACI 318. (1995). *Building Code Requirements for Structural Concrete and Commentar*y., American Concrete Institute, Farmington Hills, MI.

ACI 318. (2019). *Building Code Requirements for Structural Concrete and Commentar*y., American Concrete Institute, Farmington Hills, MI.

ACI Committee 214. (2010). *Guide for Obtaining Cores and Interpreting Compressive Strength Results*., American Concrete Institute, Farmington Hills, MI.

Ahmad, S. H., and Lue, D. M. (1987). "Flexure-Shear Interaction of Reinforced High Strength Concrete Beams." *ACI Structural Journal*. 84 (4). https://doi.org/10.14359/1662

Alcocer, S. M., and Uribe, C. M. (2008). "Monolithic and Cyclic Behavior of Deep Beams Designed Using Strut-and-Tie Models." *ACI Structural Journal*, 105 (3). https://doi.org/10.14359/19792

Angelakos, D. (1999). "The Influence of Concrete Strength and Longitudinal Reinforcement Ratio on the Shear Strength of Large-Size Reinforced Concrete Beams with, and without, Transverse Reinforcement. " Master's thesis. Department of Civil Engineering, University of Toronto, Toronto, Ontario.

Angelakos, D., Bentz, E. C., and Michael, P. C. (2001). "Effect of Concrete Strength and Minimum Stirrups on Shear Strength of Large Members." *ACI Structural Journal,* 98(3), 291-300. https://doi.org/10.14359/10220

Avendaño, A. R., and Bayrak, O. (2008). "Shear Strength and Behavior of Prestressed Concrete Beams. " Technical Report. The University of Texas at Austin, Austin, TX, 180.

Bažant, Z. P., and Kazemi, M. T. (1991). "Size Effect on Diagonal Shear Failure of Beams Without Stirrups." *ACI Structural Journal*, 88 (3). https://doi.org/10.14359/3097

Bentz, E. C. (2010). "MC2010: Shear Strength of Beams and Implications of New Approaches." fib Bulletin 57: Shear and Punching Shear in RC and FRC Elements, Salo, Italy, October 15-16, 15-30.

Bentz, E. C., and Collins, M. P. (2006). "Development of the 2004 Canadian Standards Association (CSA) A23.3 Shear Provisions for Reinforced Concrete." *Canadian Journal of Civil Engineering*, 33(5), 521-534. https://doi.org/10.1139/l06-005

Bentz, E. C., and Collins, M. P. (2017). "Updating the ACI Shear Design Provisions." *Concrete International*, 39(9), 33-38.

Bentz, E. C., and Collins, M. P. (n.d.). "Response 2000." <http://www.ecf.utoronto.ca/~bentz/r2k.htm>. Accessed 2019.

Bentz, E. C., Vecchio, F. J., and Collins, M. P. (2006). "Simplified Modified Compression Field Theory for Calculating Shear Strength of Reinforced Concrete Elements." *ACI Structural Journal*, 103(4), 614-624. https://doi.org/10.14359/16438

Birrcher, D. B., Tuchscherer, R. G., Huizinga, M., and Bayrak, O. (2013). "Minimum Web Reinforcement in Deep Beams." *ACI Structural Journal*, 110 (2), 297-306. https://doi.org/10.14359/51684409

Birrcher, D. B., Tuchscherer, R. G., Huizinga, M., and Bayrak, O. (2014). "Depth Effect in Deep Beams." *ACI Structural Journal*, 111 (4), 731-740. https://doi.org/10.14359/51687002

Birrcher, D., Tuchscherer, R., Huizinga, M., Bayrak, O., Wood, S., and Jirsa, J. (2009). "Strength and Serviceability Design of Reinforced Concrete Deep Beams." No. FHWA/TX-09/0-5253-1. Austin, Texas: Center for Transportation Research.

Bresler, B., and Scordelis, A. C. (1963). "Shear Strength of Reinforced Concrete Beams." *ACI Journal Proceedings*. 60(1), 51-74. https://doi.org/10.14359/7842

Brown, M. D., Sankovich, C. L., Bayrak, O., and Jirsa, J. (2006a). "Behavior and Efficiency of Bottle-Shaped Struts." *ACI Structural Journal,* 103(3), 348-355. https://doi.org/10.14359/15312

Brown, M. D., Sankovich, C. L., Bayrak, O., Jirsa, J., Breen, J. E., and Wood, S. (2006b). "Design for Shear in Reinforced Concrete Using Strut-and-Tie Models." No. FHWA/TX-06/0-4371-2. Austin, Texas: Center for Transportation Research.

Cao, S. (2001). "Size Effect and the Influence of Longitudinal Reinforcement on the Shear Response of Large Reinforced Concrete Members." Master's thesis. Department of Civil Engineering, University of Toronto, Toronto, Ontario.

Caprani, C. C., and Melhem, M. M. (2019). "On the Use of MCFT per AS 5100.5 for the Assessment of Shear Capacities of Existing Structures." *Australian Journal of Structural Engineering*, 1-11. https://doi.org/10.1080/13287982.2019.1664207

Chang, T. S., and Kesler, C. E. (1958). "Static and Fatigue Strength in Shear of Beams with Tensile Reinforcement." *ACI Journal Proceedings*. 54 (6), 1033-1057. https://doi.org/10.14359/11493

Chehab, A. I., and Eamon, C. D. (2018). "Regression-Based Adjustment Factor to Better Estimate Shear Capacity for Load-Rating Simple Span PC Girders." *ASCE Journal of Bridge Engineering*, 23(5), 04018017. https://doi.org/10.1061/(ASCE)BE.1943-5592.0001224

Chehab, A. I., Eamon, C. D., Parra-Montesinos, G. J., and Dam, T. X. (2018). "Shear Testing and Modeling of AASHTO Type II Prestressed Concrete Bridge Girders." *ACI Structural Journal*, 115(3), 801-811. https://doi.org/10.14359/51701917

Choi, J., Zaborac, J. and Bayrak, O. (2021). "Assessment of Shear Capacity of Prestressed Concrete Members with Insufficient Web Reinforcement using AASHTO LRFD General Shear Design Procedure." *Engineering Structures*, 242. https://doi.org/10.1016/j.engstruct.2021.112530

Clark, A. P. (1951). "Diagonal Tension in Reinforced Concrete Beams." *ACI Journal Proceedings*. 48 (10), 145-156. https://doi.org/10.14359/11876

Collins, M. P. (1987). "Towards a Rational Theory for RC Members in Shear." *Journal of Structural Division*, American Society of Civil Engineers, 104(4), 649-666. https://doi.org/10.1061/JSDEAG.0004900

Collins, M. P., Mitchell, D., Adebar, P., and Vecchio, F. J. (1996). "A General Shear Design Method." *ACI Structural Journal*, 93(1), 36-45. https://doi.org/10.14359/9838

CSA Group. (2004). *Design of Concrete Structures CSA A23.3-04*. Canadian Standards Association, Mississauga, ON, Canada.

CSA Group. (2019a). *CSA S6-14, Canadian Highway Bridge Design Code*. Canadian Standards Association, Mississauga, ON, Canada.

CSA Group. (2019b). *Commentary on CSA S6-14, Canadian Highway Bridge Design Code*. Canadian Standards Association, Mississauga, ON, Canada.

de Cossio, R. D., and Siess, C. P. (1960). "Behavior and Strength in Shear of Beams and Frames Without Web Reinforcement." *ACI Journal Proceedings*. 56 (2), 695-735. https://doi.org/10.14359/8118

de Paiva, H. A. R., and Siess, C. P. (1965). "Strength and Behavior of Deep Beams in Shear." *Journal of the Structural Division*. 91(5), 19-41. https://doi.org/10.1061/JSDEAG.0001329

Eamon, C. D., Parra-Montesinos, G. J., and Chehab, A. (2014). "Evaluation of Prestressed Concrete Beams in Shear." Michigan Department of Transportation, Report No: RC-1615, Lansing, MI, 324.

Ferguson, P. M. (1956). "Some Implications of Recent Diagonal Tension Tests." ACI Journal Proceedings. 53(8), 157-172. https://doi.org/10.14359/11507

fib. (2013). *fib Model Code for Concrete Structures (2010)*. Wilhelm Ernst & Sohn, Lausanne, Switzerland. https://doi.org/10.1002/9783433604090

Foster, S. J., and Golbert, R. I. (1998). "Experimental Studies on High-Strength Concrete Deep Beams." *ACI Structural Journal*. 95(4), 382-390. https://doi.org/10.14359/554

Frosch, R. J., Yu, Q., Cusatis, G., and Bazant, Z. P. (2017). "A Unified Approach to Shear Design." *Concrete International*, 39(9), 47-52.

Furuuchi, H., Takahashi, Y., Ueda, T., and Kakuta, Y. (1998). "Effective Width for Shear Failure of RC Deep Slabs." *Transactions of the Japan Concrete Institute*. 20, 209-216.

Ghoneim, M. (2001). "Shear Strength of High-Strength Concrete Deep Beams." *Journal of Engineering and Applied Science,* 48 (4), 675-693. https://doi.org/10.14359/10184

Hara, T. (1985). "The Shear Strength of Reinforced Concrete Deep Beams." *Transactions of the Japan Concrete Institute*. 6, 395-402.

Hassan, T. K., Seliem, H. M., Dwairi, H., Rizkalla, S. H., and Zia, P. (2008). "Shear Behavior of Large Concrete Beams Reinforced with High-Strength Steel." *ACI Structural Journal*, 105 (2), 173-179. https://doi.org/10.14359/19732

Hawkins, N. M., and Kuchma, D. A. (2007). "NCHRP 579: Application of LRFD Bridge Design Specifications to High-Strength Structural Concrete: Shear Provisions." Transportation Research Board, Washington, DC.

Hawkins, N. M., Kuchma, D. A., Mast, R. F., Marsh, M. L., and Reineck, K.-H. (2005). "NCHRP 549: Simplified Shear Design of Structural Concrete Members." Transportation Research Board, Washington, DC.

Higgins, C., Potisuk, T., Farrow, W., C., Robelo, M., J., McAuliffe, T., K., and Nicholas, B. S. (2007). "Tests of RC Deck Girders with 1950s Vintage Details." *ASCE Journal of Bridge Engineering*, 12(5), 621-631. https://doi.org/10.1061/(ASCE)1084-0702(2007)12:5(621)

Holt, J., Garcia, U., Waters, S., Monopolis, C., Zhu, A., Bayrak, O., Powell, L., Halbe, K., Kumar, P., and Chavel, B. (2018). "Concrete Bridge Shear Load Rating, Synthesis Report." FHWA-HIF-18-061. Federal Highway Administration.

Hovell, C., Avendano, A, Moore, A., Dunkman, D., Bayrak, O., and Jirsa, J. (2013). "Structural Performance of Texas U-Beams at Prestress Transfer and Under Shear-Critical Loads." FHWA/TX 13/0-5831-2. Austin, Texas. The Center for Transportation Research.

Hsuing, W., and Frantz, G. C. (1985). "Transverse Stirrup Spacing in R/C Beams." *Journal of Structural Engineering*, 111 (2), 353-362. https://doi.org/10.1061/(ASCE)0733-9445(1985)111:2(353)

Johnson, M. K., and Ramirez, J. A. (1989). "Minimum Shear Reinforcement in Beams with Higher Strength Concrete." *ACI Structural Journal*, 86 (4), 376-382. https://doi.org/10.14359/2896

Kani, M. (1979). "Kani on Shear in Reinforced Concrete." Editors: Kani, M. W., Huggins, M. W., and Wittkopp, R. R., Toronto, Ontario: University of Toronto Press.

Kong, F., Robins, P. J., and Cole, D. F. (1970). "Web Reinforcement Effects on Deep Beams." *ACI Journal Proceedings*. 67 (12), 1010-1018. https://doi.org/10.14359/7336

Kong, P. Y. L., and Rangan, B. V. (1998). "Shear Strength of High-Performance Concrete Beams." *ACI Structural Journal*, 95 (6), 677-688. https://doi.org/10.14359/581

Krefeld, W. J., and Thurston, C. W. (1966a). "Contribution of Longitudinal Steel to Shear Resistance of Reinforced Concrete Beams." *ACI Journal Proceedings*. 63 (3), 325-344. https://doi.org/10.14359/7626

Krefeld, W. J., and Thurston, C. W. (1966b). "Studies of the Shear and Diagonal Tension Strength of Simply Supported Reinforced Concrete Beams." *ACI Journal Proceedings*. 63 (4), 451-476. https://doi.org/10.14359/7633

Kuchma, D. A., Hawkins, N. M., Kim, S.-H., Sun, S., and Kim, K. S. (2008). "Simplified Shear Provisions of the AASHTO LRFD Bridge Design Specifications." *PCI Journal*, 53(3), 53-73. https://doi.org/10.15554/pcij.05012008.53.73

Larson, N., Gomez, E. F., Garber, D., Bayrak, O., and Ghannoum, W. (2013). "Strength and Serviceability Design of Reinforced Concrete Inverted-T Beams." No. FHWA/TX-13/0-6416-1. Austin, Texas: Center for Transportation Research.

Leonhardt, F., and Walther, R. (1964). "The Stuttgart Shear Tests, 1961: Contributions to the Treatment of the Problems of Shear in Reinforced Concrete Construction." London, England: Cement and Concrete Association.

MacGregor, J. G., and Hanson, J. M. (1969). "Proposed Changes in Shear Provisions for Reinforced and Prestressed Concrete Beams*." *ACI Journal*, 66(4), 276-288.

Manuel, R. F., Slight, B. W., and Suter, G. T. (1971). "Deep Beam Behavior Affected by Length and Shear Span Variables." *ACI Journal Proceedings*. 68 (12), 954-958. https://doi.org/10.14359/7246

Mathys, B., French, C., and Shield, C. (2014). "Anchorage of Shear Reinforcement in Prestressed Concrete Bridge Girders." Research Report Number MN/RC 2014-36, Department of Civil, Environmental, and Geo-Engineering, University of Minnesota.

Matsuo, M., Lertsrisakulrat, T., Yanagawa, A., and Niwa, J. (2002). "Shear Behavior of RC Deep Beams with Stirrups." *Transactions of the Japan Concrete Institute*. 23, 385-390.

Mitchell, D., and Collins, M. P. (1974). "Diagonal Compression Field theory-A Rational Model for Structural Concrete in Pure Torsion." *ACI Journal*, 71(8), 396-408. https://doi.org/10.14359/7103

Moody, K. G., Viest, I. M., Elstner, R. C., and Hognestad, E. (1954). "Shear Strength of Reinforced Concrete Beams Part 1 -Tests of Simple Beams." *ACI Journal Proceedings*. 51(12), 317-332. https://doi.org/10.14359/11680

Morrow, J., and Viest, I. M. (1957). "Shear Strength of Reinforced Concrete Frame Members Without Web Reinforcement." *ACI Journal Proceedings*. 53 (3), 833-869. https://doi.org/10.14359/11558

Muttoni, A., Schwartz, J., and Thürlimann, B. (1997). "Design of Concrete Structures with Stress Fields." Birkhäuser Basel. https://doi.org/10.1007/978-3-0348-9047-2

Naji, B., Ross, B. E., and Khademi, A. (2018). "Analysis of Bond-loss Resistance Models for Pretensioned I-girders." *PCI Journal*, 63(1), 40-56. https://doi.org/10.15554/pcij63.1-03

Nakamura, E. (2011). "Shear Database for Prestressed Concrete Members." Master's thesis, The University of Texas at Austin, Austin.

Nakamura, E., Avendaño, A. R., and Bayrak, O. (2013). "Shear Database for Prestressed Concrete Members." *ACI Structural Journal*, 110(6), 909-918. https://doi.org/10.14359/51686147

New Zealand Transportation Agency (2013). "SP/M/022 Bridge Manual." 3rd Edition. NZ Transport Agency. https://www.nzta.govt.nz/resources/bridge-manual/bridge-manual.html

Oh, J., and Shin, S. (2001). "Shear Strength of Reinforced High-Strength Concrete Deep Beams." *ACI Structural Journal*, 98 (2), 164-173. https://doi.org/10.14359/10184

Ozcebe, G., Ersoy, U., and Tankut, T. (1999). "Evaluation of Minimum Shear Reinforcement Requirements for Higher Strength Concrete." *ACI Structural Journal*, 96(3), 361-368. https://doi.org/10.14359/669

Perez, B. (2019). "Structural Evaluation and Testing of Damaged Reinforced Concrete Bent Caps." Master's thesis. Department of Civil, Architectural, and Environmental Engineering, University of Texas at Austin, Austin, Texas.

Perez, B., Zaborac, J., Bayrak, O., and Hrynyk, T. (2019). "Evaluation of a 60-year old Reinforced Concrete Bent Cap Exhibiting Shear Distress." *Concrete - Innovations in Materials, Design and Structures*, 1220-1227. Kraków, Poland: *fib*.

Quintero-Febres, C. G., Parra-Montesinos, G., and Wight, J. K. (2006). "Strength of Struts in Deep Concrete Members Designed Using Strut-and-Tie Method." *ACI Structural Journal,* 103(4), 577-586. https://doi.org/10.14359/16434

Rajagopalan, K. S., and Ferguson, P. M. (1968). "Exploratory Shear Tests Emphasizing Percentage of Longitudinal Steel." *ACI Journal Proceedings*. 65(8), 634-638. https://doi.org/10.14359/7501

Ramakrishnan, V., and Ananthanarayana, Y. (1968). "Ultimate Strength of Deep Beams in Shear." *ACI Journal Proceedings*. 65(2), 87-98. https://doi.org/10.14359/7458

Reineck, K.-H., Bentz, E. C., Fitik, B., Kuchma, D. A., and Bayrak, O. (2013). "ACI-DAfStb Database of Shear Tests on Slender Reinforced Concrete Beams without Stirrups." *ACI Structural Journal*, 110(5), 867-876. https://doi.org/ 10.14359/51685839

Reineck, K.-H., Kuchma, D. A., Kim, K. S., and Marx, S. (2003). "Shear Database for Reinforced Concrete Members without Shear Reinforcement." *ACI Structural Journal*, 100(2), 240-249. https://doi.org/10.14359/12488

Rigotti, M. (2002). "Diagonal Cracking in Reinforced Concrete Deep Beams-An Experimental Investigation." Ph.D. thesis. Department of Building, Civil, and Environmental Engineering, Concordia University, Montréal, Québec, Canada.

Rogowsky, D. M., MacGregor, J. G., and Ong, S. Y. (1986). "Tests of Reinforced Concrete Deep Beams." *ACI Journal Proceedings*. 83(4), 614-623. https://doi.org/10.14359/10558

Roller, J. J., and Russel, H. G. (1990). "Shear Strength of High-Strength Concrete Beams with Web Reinforcement." *ACI Structural Journal*, 87(2), 191-198. https://doi.org/10.14359/2682

Sarsam, K. F., and Al-Musawi, J. M. S. (1992). "Shear Design of High- and Normal Strength Concrete Beams with Web Reinforcement." *ACI Structural Journal*, 89(6), 658-664. https://doi.org/10.14359/9644

Schlaich, J., and Weischede, D. (1982). "Detailing of Concrete Structures-First Draft of a Design Manual (in German). " No. 150; p. 163. Paris: Comité Euro-International du Béton.

Schlaich, J., Schafer, K., and Jennewein, M. (1987). "Toward a Consistent Design of Structural Concrete." *PCI Journal*, 32 (3), 74-150. https://doi.org/10.15554/pcij.05011987.74.150

Shin, S.-W., Lee, K.-S., Moon, J.-I., and Ghosh, S. K. (1999). "Shear Strength of Reinforced High-Strength Concrete Beams with Shear Span-to-Depth Ratios between 1.5 and 2.5." *ACI Structural Journal*, 96 (4), 549-556. https://doi.org/10.14359/691

Shioya, T. S. (1989). "Shear Properties of Large Reinforced Concrete Member." Special Report of Institute of Technology. (25), 213.

Sivakumar, B. (2016). "Low Shear Strength near Inflection Points of Post-Tensioned Multi-Cell Box Girders." Unpublished report to AASHTO Committee T-18: Bridge Management, Evaluation and Rehabilitation.

Smith, K. N., and Vantsiotis, A. S. (1982). "Shear Strength of Deep Beams." *ACI Journal Proceedings*. 79 (3), 201-213. https://doi.org/10.14359/10899

Sritharan, S., Wibowo, H., Rosenthal, M.J., Eull, J.N., and Holombo, J. (2019). "LRFD Minimum Flexural Reinforcement Requirements." NCHRP Research Report 906, Transportation Research Board, Washington DC.

Standards Association of Australia. (2017). *AS 5100.5:2017 Bridge Design: Part 5*. Standards Australia, Sydney, Australia.

Standards New Zealand (2006). *Concrete Structures Standard, NZS3101.1.2006: The Design of Concrete Structures and NZS3101.2.2006: Commentary on the Design of Concrete Structures*. Standards® New Zealand, https://www.standards.govt.nz/shop/nzs-3101-1-and-22006/

Stanik, B. A. P. (1998). "The Influence of Concrete Strength, Distribution of Longitudinal Reinforcement, Amount of Transverse Reinforcement and Member Size on Shear Strength of Reinforced Concrete Members." Master's thesis. Department of Civil Engineering, University of Toronto, Toronto, ON, Canada.

Subedi, N. K., Vardy, A. E., and Kubotat, N. (1986). "Reinforced concrete deep beams some test results." *Magazine of Concrete Research*, 38(137), 206-219. https://doi.org/10.1680/macr.1986.38.137.206

Tan, K.-H., and Lu, H.-Y. (1999). "Shear Behavior of Large Reinforced Concrete Deep Beams and Code Comparisons." *ACI Structural Journal*, 96(5), 836-846. https://doi.org/10.14359/738

Tan, K.-H., Kong, F.-K., Teng, S., and Guan, L. (1995). "High-Strength Concrete Deep Beams with Effective Span and Shear Span Variations." *ACI Structural Journal*, 92(4), 395-405. https://doi.org/10.14359/991

Tan, K.-H., Kong, F.-K., Teng, S., and Weng, L.-W. (1997a). "Effect of Web Reinforcement on High-Strength Concrete Deep Beams." *ACI Structural Journal*, 94(5), 572-582. https://doi.org/10.14359/506

Tan, K.-H., Teng, S., Kong, F.-K., and Lu, H.-Y. (1997b). "Main Tension Steel in High Strength Concrete Deep and Short Beams." *ACI Structural Journal*, 94(6), 752-768. https://doi.org/10.14359/9735

Tanimura, Y., and Sato, T. (2005). "Evaluation of Shear Strength of Deep Beams with Stirrups." Quarterly Report of Railway Technical Research Institute. 46 (1), 53-58. https://doi.org/10.2219/rtriqr.46.53

Tuchscherer, R. G., Birrcher, D. B., and Bayrak, O. (2016). "Reducing Discrepancy between Deep Beam and Sectional Shear-Strength Predictions." *ACI Structural Journal*, 113(1), 3-15. https://doi.org/10.14359/51688602

Tuchscherer, R. G., Birrcher, D. B., Huizinga, M., and Bayrak, O. (2011). "Distribution of Stirrups across Web of Deep Beams." *ACI Structural Journal*, 108(1), 108-115. https://doi.org/10.14359/51664208

Tuchscherer, R. G., Birrcher, D. B., Williams, C. S., Deschenes, D. J., and Bayrak, O. (2014). "Evaluation of Existing Strut-and-Tie Methods and Recommended Improvements." *ACI Structural Journal*, 111(6), 1451-1460. https://doi.org/10.14359/51686926

Tuchscherer, R., Birrcher, D., Huizinga, M., and Bayrak, O. (2010). "Confinement of Deep Beam Nodal Regions." *ACI Structural Journal*, 107(6), 709-717. https://doi.org/10.14359/51664019

Uzel, A. (2003). "Shear Design of Large Footings." Ph.D. thesis. Department of Civil Engineering, University of Toronto, Toronto, ON, Canada.

Van Den Berg, F. J. (1962). "Shear Strength of Reinforced Concrete Beams Without Web Reinforcement." *ACI Journal Proceedings*. 59(11), 1587-1600. https://doi.org/10.14359/7966

Vecchio, F. J. (2000). "Analysis of Shear-Critical Reinforced Concrete Beams." *ACI Structural Journal*, 97(1), 102-110. https://doi.org/10.14359/839

Vecchio, F. J., and Collins, M. P. 1986. "The Modified Compression-Field Theory for Reinforced Concrete Elements Subjected to Shear." *ACI Journal*, 83(2), 219-231. https://doi.org/10.14359/10416

Vector Analysis Group (n.d.). "VecTor2." <http://vectoranalysisgroup.com/vector2.html>. Accessed 2019.

Walraven, J. C. (1981). "Fundamental Analysis of Aggregate Interlock." *Journal of the Structural Division*, American Society of Civil Engineers, 107(11), 2245-2270. https://doi.org/10.1061/JSDEAG.0005820

Walraven, J. C., and Lehwalter, N. (1994). "Size Effects in Short Beams Loaded in Shear." *ACI Structural Journal*, 91(5), 585-593. https://doi.org/10.14359/4177

Watstein, D., and Mathey, R. G. (1958). "Strains in Beams Having Diagonal Cracks." *ACI Journal Proceedings*. 55(12), 717-728. https://doi.org/10.14359/11384

Williams, C. S., Deschenes, D. J., and Bayrak, O. (2012). "Strut-and-Tie Model Design Examples for Bridges: Final Report." No. FHWA/TX-12/5-5253-01-1. Austin, Texas: Center for Transportation Research.

Wong, P. S., Trommels, H., and Vecchio, F. J. (2012). "VecTor2 and FormWorks User's Manual, Second Edition." Technical Report, Department of Civil Engineering, University of Toronto, 311 pp.

Xie, Y., Ahmad, S. H., Yu, T., Hino, S., and Chung, W. (1994). "Shear Ductility of Reinforced Concrete Beams of Normal and High-Strength Concrete." *ACI Structural Journal,* 91(2), 140-149. https://doi.org/10.14359/4592

Yang, K.-H., Chung, H.-S., Lee, E.-T., and Eun, H.-C. (2003). "Shear Characteristics of High-Strength Concrete Deep Beams Without Shear Reinforcements." *Engineering Structures,* 25(10), 1343-1352. https://doi.org/10.1016/S0141-0296(03)00110-X

Yoon, Y.-S., Cook, W. D., and Mitchell, D. (1996). "Minimum Shear Reinforcement in Normal, Medium, and High-Strength Concrete Beams." *ACI Structural Journal*, 93(5), 576-584. https://doi.org/10.14359/9716

Yoshida, Y. (2000). "Shear Reinforcement for Large Lightly Reinforced Concrete Members." Master's thesis. Department of Civil Engineering, University of Toronto, Toronto, Ontario.

Zaborac, J., Choi, J. and Bayrak, O. (2020). "Assessment of Deep Beams with Inadequate Web Reinforcement Using Strut-and-Tie Models." *Engineering Structures*, 218. https://doi.org/10.1016/j.engstruct.2020.110832

Zararis (2003). "Shear Strength and minimum Shear Reinforcement of Reinforced Concrete Slender Beams." *ACI Journal*, 100(2), 203-214. https://doi.org/10.14359/12484

Zhang, N., and Tan, K.-H. (2007). "Size Effect in RC Deep Beams: Experimental Investigation and STM Verification." *Engineering Structures*, 29(12), 3241-3254. https://doi.org/10.1016/j.engstruct.2007.10.005